REPORT CDOT-2020-01 February 2020

Analyze and Validate Bearing Pressure Requirements for Truncated Base Mechanically-Stabilized Earth/Geosynthetically-Reinforced Soil (GRS) Walls

APPLIED RESEARCH & INNOVATION BRANCH

Nien-Yin Chang, Hien Manh Nghiem, Shing Chun Wang

COLORADO
Department of Transportation

The contents of this report reflect the views of the authors, who are responsible for the facts and accuracy of the data presented herein. The contents do not necessarily reflect the official views of the Colorado Department of Transportation or the Federal Highway Administration. This report does not constitute a standard, specification, or regulation. Use of the information contained in the report is at the sole discretion of the designer.

Technical Report Documentation Page

1. Report No.	2. Government Accession No.	3. Recipient's Catalog No.
CDOT2020-01		

4. Title and Subtitle	5. Report Date
Analyze and Validate Bearing Pressure Requirements for Truncated Base Mechanically-Stabilized Earth/Geosynthetically-Reinforced Soil (GRS) Walls	February 2020
	6. Performing Organization Code

7. Author(s)	8. Performing Organization Report No.
Nien-Yin Chang, P.E., Ph.D., Hien Manh Nghiem, Ph.D., and Shing-Chun Wang, Ph.D., P.E.	UCD-CGES-2019-01

9. Performing Organization Name and Address	10. Work Unit No. (TRAIS)
University of Colorado Denver Campus Box 113, P. O. Box 173364, Denver, Colorado 80217	
	11. Contract or Grant No. 216.05

12. Sponsoring Agency Name and Address	13. Type of Report and Period Covered
Colorado Department of Transportation - Research 2829 W. Howard Pl. Denver, CO 80204	Final
	14. Sponsoring Agency Code

15. Supplementary Notes

Prepared in cooperation with the US Department of Transportation, Federal Highway Administration

"Truncated base MSE walls are the MSE walls with narrow base excavation length and steep excavation slope designed to save construction cost while pushing the technological envelope of geosynthetic reinforcement development. A wall with truncated geometry of a narrow base length and steep excavation slope can significantly increase its base bearing pressure. The truncated base wall, an innovated version of regular MSE wall of uniform geosynthetic reinforcement length (RL) equals to 70% of design height (DH) to linearly varied length of geosynthetic reinforcement with an average length equals to 70% of design wall height at mid-wall height. Under this assumption, for instance, the shortest reinforcement RL is 45% DH at the wall base, RL increases linearly from the base to 95% DH at the wall top. The wall with this geometry can limit the magnitude of wall-top surcharge due to potential MSE wall stability concern. The base pressures in CDOT Bridge worksheets were calculated using overturning analysis with reduced bearing width (Meyerhof method) from a regular base wall with 70% wall design height. This study aims to calibrate the values of base bearing pressures and develop optimal design geometry with the Colorado Class I backfill at different placement spacing. Large-scale Tiger Cage truncated wall tests were performed with comprehensive earth pressure measurements along the wall and base. The base bearing pressures were checked favorably with the results of finite element analyses and found much smaller than the pressures recommended in the CDOT Bridge worksheets due to the arching effects with the vertical pressure transfer from backfill and surcharge loads to the back of the block facing wall and excavated slope. The wall façade blocks experience vertical stresses that increase with the depth of backfill."

17. Keywords	18. Distribution Statement
Truncated base GRS wall, bearing pressure at the base of MSE/GRS wall, large-scale model test, geosynthetic tensile stress and strength, Colorado Class I Backfill.	No restrictions. This document is available to the public through the National Technical Information Service, 5825 Port Royal Road, Springfield, VA 22161.

19. Security Classif. (of this report)	20. Security Classif. (of this page)	21. No. of Pages	22. Price
None	None		

Form DOT F 1700.7 (8-72) Reproduction of completed page authorized

CONVERSION TABLE

U. S. Customary System to SI to U. S. Customary System

(multipliers are approximate)

Multiply (symbol)	by	To Get (symbol)	Multiply	by	To Get
LENGTH					
Inches (in)	25.4	millimeters (mm)	mm	0.039	in
Feet (ft)	0.305	meters (m)	m	3.28	ft
yards (yd)	10.914	meters (m)	m	1.09	yd
miles (mi)	1.61	kilometers (km)	m	0.621	mi
AREA					
square inches (in^2)	645.2	square millimeters (mm^2)	mm^2	0.0016	in^2
square feet (ft^2)	0.093	square meters (m^2)	m^2	10.764	ft^2
square yards (yd^2)	0.836	square meters (m^2)	m^2	1.195	yd^2
acres (ac)	0.405	hectares (ha)	ha	2.47	ac
square miles (mi^2)	2.59	square kilometers (km^2)	km^2	0.386	mi^2
VOLUME					
fluid ounces (fl oz)	29.57	milliliters (ml)	ml	0.034	fl oz
gallons (gal)	3.785	liters (l)	l	0.264	gal
cubic feet (ft^3)	0.028	cubic meters (m^3)	m^3	35.71	ft^3
cubic yards (yd^3)	0.765	cubic meters (m^3)	m^3	1.307	yd^3
MASS					
ounces (oz)	28.35	grams (g)	g	0.035	oz
pounds (lb)	0.454	kilograms (kg)	kg	2.202	lb
short tons (T)	0.907	megagrams (Mg)	Mg	1.103	T
		TEMPERATURE (EXACT)			
Fahrenheit (°F)	5(F-32)/9 (F-32)/1.8	Celsius (° C)	° C	1.8C+32	° F
ILLUMINATION					
foot candles (fc)	10.76	lux (lx)	lx	0.0929	fc
foot-Lamberts (fl)	3.426	candela/m (cd/m)	cd/m	0.2919	fl
FORCE AND PRESSURE OR STRESS					
poundforce (lbf)	4.45	newtons (N)	N	.225	lbf
poundforce (psi)	6.89	kilopascals (kPa)	kPa	.0145	psi

ACKNOWLEDGMENTS

The Colorado Department of Transportation and Federal Highway Administration jointly sponsored this study, and the Center for Geotechnical Engineering Science research team (TEAM) at the University of Colorado Denver greatly appreciates the sponsorship. The TEAM appreciates the comments from the following panelists: Shing Chun (Trever) Wang, Panel Chair, Bridge Design and Management (BDM), Ryan Sullivan-Hope, Teddy Meshesha, Matt Greer, CO Division of FHWA, Daniel Alzamora, FHWA Resource Center, Dave Thomas, Materials and Geotechnical Branch, and Martin Merklinger from the Rocsol. The TEAM includes the following members: Nien-Yin Chang, PI, Hien Manh Nghiem, Co-PI, and doctoral graduate students: Jungang Liu, Bach Pham, and Shile Dong. The Center acknowledges the devotion of the TEAM members to this study.

EXECUTIVE SUMMARY

With demand for safer and more economical MSE walls, the truncated base MSE wall is a potential design approach. To answer the demand, the Staff Bridge has issued worksheets to address the truncated base MSE walls. With these design sheets, the worker safety issues regarding steep cut during excavation are covered by OSHA or 29 CFR 1926 requirements. Truncated base MSE walls are the MSE walls applied primarily for cut wall with narrow-base highway excavation length into a steep slope. It is designed to save construction cost while pushing the technological envelope of geosynthetic reinforcement development in terms of safety. The properties of the truncated base are:

- Usually existing slope with good soil or rock with 1(H):1(V), ¾(H):1(V) & ½(H):1(V).
- Temporary wall back excavation must meet OSHA slope requirements on 1(H):1(V), ¾(H):1(V) and ½(H):1(V), the slope stability for the three temporary cut slopes with a minimum factor of safety of 1.3 for stability.
- It is assumed that the same subsurface materials prevail at the wall base and wall-back cut slopes of 1(H):1(V), ¾(H):1(V) and ½(H):1(V) with the minimum factor of safety of 1.5 for wall global stability.

These base pressures (BP) are calculated by overturning analysis with reduced bearing width of 70% wall design height for a regular base wall (Meyerhof method). For the truncated base wall, the bearing pressure (BP) is calculated based on the same methodology of the regular wall with a narrowed base of 4 feet or 45% design height. Table 1 and Figure 1 show the comparison of the factored BP between a regular equal- length reinforcement wall with 1 (H) to 1 (V) back slope (regular base wall, Fig. 2) and a truncated linearly varied reinforcement length wall with ½ (H) to 1 (V) back slope (truncated-base wall, Fig. 3). The most frequently used MSE walls have 1 (V) to 1 (H) backfill slope as specified in the CDOT Bridge worksheets based on the methodology of regular AASHTO MSE walls. Since the current AASHTO publication does not define or recognize the designs depicted in the CDOT worksheets, the CDOT designs are quite conservative. For instance, the contact toe pressures of the truncated-base GRS walls with narrow base are nearly double when compared to the regular AASHTO walls with their bases, a minimum 70% of design heights (linearly varying geosynthetic length with the same design wall height, DH, as depicted in Fig. 3 by design optimization, utilizes the same quantity of geosynthetic as in Fig 2, the average

RL in Fig. 2 is still 70% of DH). This study aims to calibrate the values of **base bearing pressures** and develop **optimal design geometry** fitting the requirements of the Colorado Class I backfill. With reference to the attached MSE worksheet B-504-C1 (CDOT, 2016), Fig. 2, the base and its uniform reinforcement lengths are both equal to 70% of design wall height. Besides, an extended Class I backfill retained soil zone requires a large volume of excavation and backfill. If during construction, sound rocks or competent soils are encountered, the standard practice involved the removal of rocks or soils stronger than Class I Backfill. In reference to the B-504-C3 (CDOT-2016), Fig. 3, the worksheet is applicable to weak rock meeting OSHA construction and global stability requirements. In addition to global stability, sufficient bearing capacity is also a design criterion for wall integrity. However, a conservative (or a large overlay) bearing pressure requirement may disqualify the selection of a truncated base wall. The current AASHTO publication regarding MSE walls provides no design guideline toward the innovation of a truncated or trapezoidal reinforced soil zone. Contemporary CDOT retaining walls do not just serve as landscape structures and/or roadway level separation, they actually support major transportation corridors and vital structures including essential bridges. This study aims to assess the safety of truncated base GRS walls, associated potential cost savings for less back-slope excavation, and to establish a unified approach for the CDOT truncated-base wall design practices.

The Center for Geotechnical Engineering Science (CGES) study team, briefed as TEAM, from the University of Colorado Denver (UCD) performed large-scale physical model tests of truncated base MSE walls to investigate the MSE wall performance. The performance database serves as a calibrator for selected finite element analysis program(s) for the analysis of truncated base MSE walls. The code was then used in generating the optimal wall design geometry. The TEAM also completed the studies on the MSE abutment performance, MSE earth pressures and innovative static load tests of driven piles using the stiff-steel Tiger Cage (T-cage). The test results of all the above studies were used in verification of the effectiveness of a finite element analysis program, SSI2D. The finite element analyses closely simulated the test results and were deemed effective. A comprehensive laboratory test program was performed to characterize the US4800 geosynthetic and backfills to provide materials parameters for the finite element analyses. Tests included the wide-width tension tests of geosynthetics and specific gravity test, gradation tests for grain size distribution characteristics, compaction tests (standard and modified Proctor tests) for moisture-

dry density relationship and triaxial tests for stress-strain-strength characteristics of selected backfills. Lab experiments were conducted to obtain the properties of backfill and US4800 geosynthetic. The wide-width tension tests provided the tensile force versus displacement curves of the geosynthetics. Test results showed reasonable tensile strength and also the average construction-caused strength loss of geosynthetic ranging from 15 to 30% with an average of around 20%. The triaxial tests provided data for the evaluation of the parameters of the hyperbolic constitutive model for Colorado Class I backfill. All tests were performed following the ASTM specifications.

Table 1. Bearing Pressure Comparison

Factored Wall Base or Toe Pressure (Tons per Square Foot)								
Wall height	6’	10’	16’	20’	26’	30’	36’	40’
Regular Base	1.942	2.577	3.377	3.703	4.216	4.721	5.262	5.673
Truncated Base	2.493	5.713	5.96	6.532	7.451	8.259	9.369	10.122

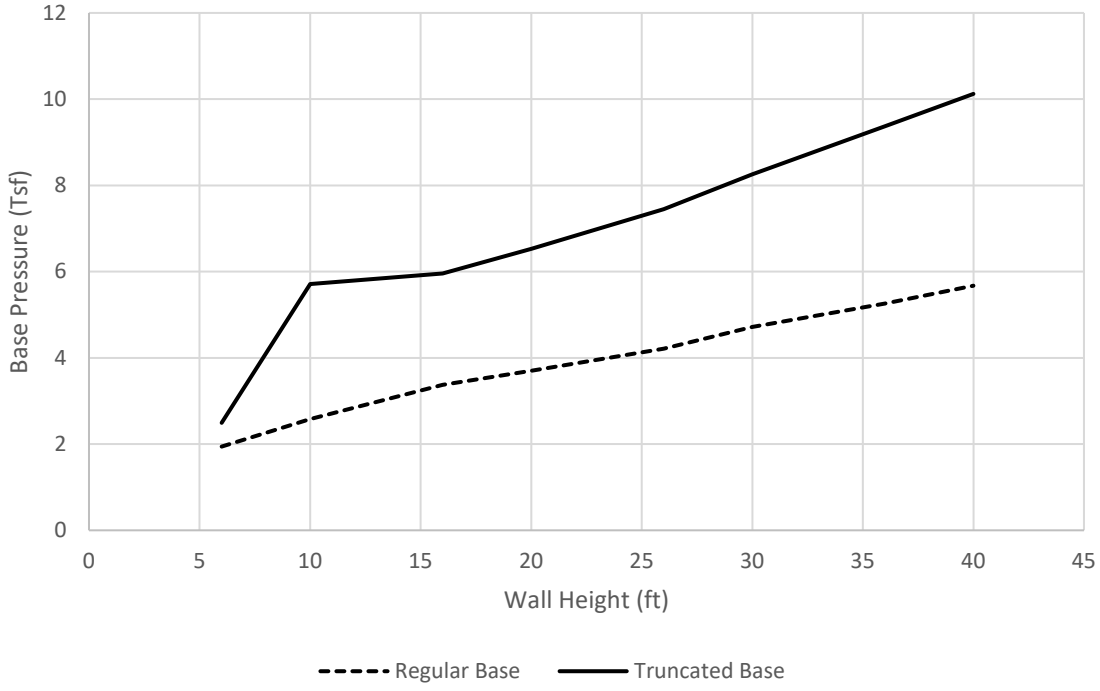

Figure 1. Bearing Pressure Comparison

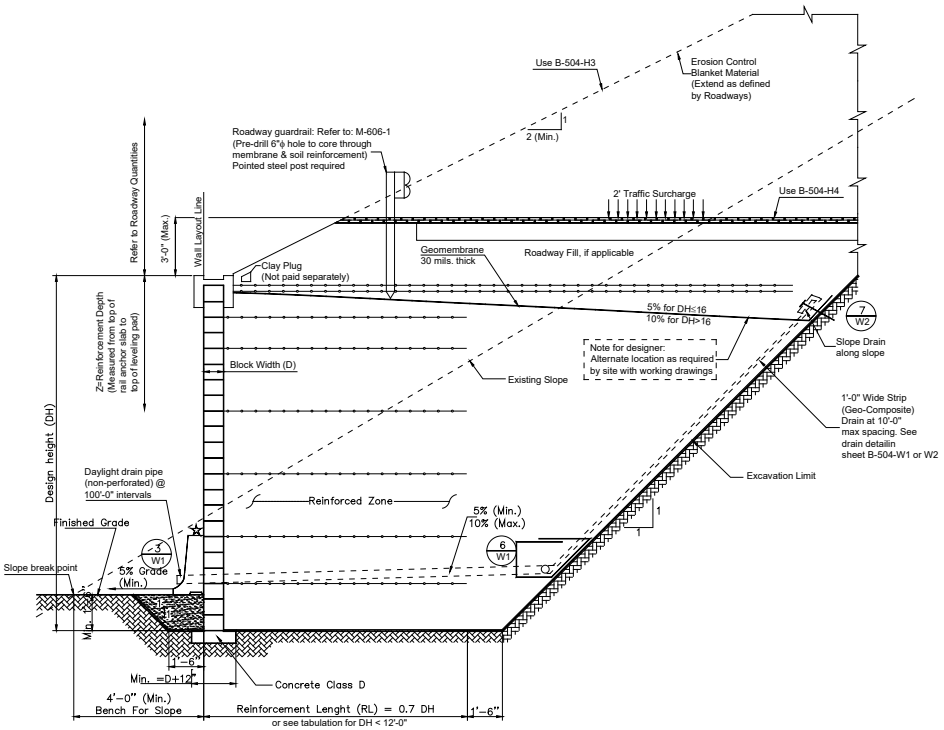

Figure 2. Regular Base MSE Wall with Base Length 0.7DH (design height) (CDOT, 2016)

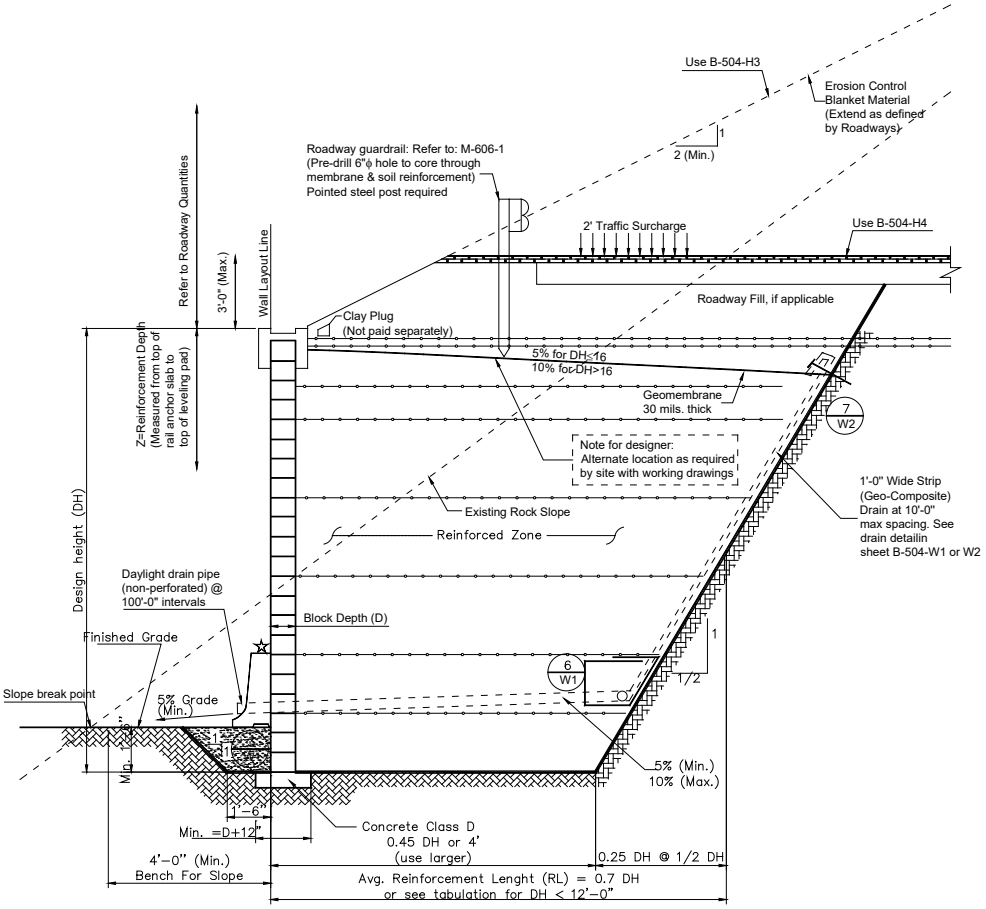

Figure 3. Truncated Base MSE Wall with Base Length 0.45DH (design height) (CDOT, 2016)

TABLE OF CONTENTS

LIST OF FIGURES

LIST OF TABLES

1. BACKGROUND

The AASHTO Section 11 on Specifications for abutments, piers, and walls gives the total reinforcement length of 0.7H in MSE wall designs, where H is the wall height. This requires a large and steep excavation, which can be both costly and unsafe. To achieve safer and more economical wall designs, a truncated mechanically stabilized earth walls are considered as a potentially more economical alternative, as indicated in CDOT Bridge Worksheet (CDOT 2016). Truncated MSE walls have a much narrower base. The AASHTO Section 11 does not provide any specification for truncated base MSE walls or define it. Knowing that the narrowed base of a truncated base wall can increase the bearing pressure at wall base, the challenges include evaluating bearing pressures and locating the site with strong foundation soils and/or rocks to safely meet the bearing pressure requirement.

The CDOT worksheet provides very conservative design requirements. As shown in Table 1 on bearing pressure specifications for walls of most popular wall heights with excavation slope of 1(H) to 1(V), the recommended bearing pressures for truncated base MSE walls nearly double the bearing pressures of regular AASHTO walls with a minimum base length of 70% of design wall heights. The above tabulated bearing pressures are evaluated using Meyerhof's overturning analysis method. Naturally once the bearing pressure is specified, the task shifts to locating a site with sufficient foundation material strength. With reference to the MSE worksheet in B-504, the width of the wall base (reinforcement) ranges from 0.45DH for truncated walls to 0.7DH for regular walls. The wall base bearing pressures in Table 1 need validation against the following design factors: **geometry of the excavation, foundation soil/rock types, types of reinforcing geosynthetics, functions of MSE wall, the roughness of backfill-excavated slope interface, toe strength improvement and external loading**.

For the truncated-base MSE walls with reinforcement length shorter than 0.45H, the external stability requirements (i.e., sliding and bearing capacity) might be insufficient due to the truncated geometry. If further top loaded, the allowable surface surcharge might be reduced. Thus, the design of a truncated base MSE walls might be dictated by both strength and performance. Some form of toe region stabilization mechanism might be needed, like sheet pile toe kicker, Jersey barrier, etc. Research on truncated MSE walls require both numerical analyses and physical model tests. The Center for Geotechnical Engineering Science has a stiff steel research apparatus, named Tiger Cage (T-cage), with the available internal dimensions of 1.875-ft wide x 6-ft high x 10-ft long.

Two studies were completed in the T-cage, the GRS bridge abutment performance and the innovative static load test of driven piles. The first **fully instrumented GRS abutment and wall tests** took place in early November 2015. The T-cage was used in this study for large-scale physical model tests of truncated base MSE walls to provide data for calibration of selected finite element codes. When finite element analysis and model test results are in good agreement, the finite element analysis code is considered valid and is used to generate performance and bearing pressure database for the formulation of truncated base MSE wall design specifications.

The overall objective of this research is an accurate prediction of truncated MSE wall base bearing distribution to make the design practical with optimal sloping excavations. Because of the narrowed base, the base bearing pressures increase and the associated safety factor decreases because of the steeper excavation slope and shorter reinforcing geosynthetics. Thus, design and construction of truncated base MSE walls, while reducing the construction cost for less extensive excavation and geosynthetics, greatly challenge the technological development of MSE wall development due to wall safety concerns. Thus, the objectives of this proposed study are to:

1. Determine the performance of truncated GRS wall models to provide data for validation of finite codes, and, use the validated finite element code to enhance the CDOT's design specifications,
2. Numerical modeling of GRS performance to assess the effectiveness of the design and the selected computer code.
3. Compare the performances from the numerical modeling and full-scale tests for mutual validation of the model tests and finite element analyses.
4. Check the CDOT design to see if there is room for improvement.

The benefit of this study and implementation plan

This study is to provide a unified and cost-saving design approach of MSE walls for 75-year design life. The plan is to perform three large-scale model tests of MSE walls with truncated bases with Colorado Class I backfill with excavation slopes of 45^o, 53^o, and 60^o. This physical model test results will serve to calibrate a selected numerical analysis computer code. When proved effective, a comprehensive finite element analysis program will be performed to provide data for the formulation of design specifications for inclusion in CDOT truncated MSE wall design worksheets. A selected backfill is tested for index properties (specific gravity, Atterberg's limits

and gradation characteristics), moisture-dry density relationship and stress-strain-strength characteristics to provide parameters for finite element analyses of walls. The TEAM will perform triaxial tests for the evaluation of hyperbolic model parameters of backfill for use in finite element analyses. The research results are organized into an appropriate format for implementation in the CDOT MSE wall design worksheet (CDOT 2018). This study accomplished the following tasks:

1) A comprehensive literature review of truncated base MSE/GRS walls addressed the base bearing pressures and wall performance. The findings were synthesized to shape the research direction,

2) Perform laboratory tests of geosynthetic reinforcing materials and backfill that meets CDOT Class 1 backfill specification. Laboratory tests were carried out to provide the material parameters of backfill and geosynthetics for finite element evaluation of truncated base MSE/GRS wall performance and base bearing pressures,

3) Finite element analyses were performed to model the truncated base wall with straight slope excavations,

4) Three physical model tests were performed to provide data for computer code validation and selection, 5) Compared the model test and finite element analysis results and selected SSI2D, code for comprehensive finite element analysis program to provide a database for a base bearing pressures and wall performance.

6) Summarized the wall performance and base bearing pressure distribution for adoption in the CDOT truncated base MSE wall design worksheet.

2. LITERATURE REVIEW

2.1 Truncated base MSE wall

As discussed earlier, the preliminary literature review revealed that available literature on truncated base MSE walls are very limited. Thus, this review is extended to include shored MSE walls with soil nail stabilized excavation slope. Woodruff (2003) completed his work on the MSE shoring composite walls. Federal Lands Highway, Federal Highway Administration (FLH, FHWA (2006) published design guidelines on "Shored Mechanically Stabilized Earth Wall Systems." It addresses mainly the MSE wall with soil-nailed excavated slope. Lee, McCartney, and Ko (2010) through their centrifuge research concluded that the base length of 30% wall height is possible when the excavated slope is stabilized with soil nails. The above publications do not address the issue facing this Statement of Work. AASHTO Section 11 never defines the truncated base MSE wall and no related specifications are available. Wu, et. al. (2006) recommended configuration of the truncation with reinforcement length 0.35 DH at the foundation level (DH is the design height of abutment wall) and increases upward at a 45° angle. The allowable bearing pressure of the sill, as determined by the three-step procedure, should be reduced by 10 percent for truncated-base walls.

A wall with uneven length of geosynthetics is allowed in FHWA NHI manual (Berg et. al., 2009). This wall can be considered as a truncated base wall, Fig. 4. Use of this type of reinforcement geometry should be considered only if the base of the MSE structure is in rock or *competent foundation soil* (foundation materials exhibiting minimal post-construction settlements). The design of these walls requires two analyses: 1) A design using simplified design rules for determining external stability; 2) A global stability analysis, performed using a reinforced soil stability program. Simplified design rules for these structures are as follows: 1) The wall is represented by a rectangular block with width equals reinforcing length (L_o) and height equals the wall design height (DH); 2) Cross-sectional area as the trapezoidal section for external stability calculations; 3) The maximum tensile force line is the same as in rectangular walls (bilinear or linear according to the extensibility of the reinforcements); 4) Minimum base length

$L_3 \geq 0.4DH$, with the difference in length in each zones being less than 0.15 DH; 5) For internal stability calculations, the wall is divided in rectangular sections and for each section the appropriate L (L_1, L_2, L_3), as shown in Fig. 4, is used for pullout calculations.

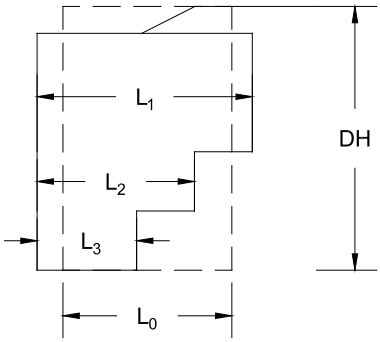

Figure 4. Dimensioning an MSE wall with uneven reinforcement lengths (Berg et. al., 2009)

Adams, et al. (2006) reported a number of GRS abutments with a truncated base with a satisfactory vertical settlement and lateral deformation performances. Wu and Ooi (2015) presented the synopsis addressing the issues of structures with short reinforcement lengths, less than 0.7DH at wall face. Nonuniform reinforcement lengths were used in truncated base reinforced soil walls with reduced reinforcement length, typically in the lower part of the wall. The evidence offered in researches and case histories on truncated base walls shows satisfactory wall performance as long as the base of a reinforced soil wall is founded on a competent foundation with the assured external stability, especially against sliding. The reinforcement length at the lowest level should generally be at least 0.3DH.

Saghebfar, et. al. (2017) presented the detailed instrumentation plan for short-term behavior monitoring of bridge deformations, settlements, reinforcement strains, vertical and horizontal stresses within the abutment, and pore water pressures, and experiences gained from the implementation of the first GRS-IBS with the truncated base project in Louisiana. Ardah, et. al. (2017) presented the results of a finite element analysis that was developed to simulate the fully-instrumented Geosynthetic Reinforced Soil Integrated Bridge System (GRS-IBS) at the Maree Michel Bridge in Louisiana. Four different loading conditions were considered in the evaluation of the performance of GRS-IBS abutment due to dead load, tandem axle truckload, service load, and abnormal load. The measured pressures at the truncated base were compared to those of FE analysis.

2.2. Bearing pressure

The Federal Lands Highway (FLH) Program of the Federal Highway Administration (FHWA) has recent experience with compound wall systems involved repair of roadways in steep mountainous terrain by construction of fill-side retaining walls after fill failures or excessive erosion as a result of landslides and/or flooding (Morison et. al., 2006). MSE walls with shortened reinforcements (0.4DH minimum) constructed in front of a permanent full-height soil nail wall with a mechanical connection between the MSE and shoring components.

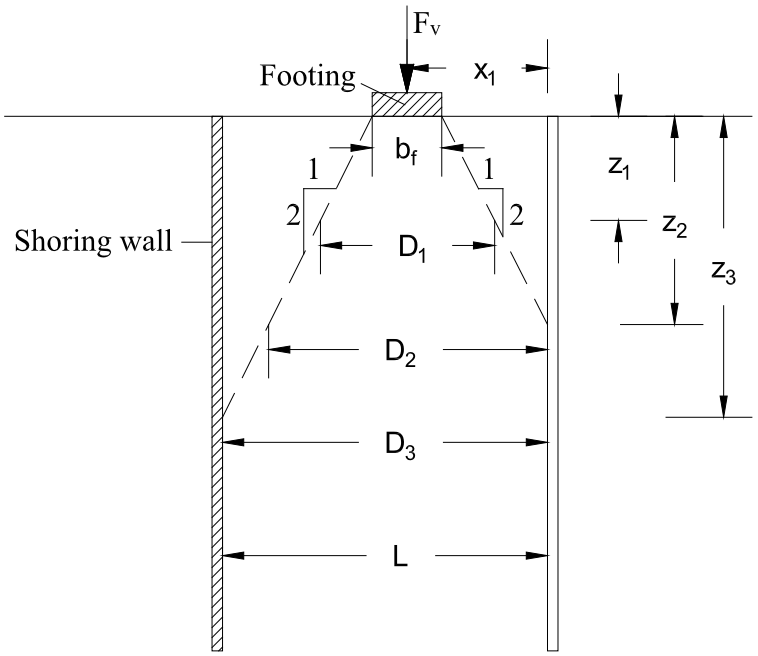

Figure 5. Calculation of vertical stress at the foundation level (Morison et. al., 2006)

The vertical stress at the base of the wall is calculated for the MSE wall component of a shored MSE wall using Fig. 5 for loading from the weight of the reinforced wall and surcharge pressures. Where applicable, the influence of concentrated vertical loading $\left(\Delta\sigma_v\right)$ should be added, calculated as illustrated in Fig. 5. The calculation illustrated in Fig. 5 includes the transfer of vertical stress to the shoring wall, where battered. However, it conservatively neglects arching effects near the shoring wall at the base. Based on the field-scale testing, this simplified method of calculating the vertical stress should be conservative for bearing capacity analysis.

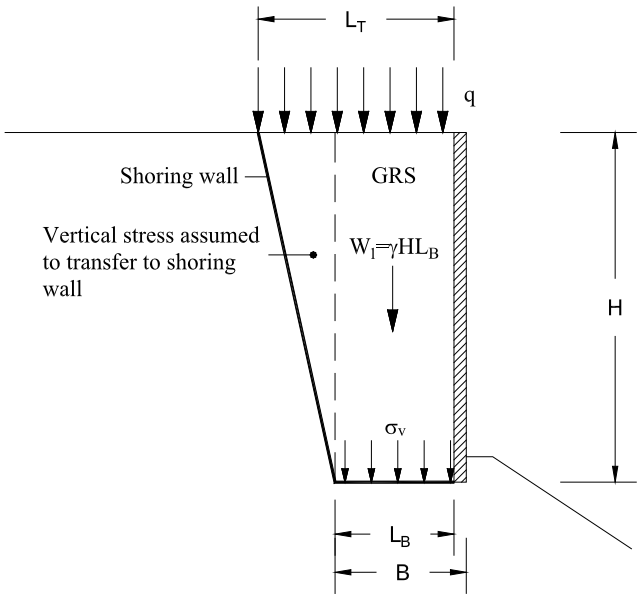

Figure 6. Calculation of vertical stress at the foundation level (Morison et. al., 2006)

The vertical stress, σ_v, acting at the base of the MSE wall component for the case presented in Fig. 6 with horizontal backfill and traffic surcharge is given by:

$$\sigma_v = \frac{W_1 + qL_B}{L_B} \tag{1}$$

The truncated base MSE walls do save construction cost because of the significant reduction in the excavation. CDOT has the right idea of promoting the idea of truncated base MSE walls and, meanwhile, it pushes the envelope of the technological development of MSE walls. However, it is critical to evaluate the bearing pressures along the excavation base and also the wall performance for safety assurance of MSE walls. This high bearing pressure might limit the top surcharge application for the wall top. Besides, the site with sufficient bearing capacity (strength) is needed to assure wall safety. Additionally, it may be necessary to strengthen the toe area with short sheet piles and/or berm to avoid excessive kicker movement.

For the purpose of computing bearing resistance, an equivalent footing is assumed to have a length equals to the length of the wall, and the width is the length of the geosynthetic at the foundation level. The bearing pressure is computed by the Meyerhof's distribution, which considers a uniform base pressure distribution over an effective base as shown in Figs. 7 and 8. Due to the flexibility of MSE walls, a triangular pressure distribution at the wall base cannot develop even if the wall base is founded on a rock, as the MSE wall has limited ability to transmit moment. Therefore, an

equivalent uniform pressure distribution at the base is suitable for MSE walls founded on either soil or rock.

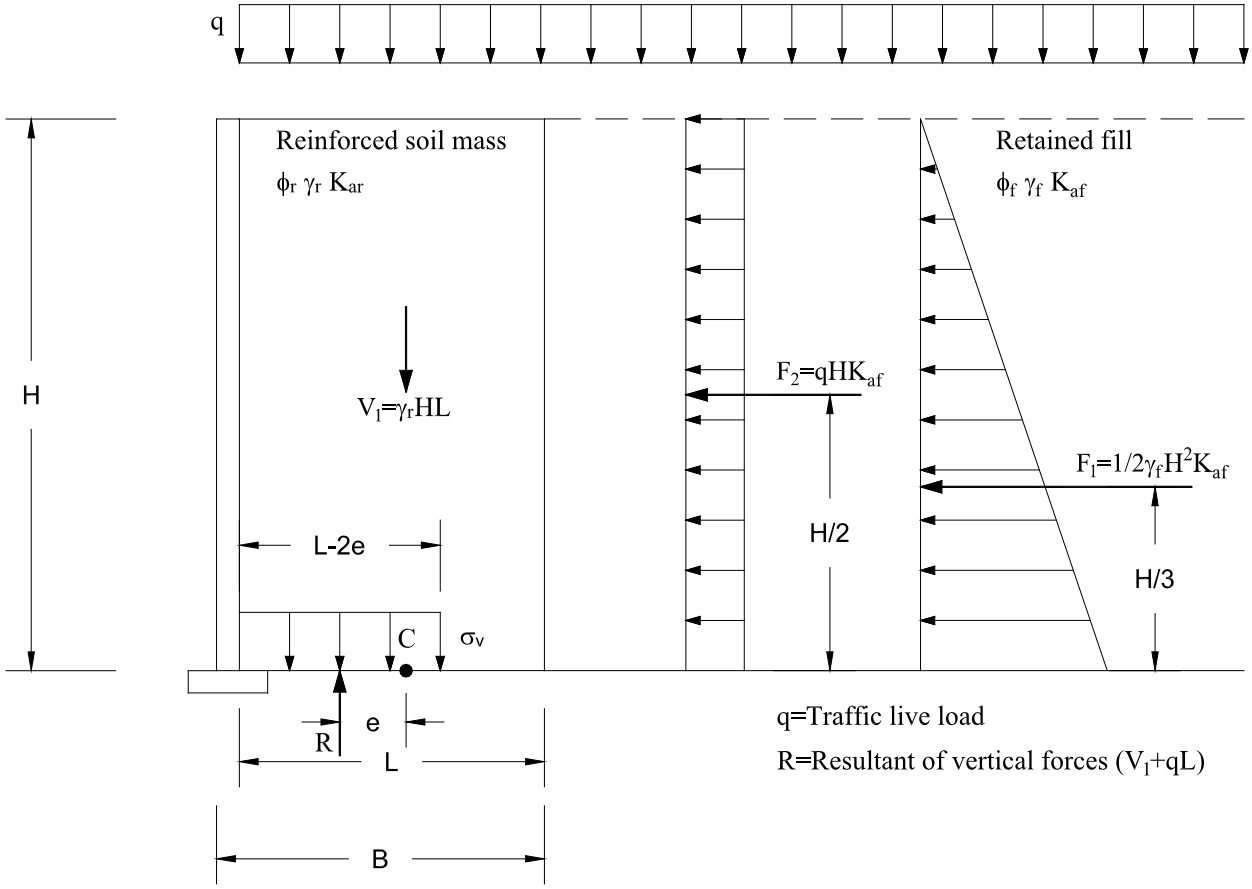

Figure 7. Vertical stress at the foundation level for bearing capacity calculation (Horizontal backslope condition)

Summing moments about point C:

$$e = \frac{F_1(H/3) + F_2(H/2)}{V_1 + qL} \tag{2}$$

Bearing stress is calculated as:

$$\sigma_v = \frac{V_1 + qL}{L - 2e} \tag{3}$$

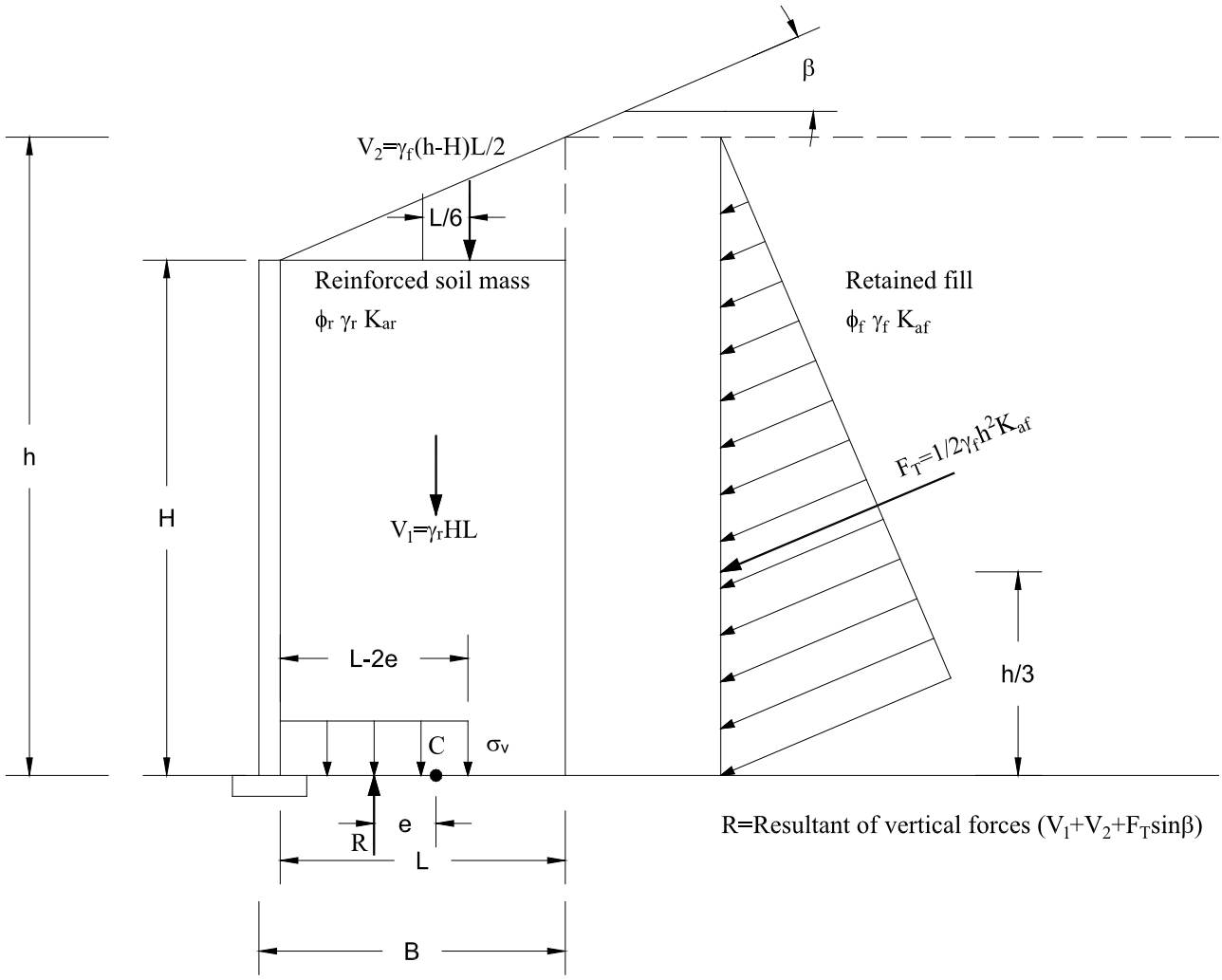

Figure 8. Vertical stress at the foundation level for bearing capacity calculation (Sloping backslope condition)

Summing moments about point C:

$$e = \frac{F_T \cos\beta\left(H/3\right) - F_T \sin\beta\left(L/2\right) - V_2\left(L/6\right)}{V_1 + V_2 + F_T \sin\beta} \tag{4}$$

Bearing stress is calculated as:

$$\sigma_v = \frac{V_1 + V_2 + F_T \sin\beta}{L - 2e} \tag{5}$$

The effect of eccentricity and load inclination is accommodated by the introduction of an effective width B'=L-2e, instead of actual width. For relatively thick facing elements, use B in lieu of L to include the facing dimension and weight in bearing calculations. If e<0, use B'=L.

3. LABORATORY TESTING OF GEOSYNTHETIC AND BACKFILL

3.1 Wide-Width Tension Test of US4800 Geosynthetic

ASTM D 4595 requires the entire width of the sample be clamped. The clamps are 8" x 2". The geosynthetic sample is 8" wide x 8" long (minimum). Since the entire width of the sample is held by the clamps, the test is considered to provide a true tensile strength, where the "pounds of force" is then divided by 8, multiplied by 12, and reported as pounds per foot.

Three geosynthetic samples with unloading-reloading are shown in Fig. 9. Sample dimensions are 8 in. in width and 12 in. in length. The properties of the geosynthetic used in analyses are shown in Table 2.

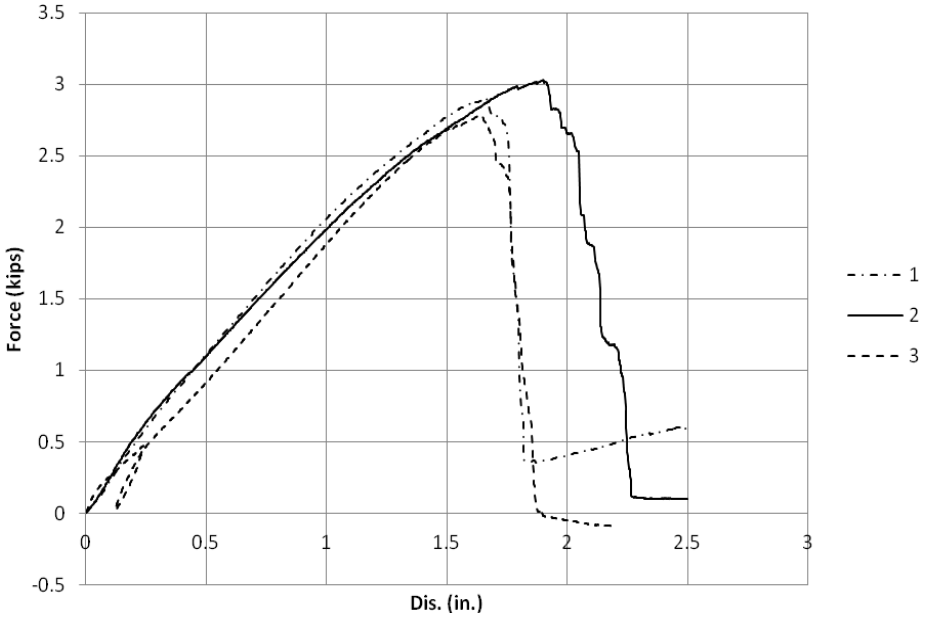

Figure 9. Load-Displacement curves of geosynthetic from tension tests

Table 2. Geosynthetic properties

Properties	Unit	Value
EA_i	lb/ft [kN/m]	44250 [659]
EA_{ur}	lb/ft [kN/m]	69000 [1028]
Fmax	lb/ft [kN/m]	4353 [65]

3.2 Triaxial Compression Tests of Colorado Class I Backfill

Both conventional compression and hydrostatic compression triaxial tests were performed and results presented in Figs. 13 to 16 and summarized in Tables 4 and 5.

3.2.1 Hydrostatic Compression Tests

Hydrostatic compression (or isotropic compression) tests are performed and shown in Fig. 10.

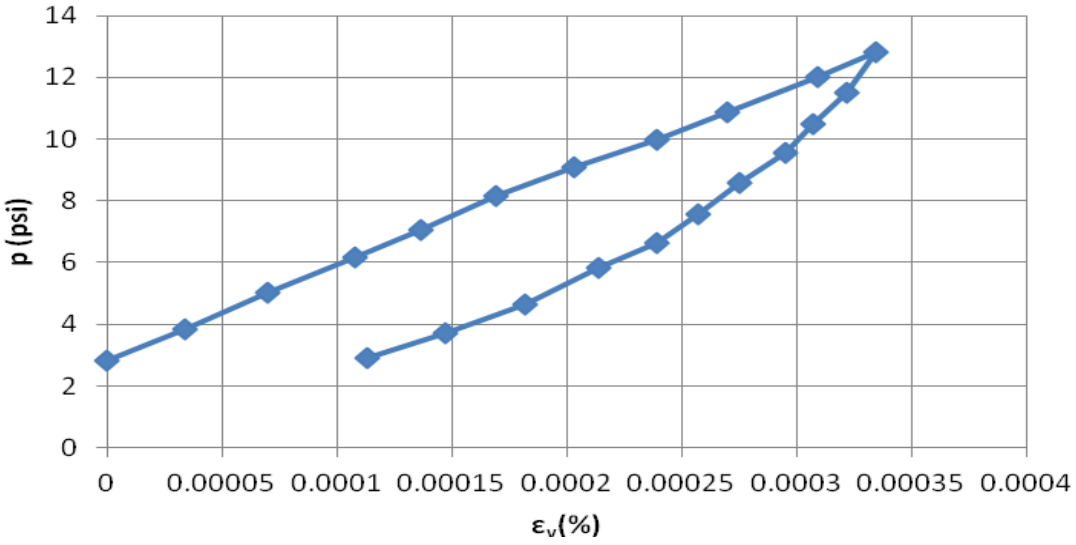

Figure 10. Hydrostatic test

3.2.2 Conventional Triaxial Compression Tests

Several conventional triaxial compression tests were conducted in the Geotechnical/structural laboratory at the University of Colorado Denver. Samples were 6 inches in diameter, 12 inches in length. Dry soil was mixed with water to attain its optimum moisture content and compacted in a mold using the modified Proctor compaction. The triaxial compression tests were performed at confining pressures of 10psi, 20psi, and 30psi. Test results are shown in Fig. 11 without volume change measurement. From these tests, the soil strength parameters are determined and shown in Table 8. The method to determine the friction angle and cohesion is presented in Figs. 12 and 13. Two isotropic compression tests, one on dry soil and other on moisture soil, were performed to assess the effect of moisture on volume change, Fig. 14. Both tests yielded similar results. This test is also used to determine the dilatancy angle, as shown in Figs. 15 and 16 and Table 3.

The Young's moduli can be determined from triaxial tests as follows:

$$E_i = K_L P_a \left(\frac{\sigma_3}{P_a} \right)^{n_L} \qquad (6)$$

$$E_{ur} = K_{ur} P_a \left(\frac{\sigma_3}{P_a} \right)^{n_{ur}} \qquad (7)$$

where E_i and E_{ur} are initial tangent modulus and unloading-reloading modulus, respectively, as functions of confining stress, σ_3; K_L and K_{ur} are loading and unloading-reloading moduli, respectively; p_a is atmospheric pressure (used as a normalizing parameter); σ_3 is confining stress; and n_L and n_{ur} are exponents for defining the influence of the confining pressure on the moduli.

The Poisson's ratio is back calculated from the coefficient of the lateral earth pressure at rest $k_0 = 0.17$ as $\nu = k_0/(1+k_0) = 0.17/1.17 = 0.145$. The elastic parameters are presented in Table 4.

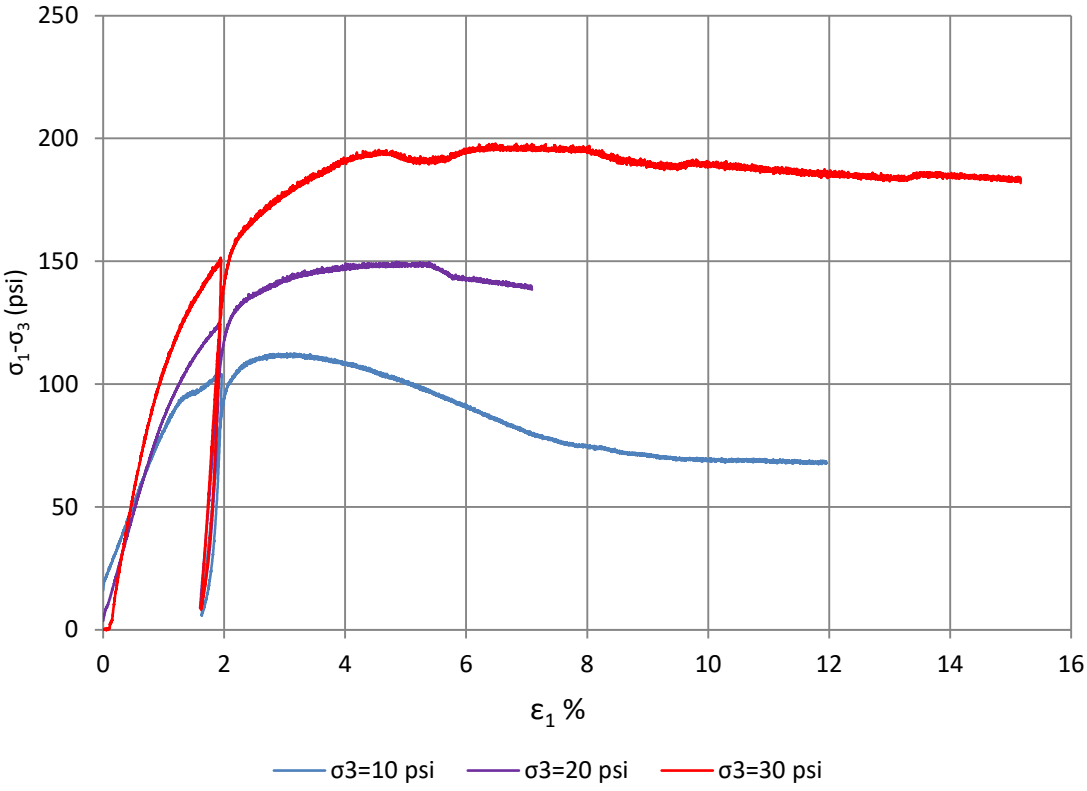

Figure 11. Triaxial test results

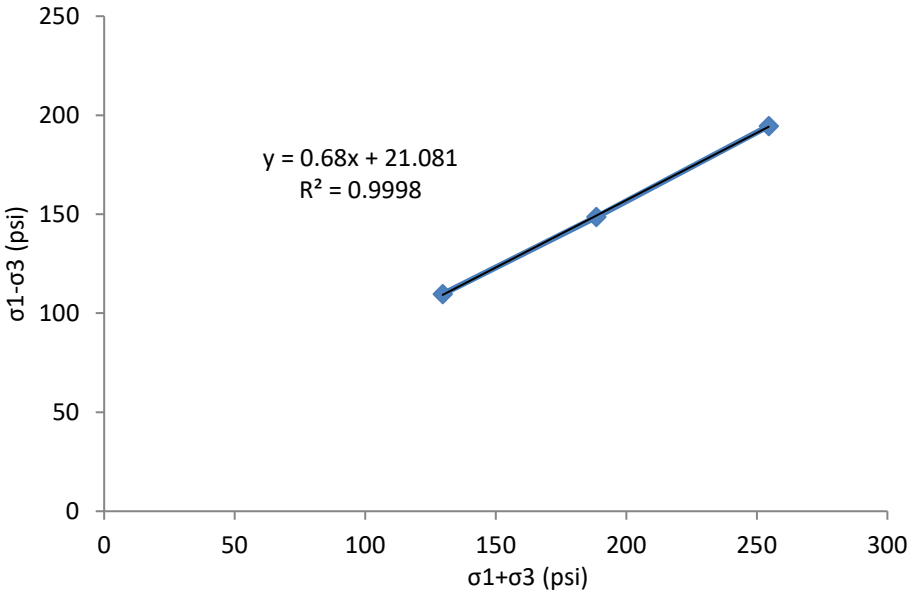

Figure 12. Determination of friction angle and cohesion

Table 3. Friction angle and cohesion from triaxial tests

Properties	Units	Value
Friction angle, φ	(^{0})	42.8
Cohesion, c	(psi)	14.4
Dilatancy angle, ψ	(^{0})	8.7

Table 4. Modulus from triaxial tests

Parameter	Value
K_L	532.4
n_L	0.477
K_{ur}	1975.6
n_{ur}	0.344
ν	0.145

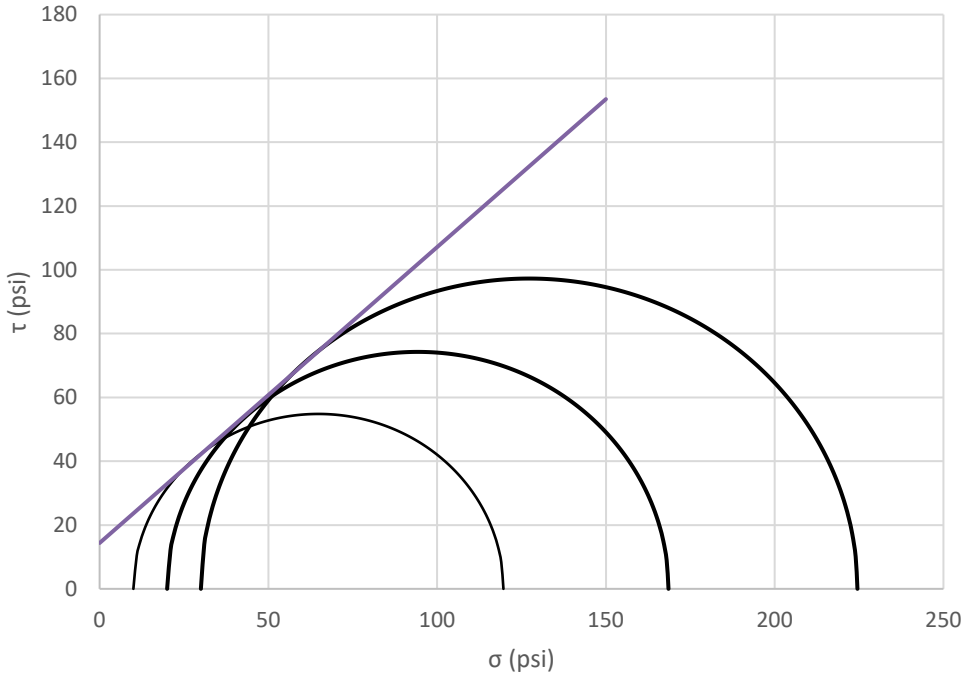

Figure 13. Mohr circle and failure line

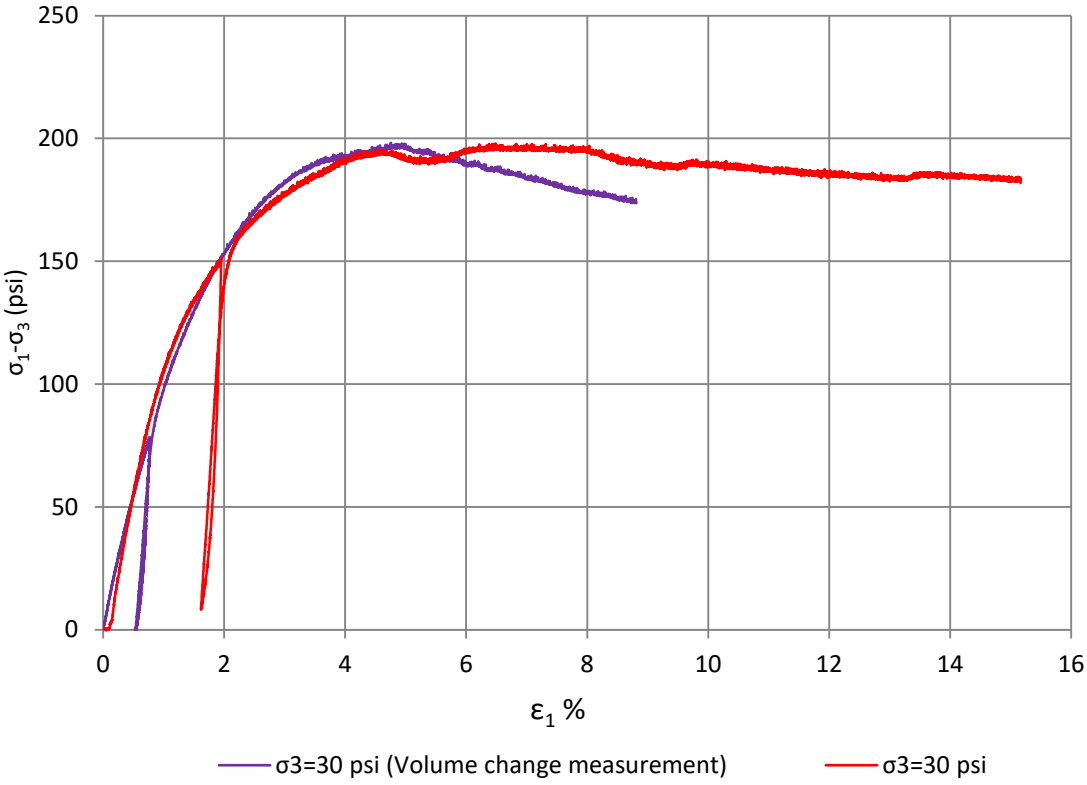

Figure 14. Comparison of triaxial compression tests (σ_3=30 psi)

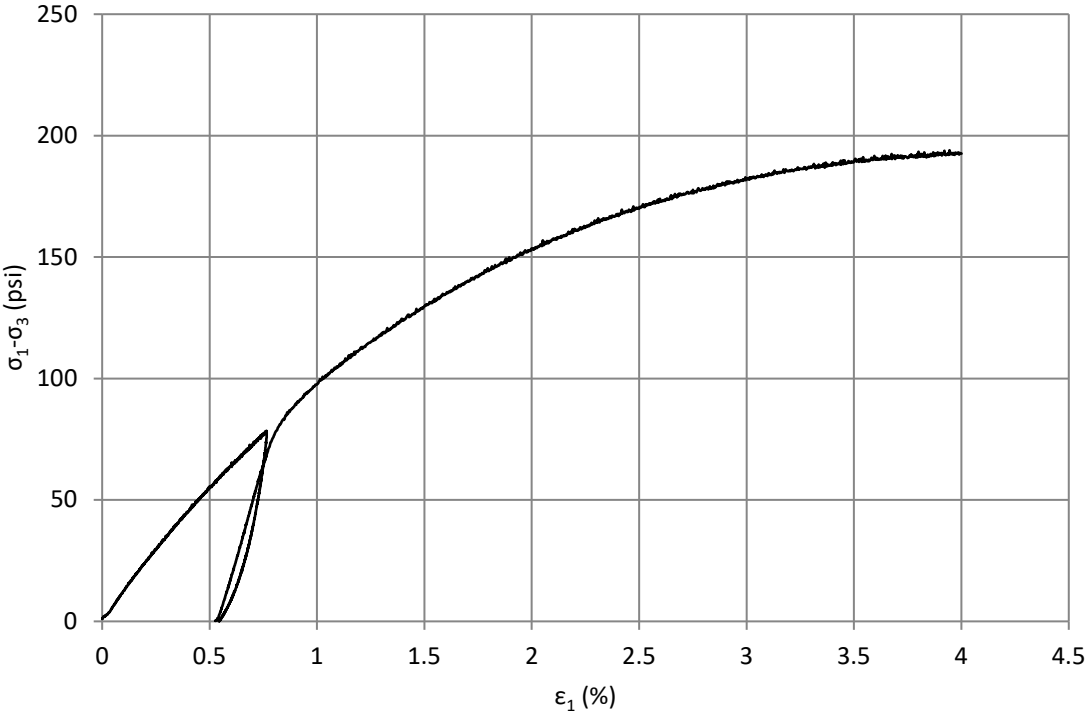

Figure 15. Triaxial test (σ_3 = 30 psi) with volume change measurement

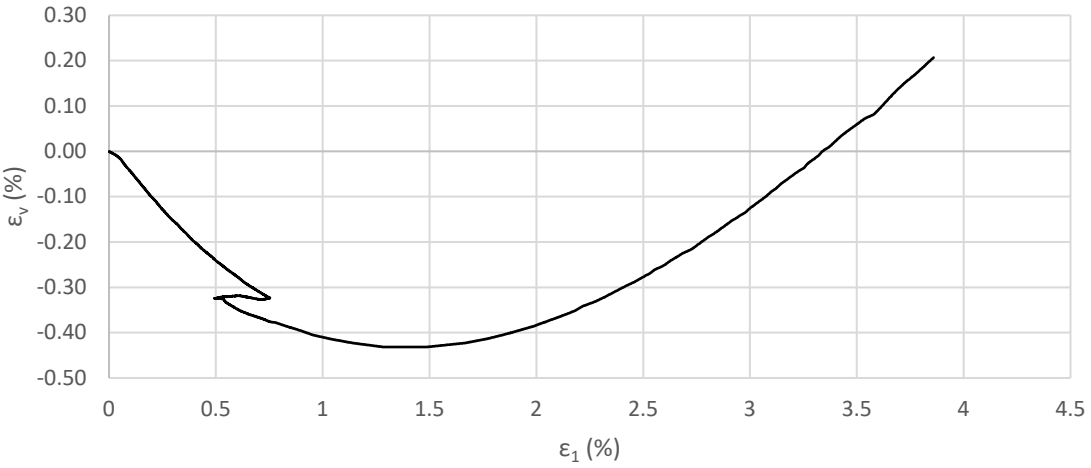

Figure 16. Volume change measurement

3.3 Oedometer and Direct Shear Tests

3.3.1 Device Description

The 305MM with 12" x 12" square direct shear box was specifically designed for testing large samples for evaluating the soil-geosynthetic interface coefficient of friction (Figs. 17 ánd 18). It could also be used to evaluate soil-soil, soil-geosynthetic, geosynthetic-geosynthetic, interface characteristics. The device utilizes the Karol Warner "CONBEL" concept for the application of loads pneumatically using pneumatic pistons.

SPECIFICATIONS

Machine Dimensions: 58.4 cm x 109 cm x 102 cm high (23" x 43" x 40" high)

Compaction Table Dimensions: 356 mm x 508 mm x 551 mm high (14" x 20" x 21.69" high)

Power: 110 Volts 60 Hz - 220-240 Volts 50 Hz

Net Weight: 381 kg (840 lbs)

Shipping Weight: 465 kg (1,025 lbs)

Shear Box

- Top 100 mm deep x 305 mm sq (3.97" x 12" sq), area = 929 cm (144" sq)
- Bottom 305 mm x 406 mm x 100 mm deep

(12" x 16" x 3.97” deep)

Easy access water chamber Aluminum with hard coat anodize finish with water control valves

Horizontal and Vertical Load 45 kN (10,000 lbs)

Consolidation Loading Pistons (2) 4 kN & 45 kN (809 lb & 10,000 lb) capacity

Four Channel Readout With RS232 output

Displays - Pressure for setting consolidation load

- Horizontal Load

- Horizontal Displacement

- Vertical Displacement

RS 232 Serial Output - ASCI Format Cable included

Get Data Software Export of data into “Excel” in computer

Horizontal Load Cell 45 kn (10,000 lbs)

Vertical Displacement Transducer: 50 mm (2.0")

Horizontal Displacement Transducer: 100 mm (4")

Geosynthetic Platform: 303 mm x 405 mm x 100 mm H (11.94" x 15.94" x 3.94")

100 mm (4.0") sq Filler Block 100 mm sq x 304 mm long (4.0" sq x 11.95")

Air Pressure Required 827 kPa (120 psi) for max sample load of 45 kn (10,000 lbs)

Horizontal Strain Rate: 0.0508 mm to 5.08 mm/min (0.002" to 0.20”/min).

Figure 17. Direct shear test device

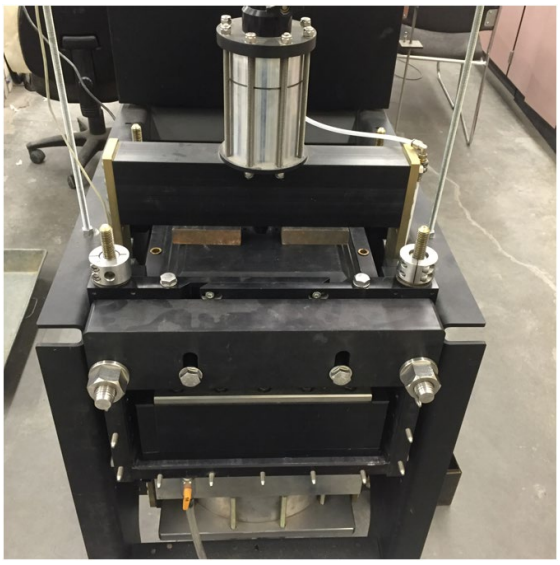

Figure 18. The loading system of direct shear box

3.3.2 Oedometer Tests

The direct shear device is used for the one-dimensional compression test. Three samples of 12"x12"x7.94” was compressed under vertical load. The relationship between vertical pressure

and vertical strain are shown in Fig. 19. From the curves, constraint moduli are computed and shown in Fig. 20.

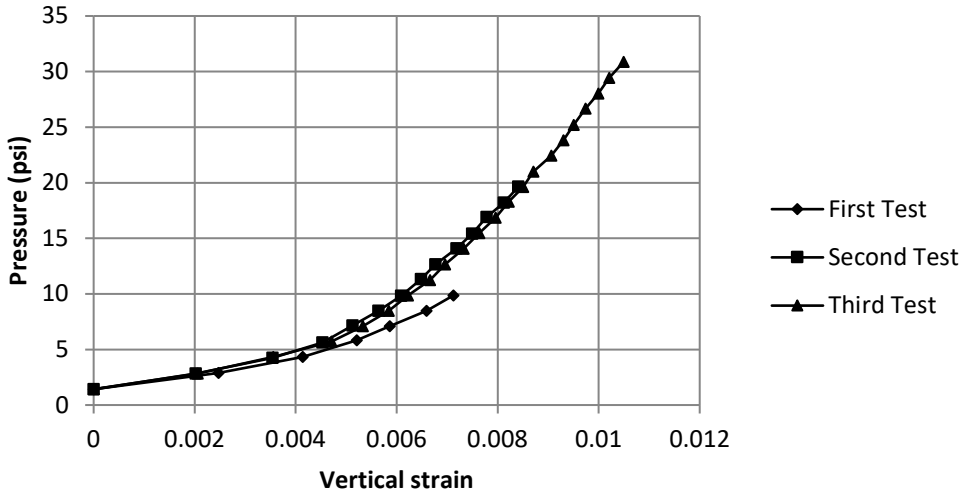

Figure 19. Oedometer tests

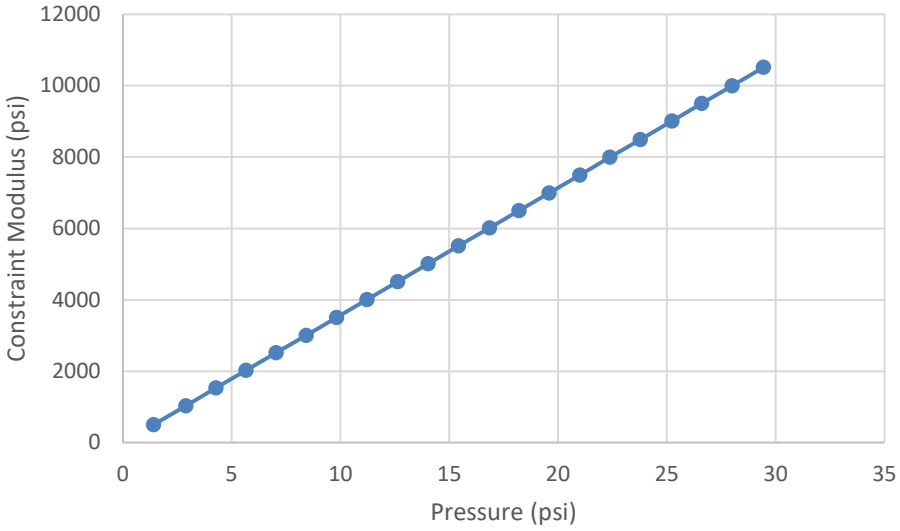

Figure 20. Constraint moduli

3.3.3 Direct Shear Tests

Three direct shear tests were conducted at different normal stresses to determine the shear strength of the soil. Soil sample after shearing is shown in Fig. 21. Shear stress-displacement curves are shown in Fig. 22 and vertical displacements and horizontal displacements curves are shown in Fig. 23.

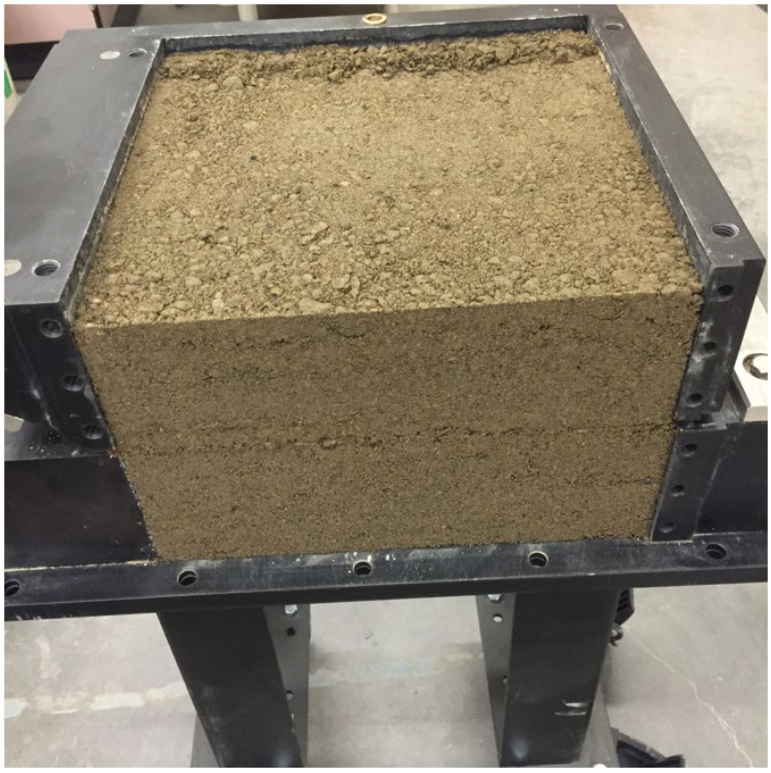

Figure 21. Soil sample after shearing

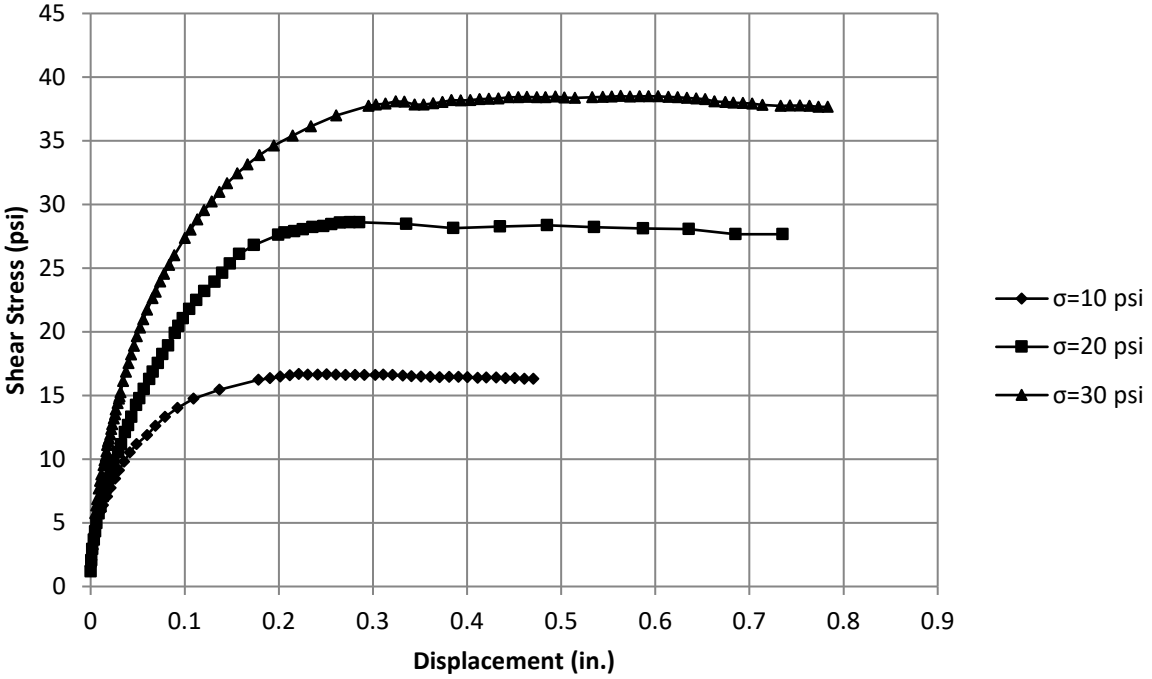

Figure 22. Shear stress and displacement curves

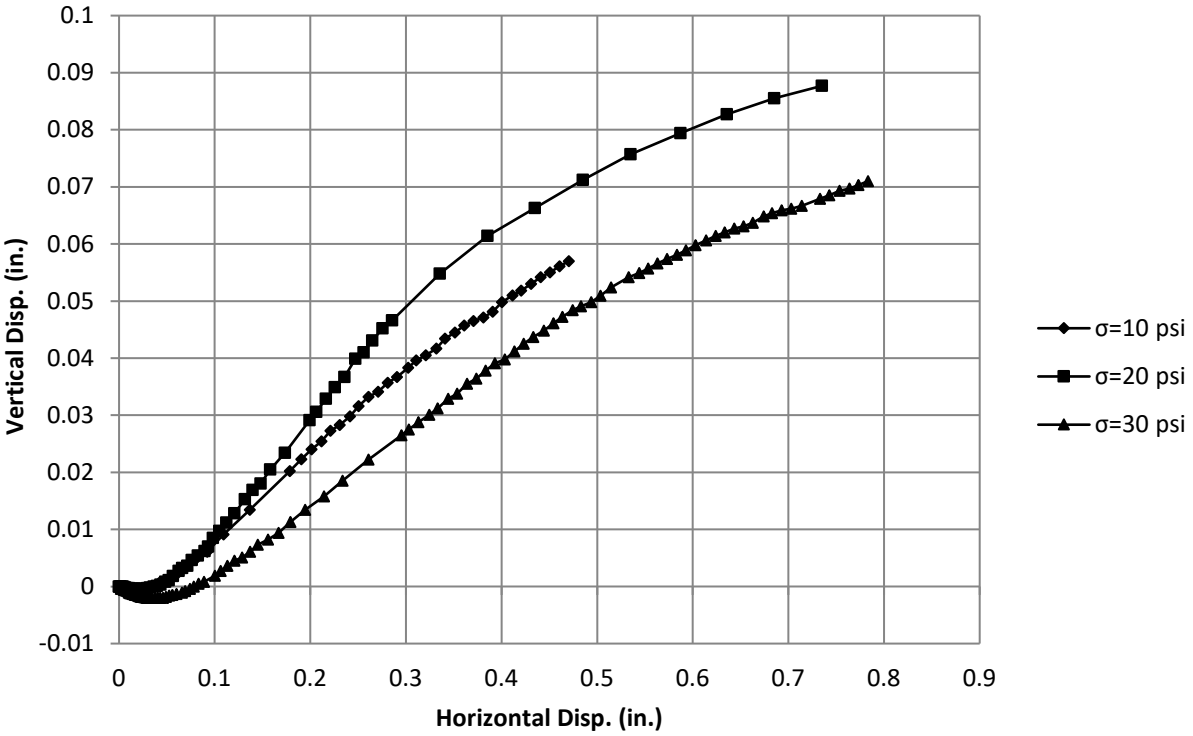

Figure 23. Vertical displacement and horizontal displacement curves

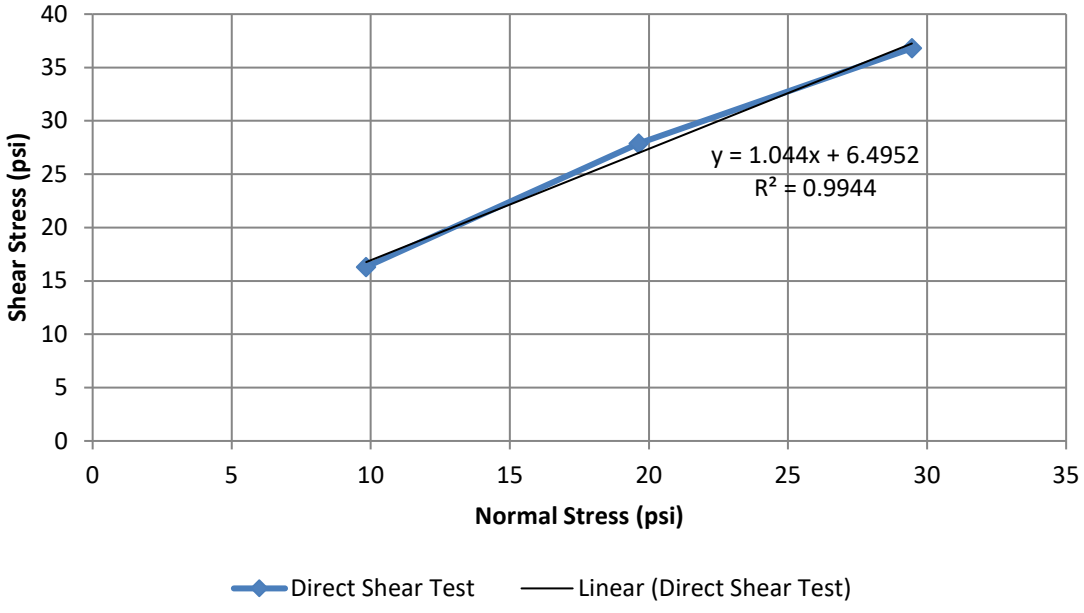

Figure 24. Determination of shear strengths

Using Mohr-Coulomb criterion, $\tau = \sigma \tan\varphi + c$, friction angle and cohesion from these tests are calculated as shown in Fig. 24. Dilatancy angle is calculated by $\tan\psi = \Delta u_y / \Delta u_x$ where Δu_y is vertical displacement increment and Δu_x horizontal displacement increment. Soil strength properties are shown in Table 5.

Table 5. Friction angle and cohesion from direct shear tests

Properties	Units	Value
Friction angle, ϕ	(^{0})	45
Cohesion, c	(psi)	6.49

3.3.4 The interface between Soil and Geosynthetic

The direct shear device was also used to determine friction angle and cohesion of interface between soil and geosynthetic. Figure 25 shows the failure line between soil and geosynthetic after a test. Test results are shown in Figs. 26 to Fig. 28.

Figure 25. Backfill with geosynthetic inclusion after shearing

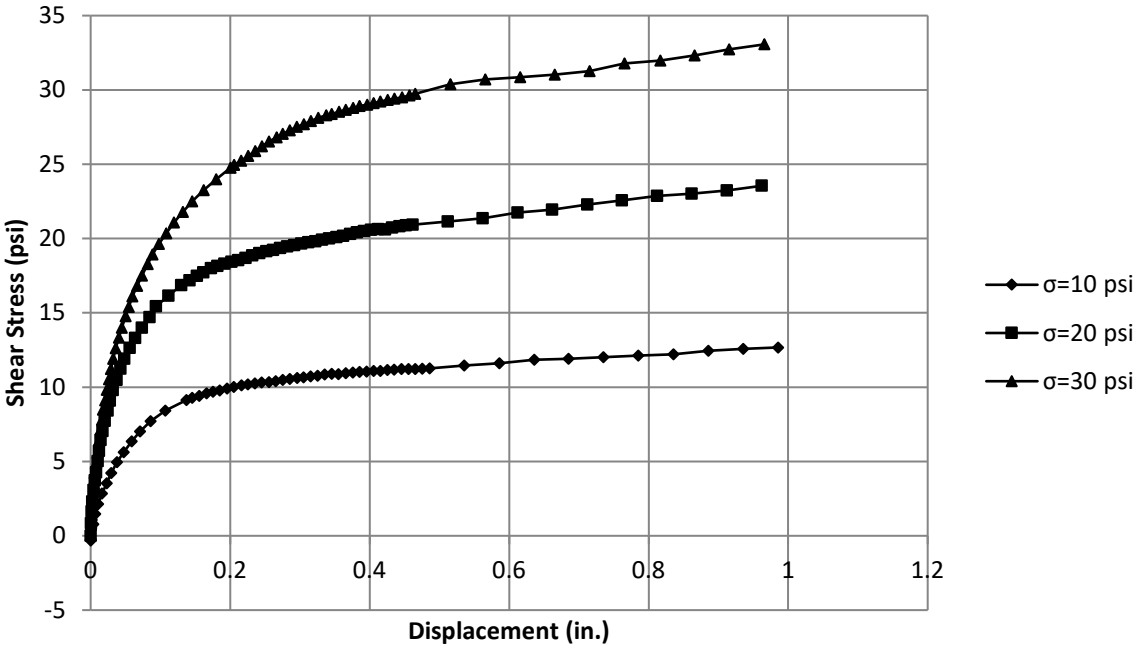

Figure 26. Shear stress and displacement curves for the backfill

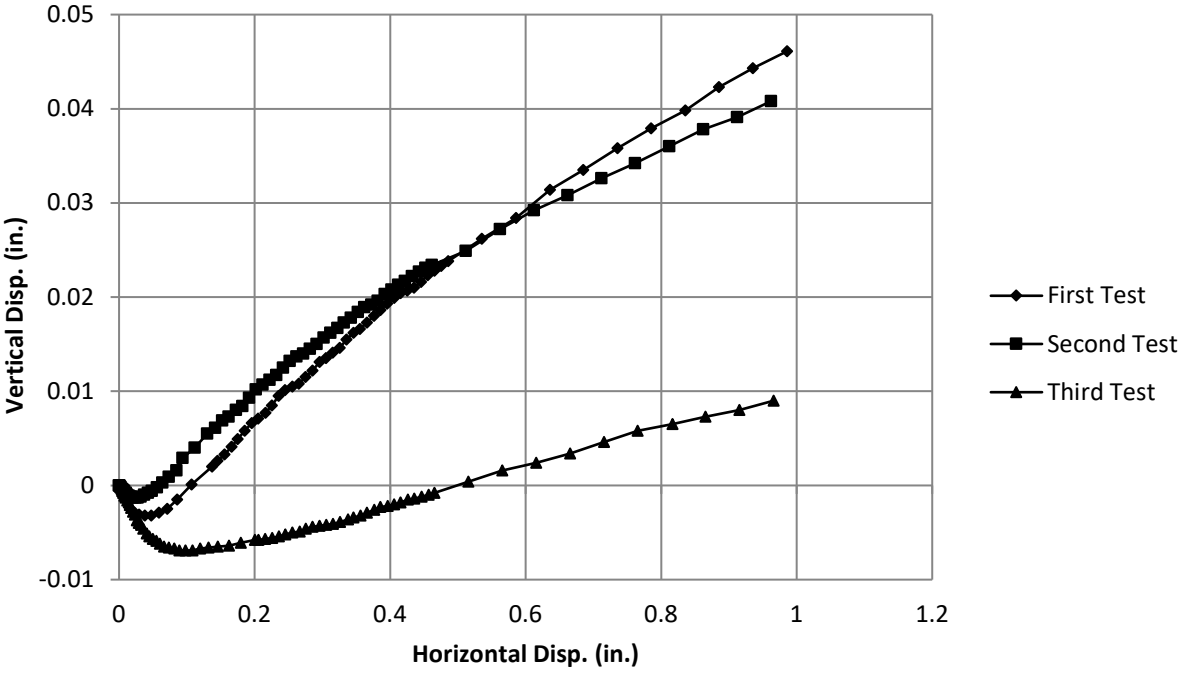

Figure 27. Vertical displacement and horizontal displacement curves

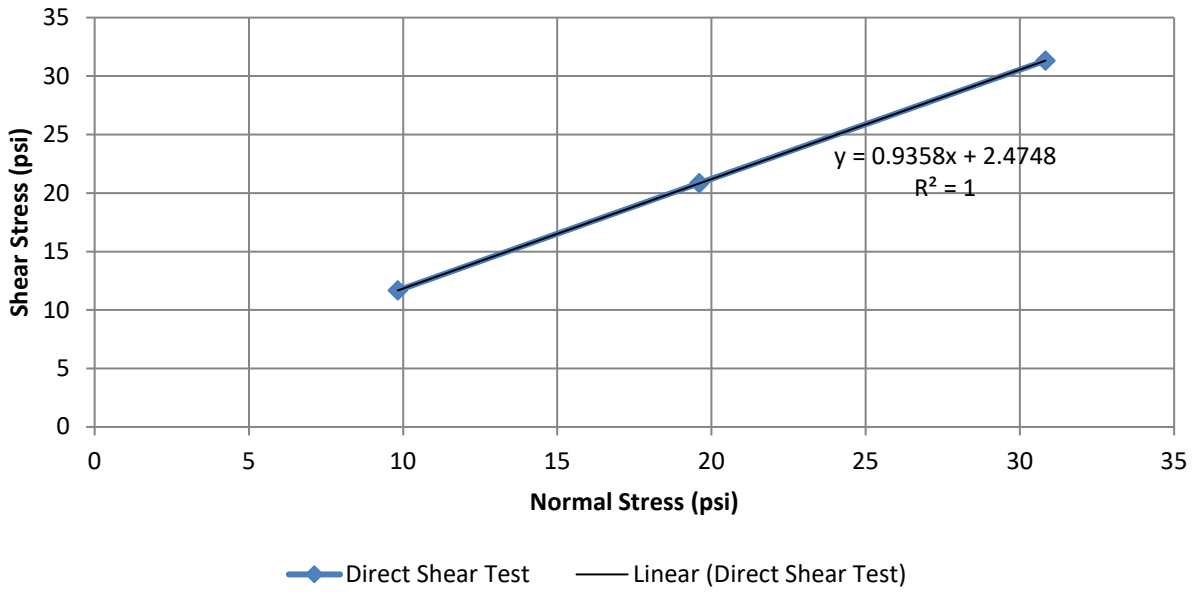

Figure 28. Interface shear strengths

Using the same method for soil, friction angle, and cohesion are computed from these tests for the interface as shown in Fig. 28 and also shown in Table 6 as below:

Table 6. Friction angle and cohesion of soil and geosynthetic interface from direct shear tests

Properties	Units	Value
Friction angle, ϕ	(^{0})	43
Cohesion, c	(psi)	2.47

As can be seen, the frictional angle and cohesion of soil and soil-geosynthetic differ insignificantly.

3.4 Index Property Tests and Density-Moisture Relationship

Index properties and density-moisture relation of the backfill were also evaluated via corresponding tests and their results are:

1) **S**pecific gravity test gave the specific gravity value of 2.80,
2) Gradation analysis gave the following results: D_{60} = 3.64 mm, D_{30} = 1.05mm, D_{10} = 0.16 mm, Cu = 22.75 and Cc = 1.86.
3) Both Standard Proctor Compaction and Modified Proctor Compaction tests were performed and their results are:

a. Standard Proctor Compaction Test: maximum dry density, γ_{dmax} = 131.5 pcf and Optimum moisture content, ω_{opt} = 10%

b. Modified Proctor Compaction Test: maximum dry density, γ_{dmax} = 142 pcf and optimum moisture content, ω_{opt} = 6.5%

Details of the above tests are given in Appendix A.

3.5 Base foundation soil

The clay soil was compacted in the T-Cage used as the soil at the base of GRS wall. The clayey soil was tested by using UU triaxial tests. Test results are shown in Fig. 29 and Table 7.

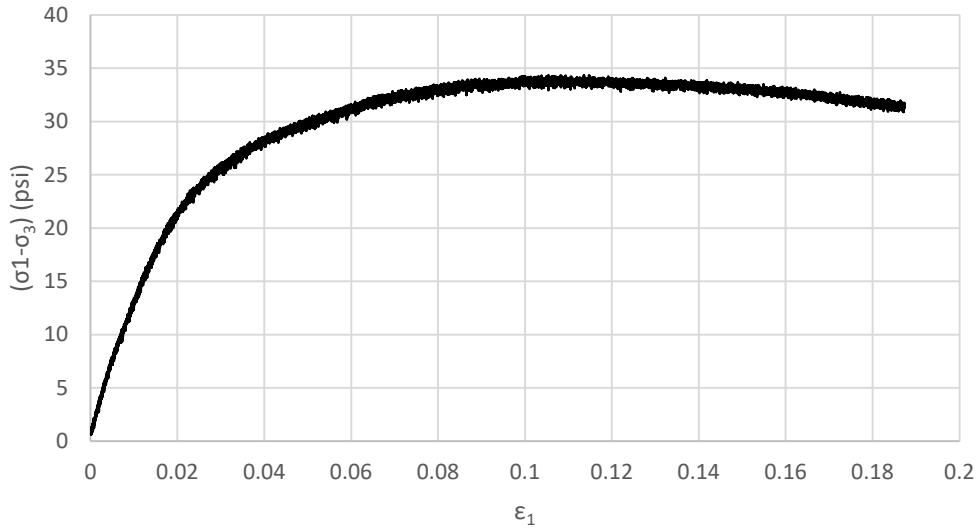

Figure 29. Stress-strain curve of the base foundation soil

Table 7. Properties of the base foundation soil

Properties	Units	Value
Young's Modulus	(psi)	4124
Undrained shear strength	(psi)	17
Poisson's Ratio	-	0.495

4. MODEL TEST

4.1 Tiger cage

A stiff steel cage, Tiger Cage (Volmer, et.al., 2017), was designed and fabricated by a team of ten persons over one and a half years. The dimensions for the T-cage are 22.5 in. inside width x 6' in height x 12' in length. It was equipped with a stiff wall constructed of ¼" x 8" x 8" and ¼" x 4" x

8” rectangular steel pipes rotating about its lower end. The rotation is designed to induce active, at rest and passive earth pressures to fulfill the goal of earth pressure evaluation with GRS/MSE backfill. Each construction can be used for wall pressure measurement during compaction and testing and also for establishing the load-settlement curve of GRS block facing wall. Airbag also can be used to apply a uniform load as surcharge to the top of the GRS wall. The maximum pressure can apply to the GRS wall by using Airbag is 14 psi which is higher than the required uniform pressure of 2 psi.

4.2 Truncated base GRS Wall model tests in Tiger-Cage

Three truncated base GRS Wall model tests were performed in Tiger-Cage at the Geotechnical-Structural Laboratory at the University of Colorado Denver. The first wall is 45^0 of back slope (Wall No.1), the second wall is 60^0 of back slope (Wall No.2), and the third wall is 53^0 of back slope (Wall No.3). All walls are constructed to a height of 52.5 inches with base widths of 24 inches. All test walls have 7 layers of concrete block façade, 11 geosynthetic layers for Wall No. 1 and No. 2 and 13 geosynthetic layers for Wall No. 3. Modular blocks are used for vertical block façade, shown in Fig. 30. The cross-sectional areas of the block facing walls are Type 1 of 53.75 in^2, Type 2 of 30.625 in^2. Geosynthetic spacing is 4 inches for the top 10 layers and 8 inches for two bottom layers for Wall No. 1 and 2, and 4 inches for all layers for Wall No. 3. The gap between the near-wall tip of geosynthetics and wall façade is 3 inches. Lengths of the geosynthetics vary with depth and slope angles. Rubber membranes are attached to both side walls of the Tiger-Cage to reduce friction between soil and side walls. Geometries of all wall are shown in Figs. 31, 32 and 33.

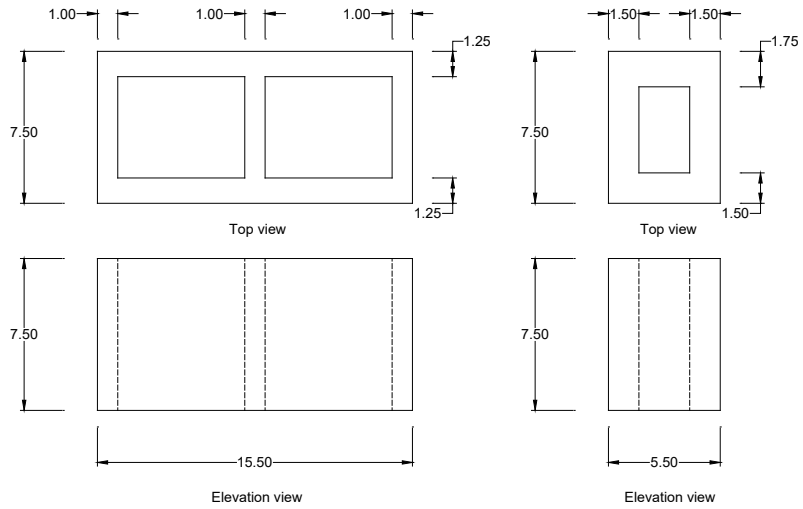

a) Type 1 a) Type 2

Figure 30. Modular block for facing wall (unit in inches.)

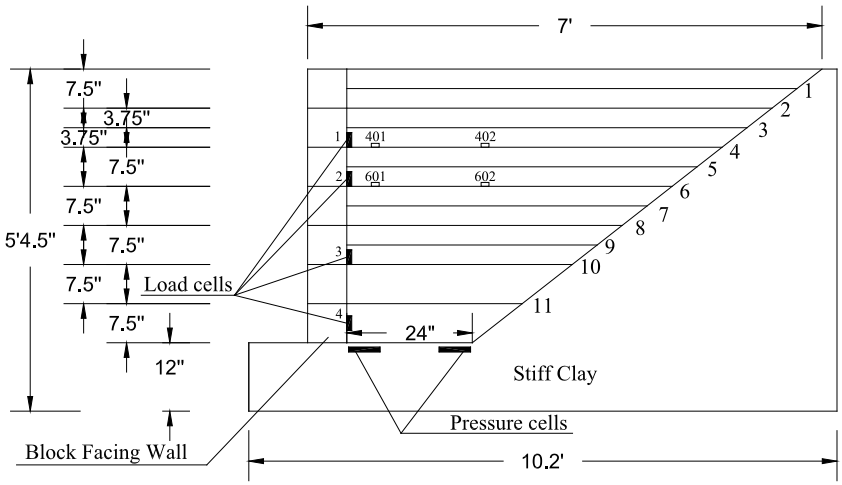

Figure 31. No. 1 GRS Wall (45^0)

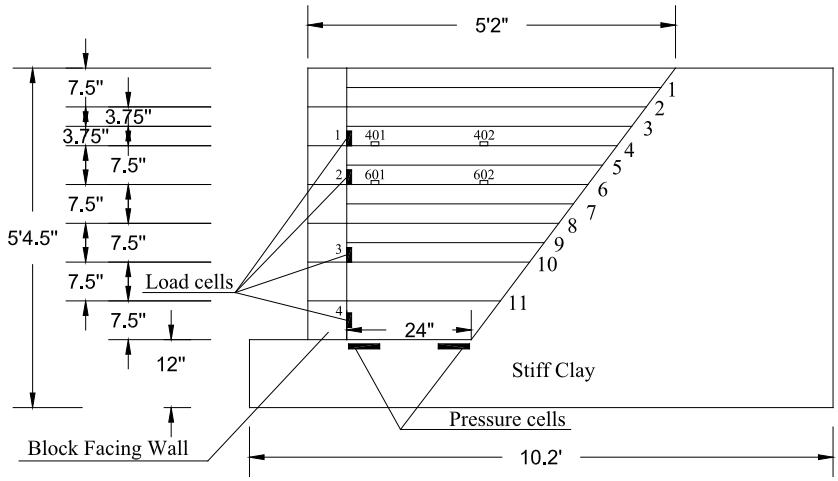

Figure 32. No. 2 GRS Wall (60^0)

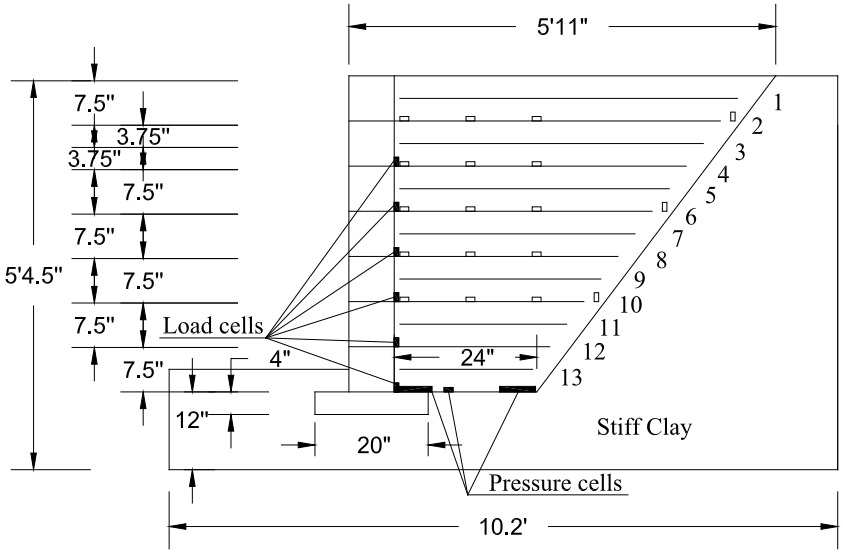

Figure 33. No. 3 GRS Wall (53^0)

4.3 Instrumentation

The experimental program consisted of instrumentation of the three truncated-base GRS walls. In order to monitor and evaluate wall performance, various types of the instrument were installed in the GRS wall to record the measurements of interest, primarily vertical pressures along the base, lateral pressures and the lateral deformation along the back of block facing wall, and distribution of strains along the geosynthetics. Two earth pressure cells with semiconductor transducer were used to monitor vertical pressures at the base of the excavation, one measures pressure near the block facing wall and another measures pressure near the back slope. Four load cells were installed along the block facing wall to measure the lateral pressures. Three displacement censors (LVDT) were installed horizontally to monitor the lateral displacements of the block facing wall. Four electrical resistant-type/foil-type strain gauges were installed on the geosynthetics to measure the strains developed along the geosynthetics. The strain gauges were protected by styrofoam to prevent punching from sharp particles of soil as shown in Fig. 34. Locations of all instruments are shown in Figs. 31 to 33.

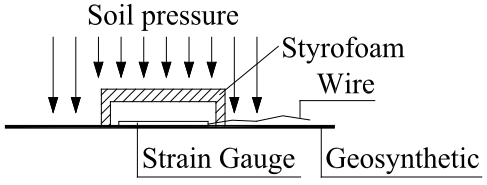

Figure 34. Strain gauge with protection

Figures 35 to 38 present calibration curves for load cells used to monitor the lateral pressures along the block facing wall numbered sequentially from the top to the bottom. Figure 39 shows the equation to calibrate the pressure transducer, which is used to monitor a vertically applied load on the surface.

Calibration equations for the earth pressure cells provided by the manufacturer are given as follows:

Calibration equation for vertical pressure cell No. 2397 is:

$$p = 62.805A - 254.879 \text{ (kPa)}$$

Or

$$p = 9.109A - 36.967 \text{ (psi)}$$

Calibration equation for vertical pressure cell No. 2398 is:

$$p = 62.742A - 256.45 \text{ (kPa)}$$

Or

$$p = 9.1A - 37.195 \text{ (psi)}$$

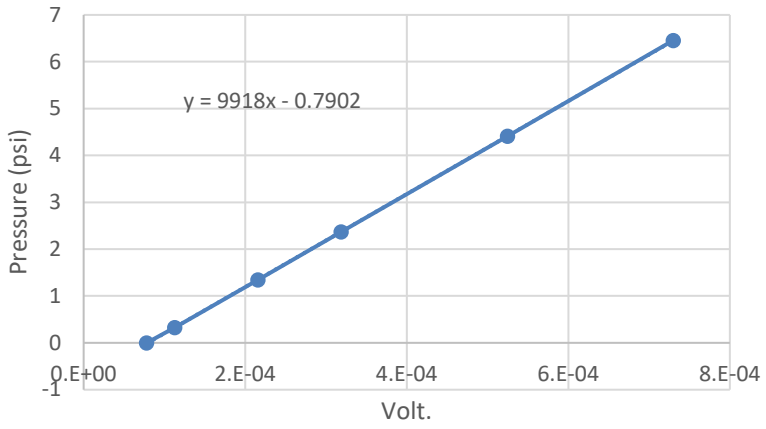

Figure 35. Calibration curve for Load Cell No.1

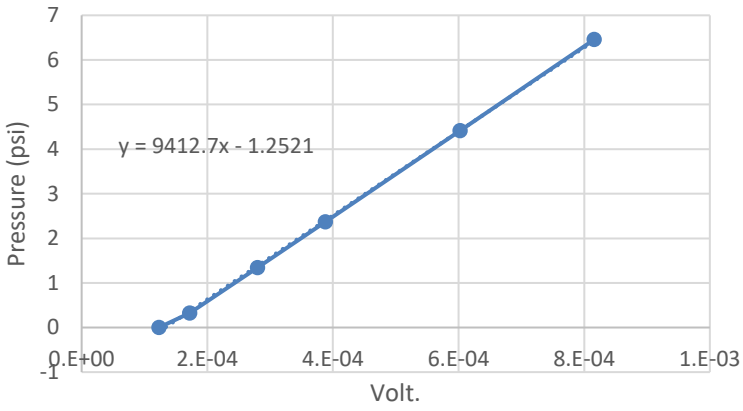

Figure 36. Calibration curve for Load Cell No.2

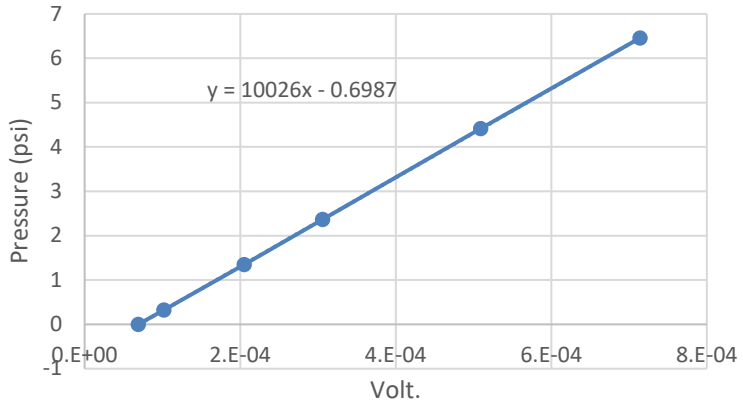

Figure 37. Calibration curve for Load Cell No.3

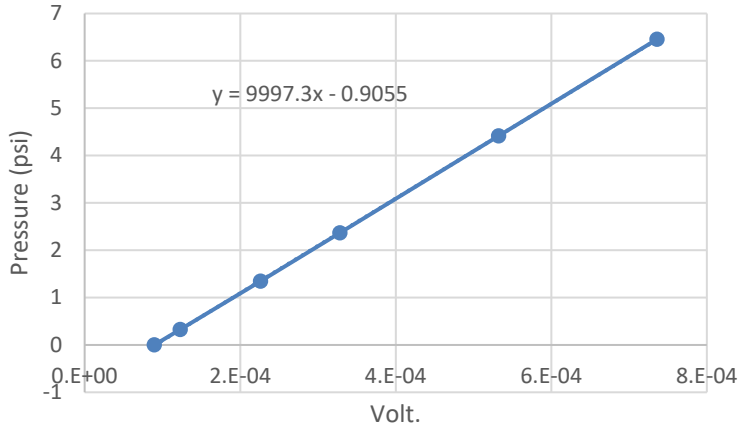

Figure 38. Calibration curve for Load Cell No.4

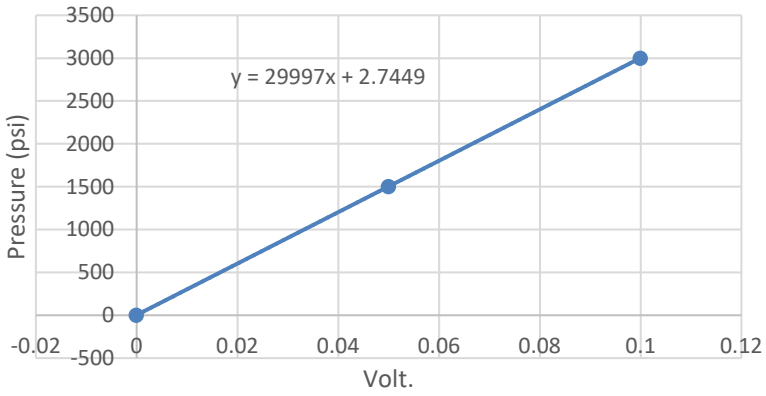

Figure 39. Calibration curve for Pressure Transducer

4.4 Construction procedure

A clayey soil was compacted in Tiger Cage at a maximum dry density of Proctor compaction or density required to provide strength equivalent to that of clay shale. The compacted clay was then excavated to reach a designed excavation slope of GRS wall with, 45°, 60°, or 53° of back slopes to the horizontal plane. The backfill was compacted layer by layer to reach a geosynthetic reinforcing spacing of 3.75 inches. The backfill is compacted to reach a maximum dry density determined in Modified Proctor compaction tests.

The construction procedure was performed as follows (Figs. 40 to 42):

1) Install vertical pressure cells at the wall base and the first facing block.
2) Fill and compact one layer of the Colorado Class I backfill.
3) Install geosynthetic and load cell

4) Repeat step 2 to step 3 until reaching the final layer.

Figure 40. Install vertical pressure cells at the wall base

Figure 41. Compacting Backfill soil layer by layer

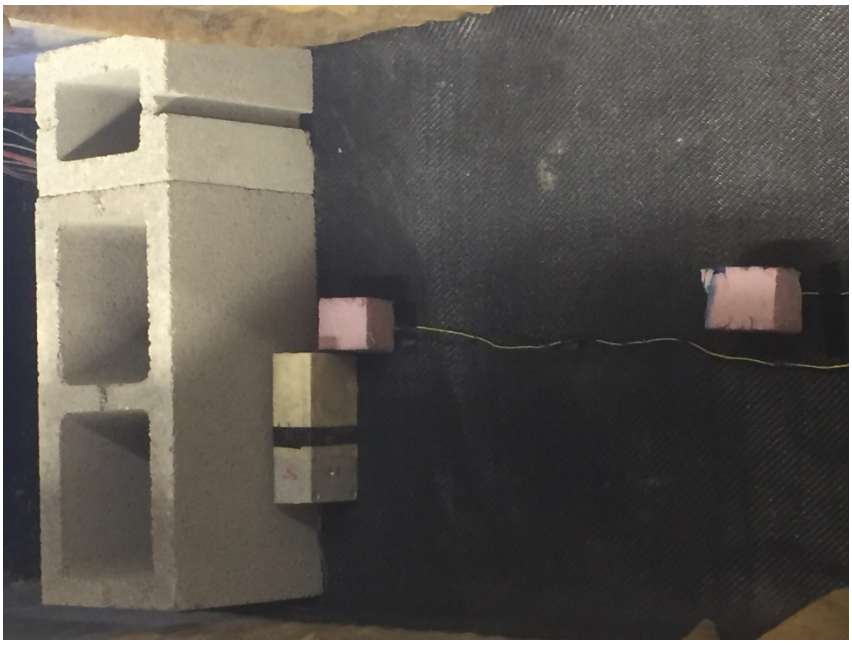

Figure 42. Install strain gauges and load cells

When the construction of the wall is finished, loading plate, load frame, airbags, and instrumentations are also installed (Figs. 43 and 44), and the test specimen is ready.

Figure 43. Install the loading plate, vertical displacement sensors, and airbag

Figure 44. Install airbags

4.5 Test results

4.5.1 Base pressure from soil weight

Base pressure initially caused by compacted soil weight. The base pressure was recorded during the construction and compared to the hand calculated values using the maximum soil density at the end of construction of each layer, as shown in Figs. 45.

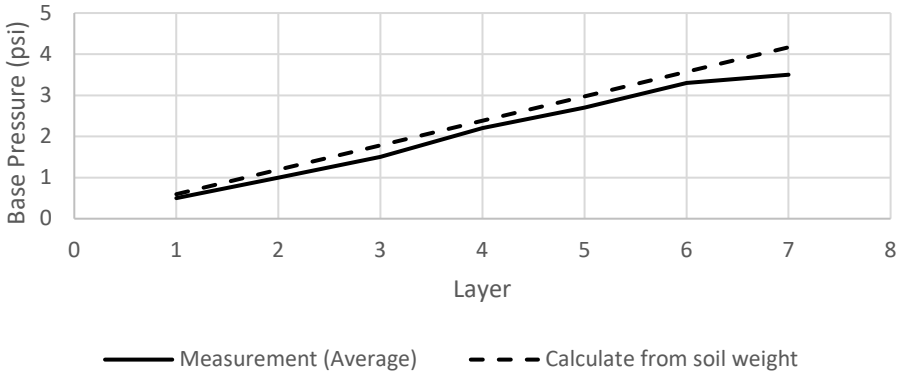

a) 45^0

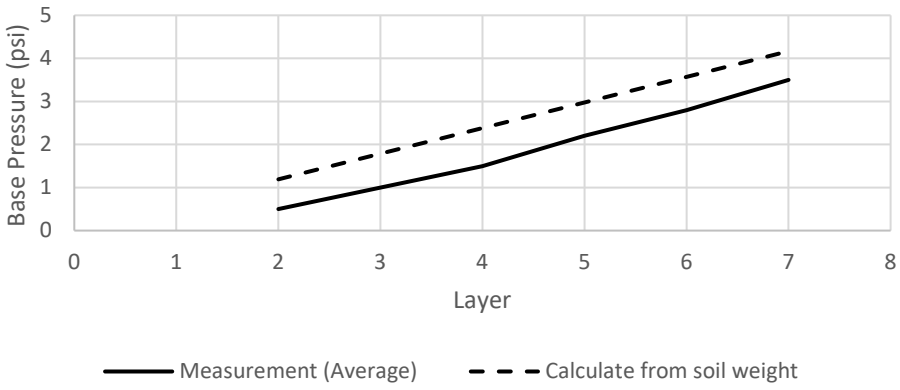

b) 60^0

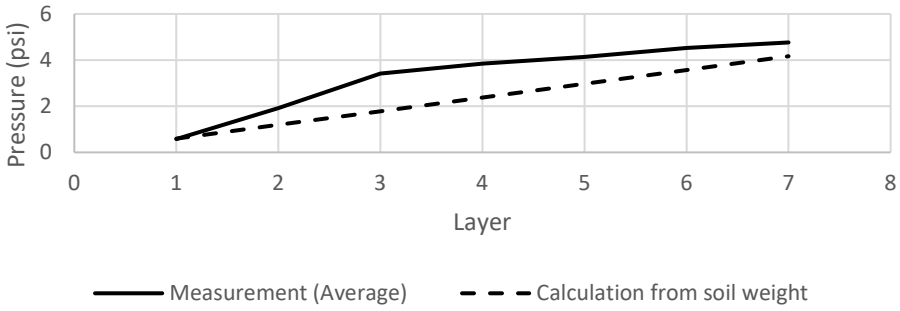

c) 53^0

Figure 45. Base pressure under backfill soil weight

4.5.2 Base pressure from the surcharge

Surcharge load of 14 psi is applied on the surface of the truncated GRS wall to evaluate the base pressure.

Pressures at the base

Figures 46a, b, and c show that the vertical base pressures measured by two pressure cells increase with the increase in surcharge pressure. For both No. 1 and No.2 walls, Fig.46.a, and, Fig.46.b, under 14 psi surcharge, the measured maximum base pressures are higher at the front pressure cell than the back pressure cell. At No. 3 Wall, Fig. 46.c, the pressures at the front and the back are almost the same and the middle pressure is higher.

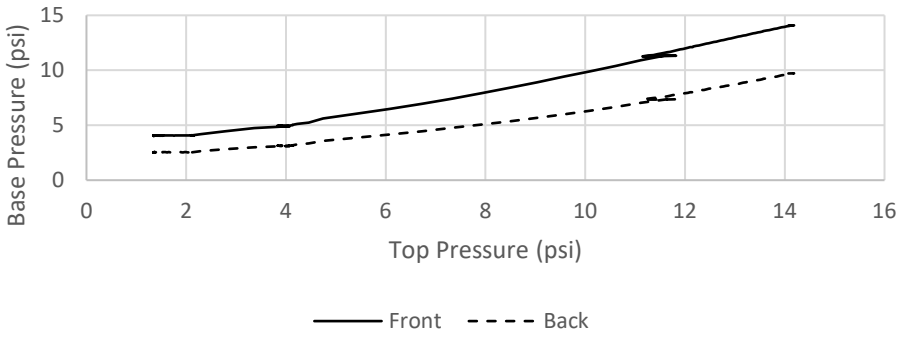

a) 45^0

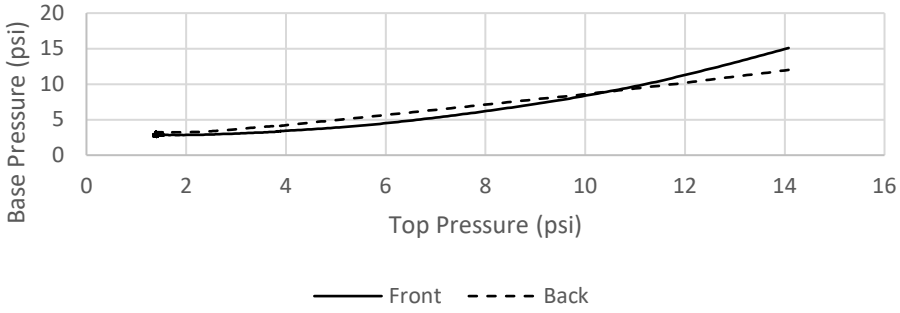

b) 60^0

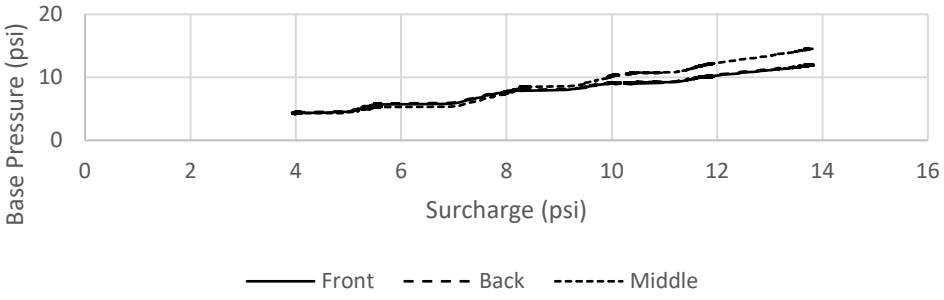

c) 53^0

Figure 46. The top-base pressure curves

5. FINITE ELEMENT ANALYSES

5.1 Finite element program

5.1.1 Introduction

To investigate the truncated base wall performance requires an effective comprehensive numerical analysis program to simulate and check the measured performance as a cross-check effort to assure accurate computation and measurement. A general-purpose computer software, SSI2D, was selected to serve the purpose. SSI2D was developed by Dr. Hien Nghiem at CGES at the University of Colorado Denver, and enhanced after rejoining the Hanoi Architectural University. The analysis

results were calibrated against the results of the Truncated Base MSE Wall tests. The comparison gives excellent agreement, and SSI2D is deemed effective for further used in other CDOT-FHWA sponsored projects.

5.1.2 Soil model

Triaxial and direct shear test results show that this backfill material is highly dilative, and the geologic cap model may not be the most suitable soil model for simulating its dilative behavior, and the modified hyperbolic model is adopted, instead. The Duncan and Chang model (Duncan and Chang, 1970) represents the nonlinear stress-strain curve of soils as a hyperbola in the shear stress, $\sigma_1 - \sigma_3$, versus axial strain space, as shown in Fig. 47, and written in written in the following equation:

$$\left(\sigma_1 - \sigma_3\right) = \frac{\varepsilon_1}{a + b\varepsilon_1} \tag{8}$$

where a and b are related to the initial tangent modulus and asymptotic deviator stress:

$$E_i = \frac{1}{a};\ \left(\sigma_1 - \sigma_3\right)_{ult} = \frac{1}{b} \tag{9}$$

where E_i is initial tangent modulus as a function of confining stress, σ_3.

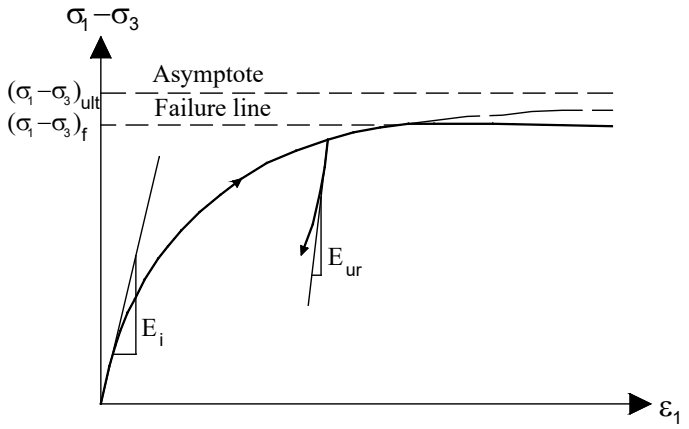

Figure 47. Nonlinear stress-strain behavior

The ultimate shear stress, $\left(\sigma_1 - \sigma_3\right)_{ult}$ related to shear stress at the failure of Mohr-Coulomb criterion by model parameter, R_f. The following equation determines the value of failure ratio for each of the tests:

$$R_f = \frac{(\sigma_1 - \sigma_3)_f}{(\sigma_1 - \sigma_3)_{ult}} \tag{10}$$

where $(\sigma_1 - \sigma_3)_f$ is deviator stress at failure determined from the stress-strain plots of the tests. Typical values R_f range from 0.5 to 0.9 for most soil (Duncan et al., 1980). The modified hyperbolic model adopted the Mohr-Coulomb failure surface. The failure occurs when the state of shear stress, τ, and the normal stress, σ, on any surface in the material, satisfy the equation below:

$$|\tau| + \sigma \tan\varphi - c = 0 \tag{11}$$

where φ and c denote the friction angle and cohesion of soils.

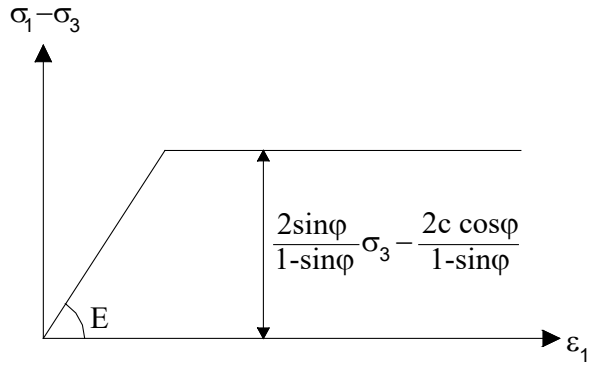

Figure 48. Mohr-Coulomb failure criteria

The Mohr-Coulomb criterion, as shown in Fig. 48 can be written in terms of principal stresses as follow:

$$-\frac{1}{2}(\sigma_1 - \sigma_3) = -\frac{1}{2}(\sigma_1 + \sigma_3)\sin\varphi + c\cos\varphi \tag{12}$$

The full Mohr-Coulomb yield criterion takes the form of a hexagonal cone in principal stress space, as shown in Fig 49. Main stress can be related to invariant stresses as:

$$(\sigma_1 - \sigma_3) = \frac{2}{\sqrt{3}}\sqrt{J_2}\left(\sin\left(\theta - \frac{2\pi}{3}\right) - \sin\left(\theta + \frac{2\pi}{3}\right)\right) = -2\sqrt{J_2}\cos\theta \tag{13}$$

$$(\sigma_1 + \sigma_3) = \frac{2}{\sqrt{3}}\sqrt{J_2}\left(\sin\left(\theta - \frac{2\pi}{3}\right) + \sin\left(\theta + \frac{2\pi}{3}\right)\right) + \frac{I_1}{3} = -\frac{2}{\sqrt{3}}\sqrt{J_2}\sin\theta + \frac{2I_1}{3} \tag{14}$$

Substitute Eqs. (13) and (14) to Eq. (12), and failure criterion can be written in invariants shown as following (Smith and Griffiths, 1997):

$$f_1 = \frac{I_1}{3}\sin\varphi - \sqrt{\frac{J_2}{3}}\sin\theta\sin\varphi + \sqrt{J_2}\cos\theta - c\cos\varphi \qquad (15)$$

where θ is Lode angle.

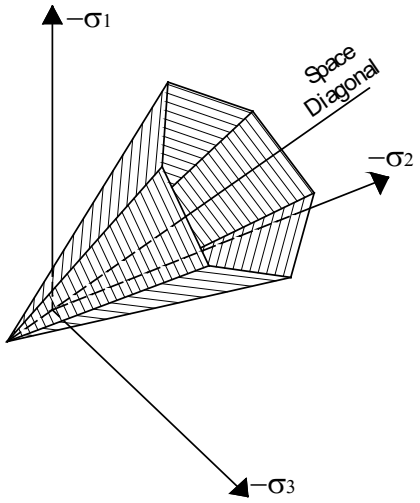

Figure 49. Mohr-Coulomb failure criteria in principal stress space

In this plastic behavior of soil, an associated flow rule is followed, and the potential function has the same form as the associated yield function and is defined for the Mohr-Coulomb model by replacing friction angle, φ, by dilation angle, ψ, in the yield function. The plastic potential function is given by:

$$g_1 = \frac{I_1}{3}\sin\psi - \sqrt{\frac{J_2}{3}}\sin\theta\sin\psi + \sqrt{J_2}\cos\theta - c\cos\psi \qquad (16)$$

The dilation angle, ψ, is required to model positive plastic volumetric strain increments as actually observed for dense soils. Soil starts to dilate when the stress state reaches the Mohr-Coulomb failure surface.

In reality, soil can sustain none or small tensile stress. This behavior can be specified as a tension cut-off. The functions of tension cut-off (which is related to maximum principal stress) are:

$$f_2 = \sigma_3 - T \qquad (17)$$

where T is maximum tensile stress. For these three yield functions, an associated flow rule is adopted.

Yield and cap surfaces for a modified hyperbolic model are shown in Fig. 50, and Fig. 51. Parameters for this model are shown in Table 8.

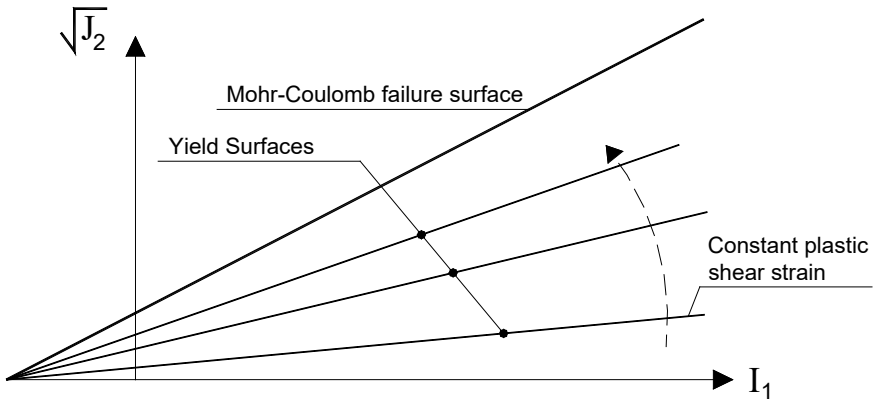

Figure 50. Yield surface of the modified hyperbolic model

The plastic volumetric strain measured in the hydrostatic compression test is not explained in shear hardening yield surfaces, as in Fig. 50. It requires a second yield surface, cap yield surface, to explain the contractive soil behavior. This cap yield surface is defined as:

$$f_c = J_2\left(\cos\theta - \sqrt{\frac{1}{3}}\sin\theta\sin\varphi\right)^2 + \left(2\frac{I_1}{3} - c\cot\varphi - \frac{I_{1c}}{3}\right)^2 - \left(c\cos\varphi - \frac{I_{1c}}{3}\sin\varphi\right)^2 \qquad (18)$$

The hardening law relating I_{1c} to plastic volumetric strain is:

$$d\varepsilon_v^p = \kappa\frac{dI_{1c}}{I_{1c}} \text{ or } \varepsilon_v^p = \kappa\ln\left(\frac{I_{1c}}{3}\right) \qquad (19)$$

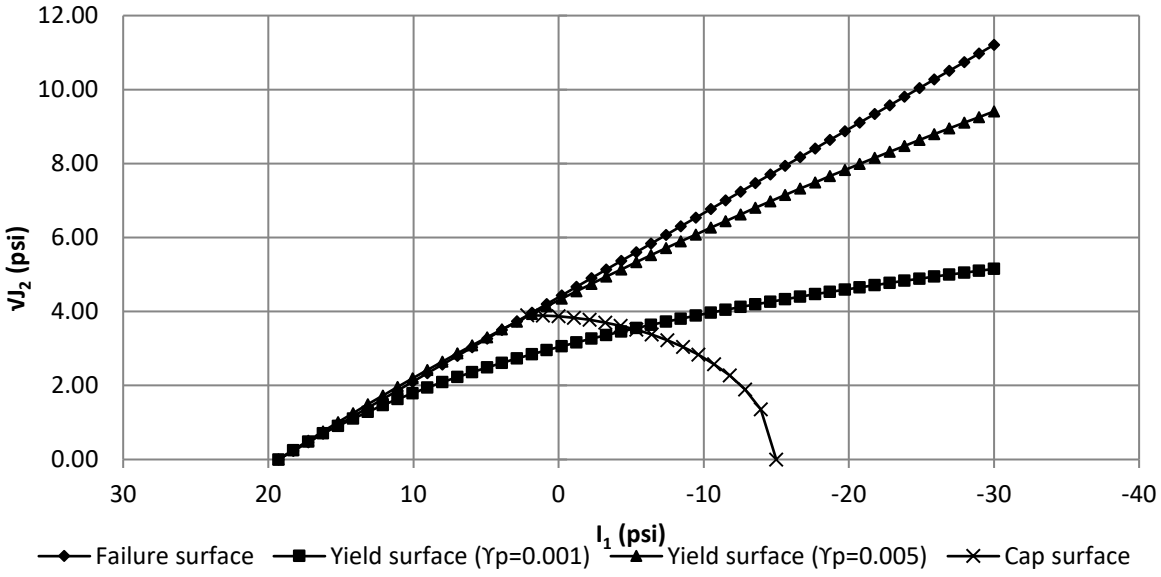

Figure 51. Yield, cap and failure surfaces

Table 8. Parameters of the modified hyperbolic model

Parameter	Description
K_L	Loading modulus number
K_{ur}	Unloading-reloading modulus number
n	Modulus exponent
R_f	Ratio between the asymptote to the hyperbolic curve and the maximum shear strength
c	Cohesion
φ	Friction angle
ψ	Dilatancy angle
OCR	Over-consolidation ratio
K	Cap surface parameter

5.1.3 Geosynthetic model

The geosynthetic reinforcement was modelled as a linear elastic perfectly-plastic material, in which three parameters are required (Fig. 52). The linear elastic perfectly-plastic model possesses a bilinear stress-strain curve. Note that the slope of tensile load-strain curve is the product of modulus (e.g., Young's modulus E or tangent modulus E_t) and thickness of the geosynthetic. The tensile load is typically expressed in units of force per unit width of the reinforcement. Inversely,

the modulus was calculated by dividing the slope of the tensile load-strain curve by the geosynthetic thickness. Similarly, the yield stress f_y for the bilinear model was found by dividing the yield tensile load by the thickness of geosynthetic.

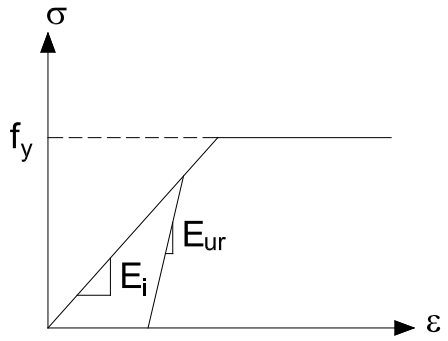

Figure 52. Stress-strain curve for geosynthetic

5.1.4 Interface model

The interfaces between soil-geosynthetic, soil-block facing wall, geosynthetic-block facing wall, and backfill-foundation soil are modeled by interface elements. The Mohr-Coulomb model is used for failure criterion and characterized by friction angle φ, cohesion, c, and dilatancy angle ψ.

5.2 Materials and properties

Model parameters and SSI2D details Materials considered in this study include (1) geosynthetic reinforcement, (2) backfill, (3) base, and (4) block facing wall.

In the FE model, the parameters for all interfaces between soil and geosynthetic are given in Table 6.

The model parameters for the geosynthetic reinforcement are presented in Table 2. A geosynthetic reinforcement manufactured by Tensar Corporation (i.e., US 4800) is used in the truncated base wall construction, which has a wide width tensile strength of 4353 lb/ft (or 65 kN/m). According to the assumed load-strain curve, the tensile strength of 4353 lb/ft would occur at a strain of 14%. The geosynthetic reinforcement mesh modeled with two-node tension bar elements. The thickness of geosynthetics was assumed as 0.06 in. or 1.5 mm. Material properties of the block facing wall are shown in Table 9.

Table 9. Properties of facing wall material

Parameter	Unit	Value
Young's Modulus	psi	4354136
Poisson's Ratio	-	0.2

5.3 Finite element model

Plane strain FE analysis was developed and verified using the results from the model tests of the fully-instrumented GRS walls. The SSI2D was selected for the numerical analysis of this study. In the FE model, the soil and the facing block were represented by a plane strain second-order, 6-noded triangle elements to describe the stress-deformation behavior. The geotextile was represented by a special tension 2-noded elements to describe the axial forces. The interface between the backfill soil and geosynthetic was simulated using interface elements to model the soil-structure interface behavior, which is represented by 6-joint element (also compatible with the soil element) to simulate the thin zone of intensely shearing at the contact between the geotextile and the surrounding soil.

Three FE models and meshes of GRS wall are shown in Figs. 53 and 54. Stage constructions are also modeled to take into account the effect of construction sequences. Deformation shapes for all walls are shown in Fig. 55. Figure 56 shows the comparison between FEA and test results for the base pressures during construction. For the second and third layer (16" to 24" thick), the base pressures from measurement increase faster than those from FEA and in good agreement at the final layer (No. 3 Wall). Similarly, Figure 57 shows the comparison between FEA and test results for the base pressures under surcharge of 14 psi. The comparisons for the base pressures at the end of the construction and under 14 psi surcharge are shown in Tables 10 and 11, respectively. the results of the base pressure calculated from finite element analysis and measurement are in good agreement.

Table 10. Average base pressure (psi) before applying vertical load

Wall	Test	Analysis
45^0	3.4	4.0
53^0	4.0	3.86
60^0	3.5	3.43

Table 11. Average base pressure (psi) at 14 psi surcharge

Wall	Test	Analysis
45^0	14.28	14.4
53^0	15.5	15.3
60^0	15.0	16.0

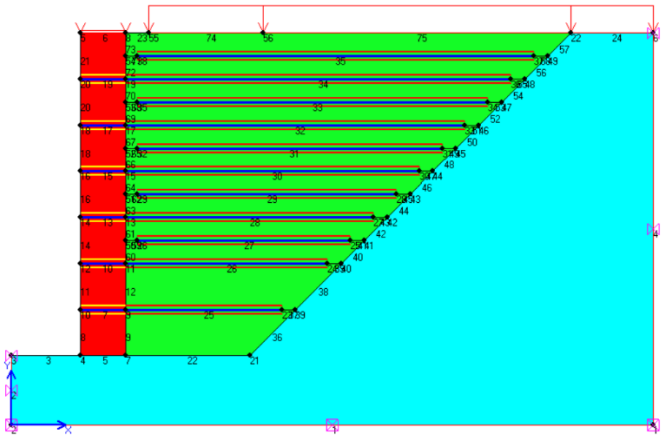

a) 45^0

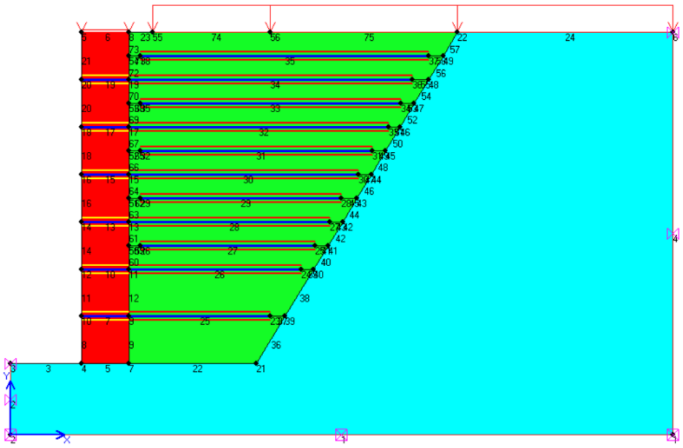

b) 60^0

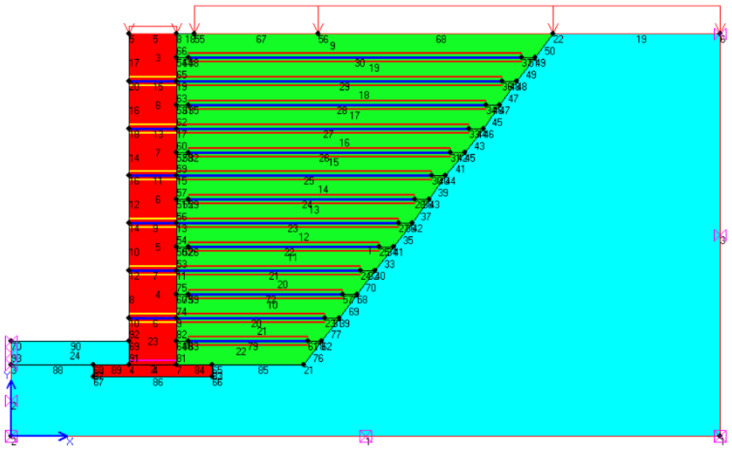

c) 53^0

Figure 53. Analysis models

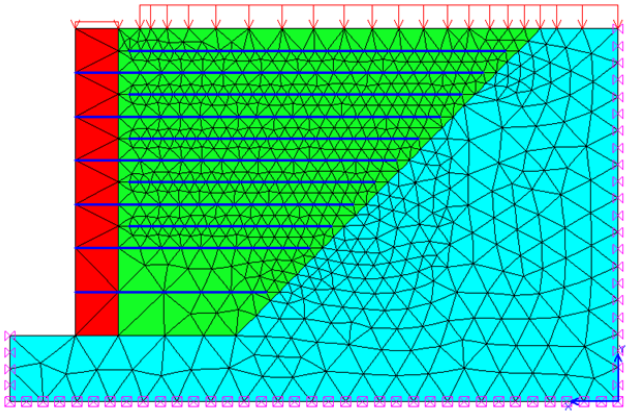

a) 45^0

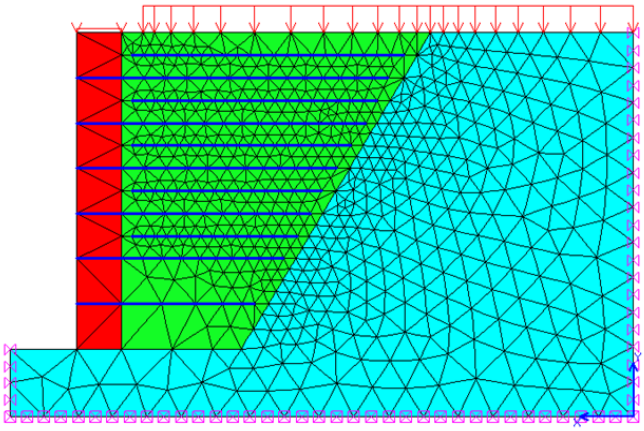

b) 60^0

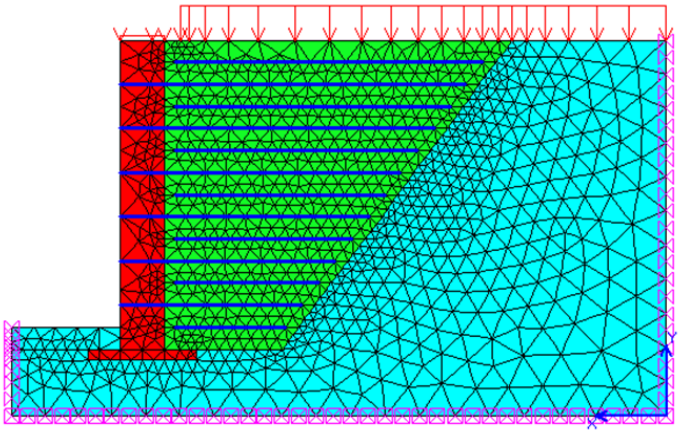

c) 53^0

Figure 54. Finite element mesh

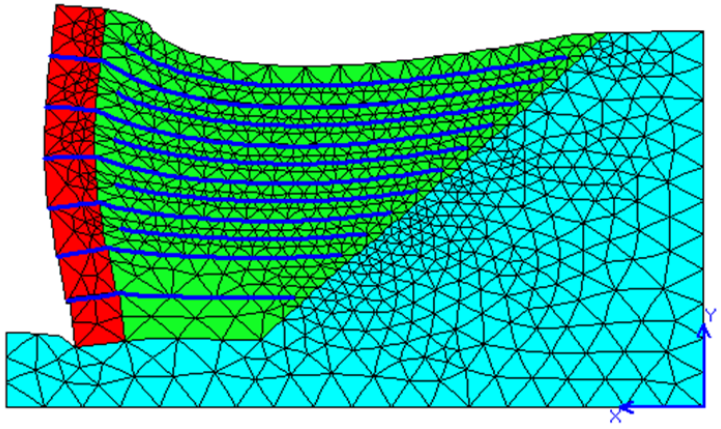

a) 45^0

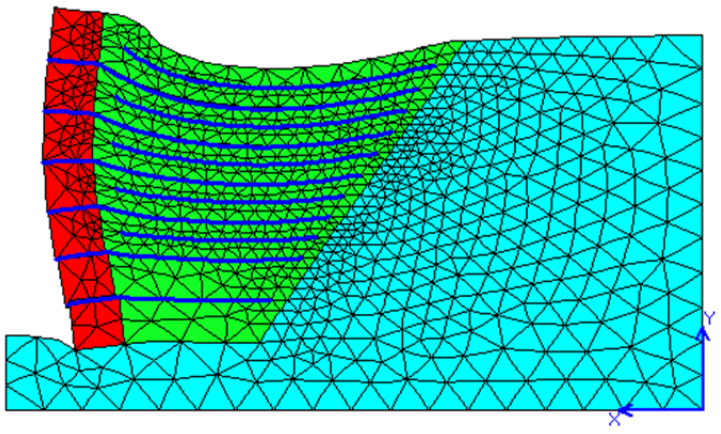

b) 60^0

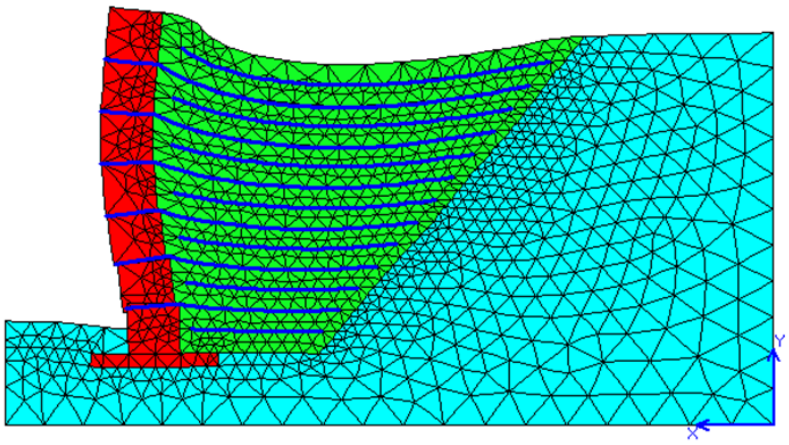

c) 53^0

Figure 55. Deformation under surcharge

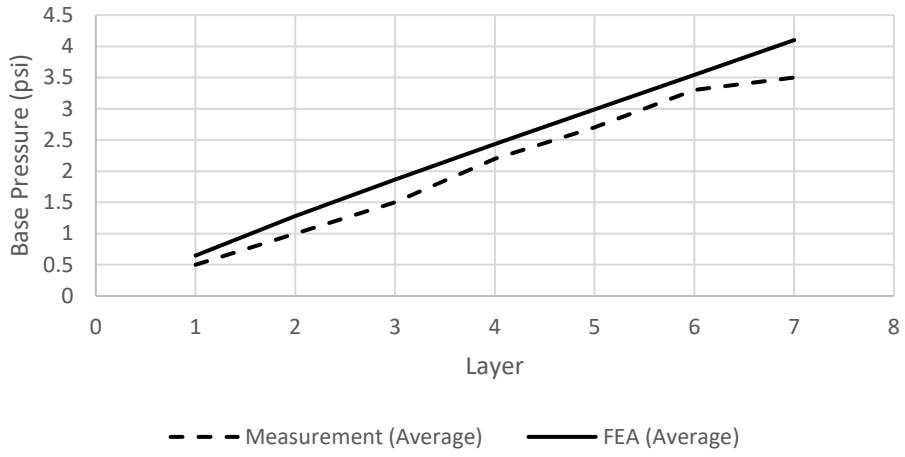

a) 45^0

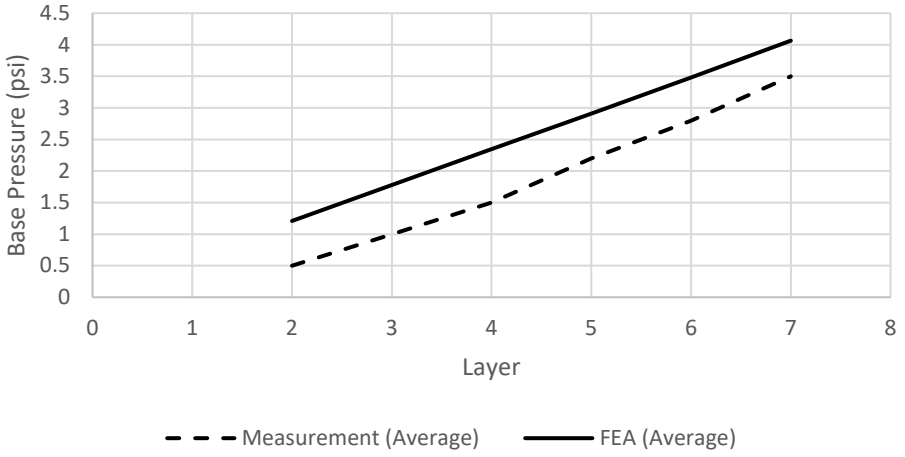

b) 60^0

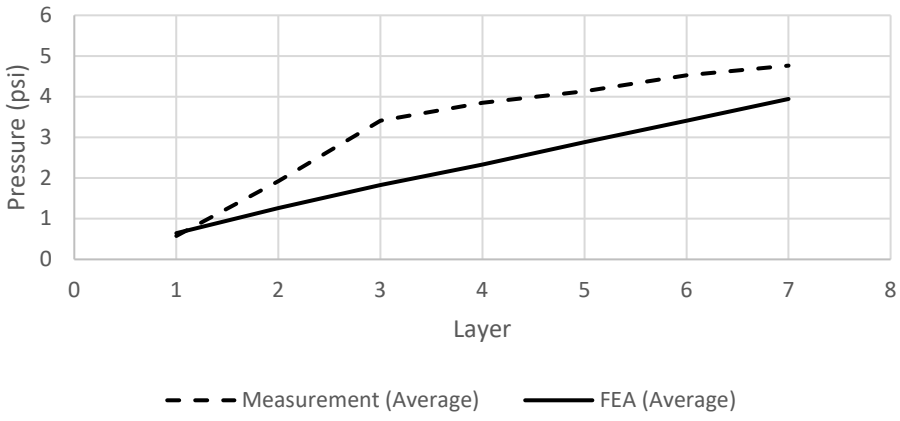

c) 53^0

Figure 56. Comparison of the base pressures during construction

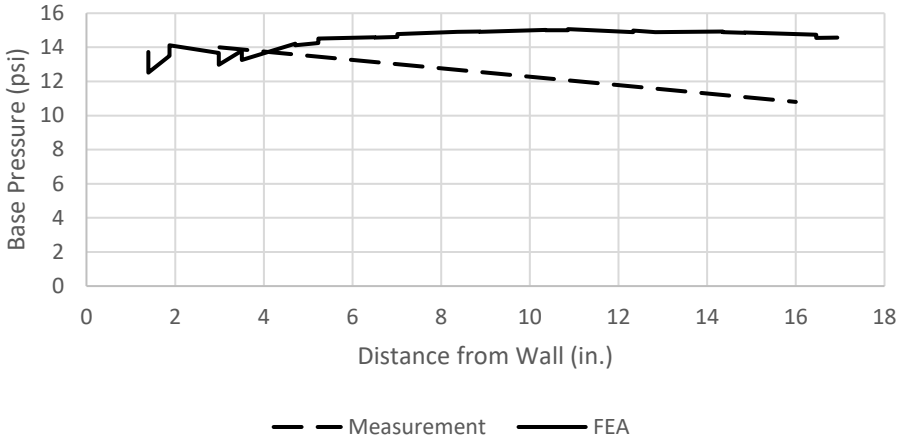

a) 45^0

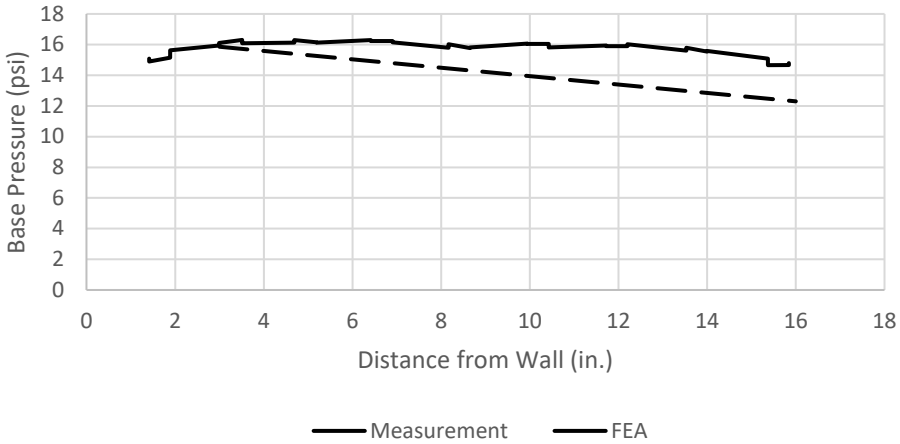

b) 60^0

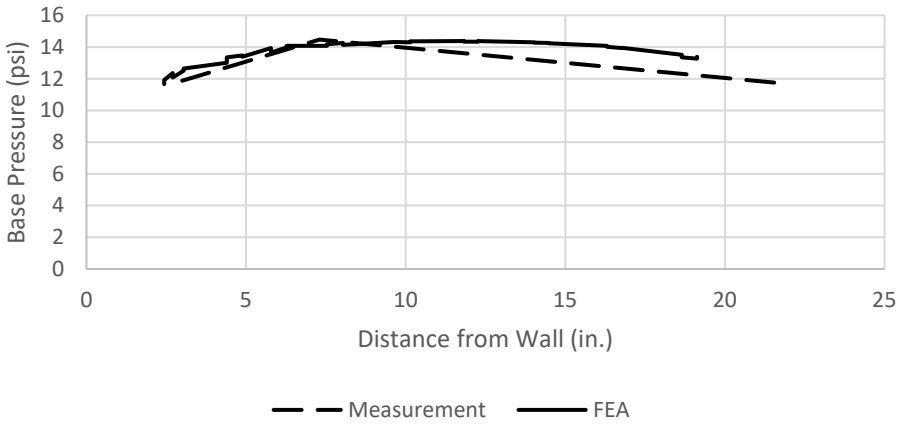

c) 53^0

Figure 57. Comparison of the base pressures at 14 psi surcharge

Pressure transfer

The test and FE analysis results showed that the base pressure is less than the summation of soil weight and the surcharge because loads transfer not only to the soil but also to the facing wall and the back slope. Pressure from surcharge transfers partly to the base of the wall.

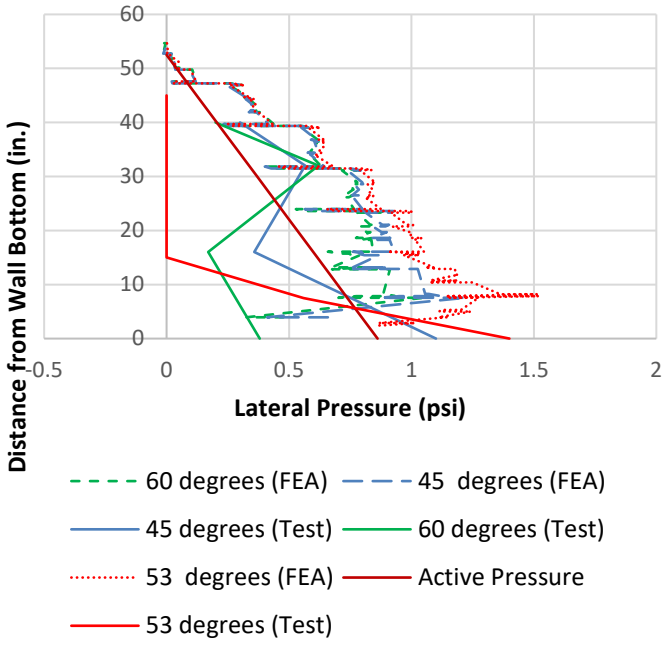

Figure 58. Lateral Pressures under Gravity

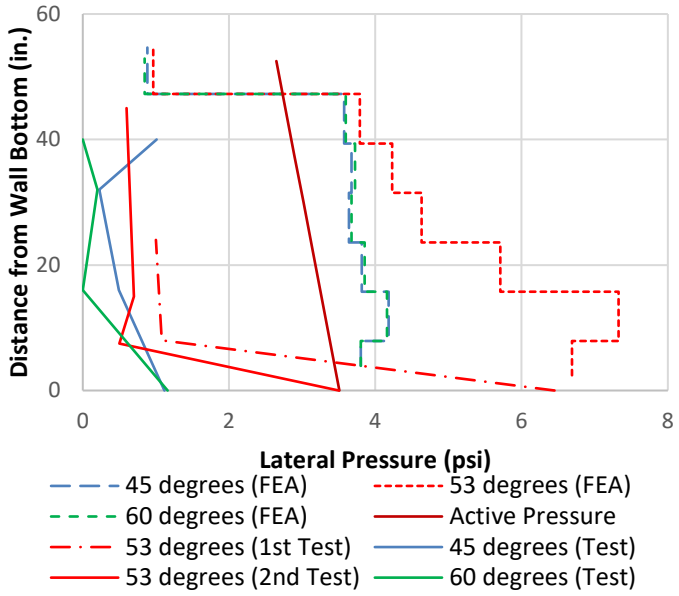

Figure 59. Average Lateral Pressures under Gravity and 14 psi Surcharge

Effect of the base foundation soil

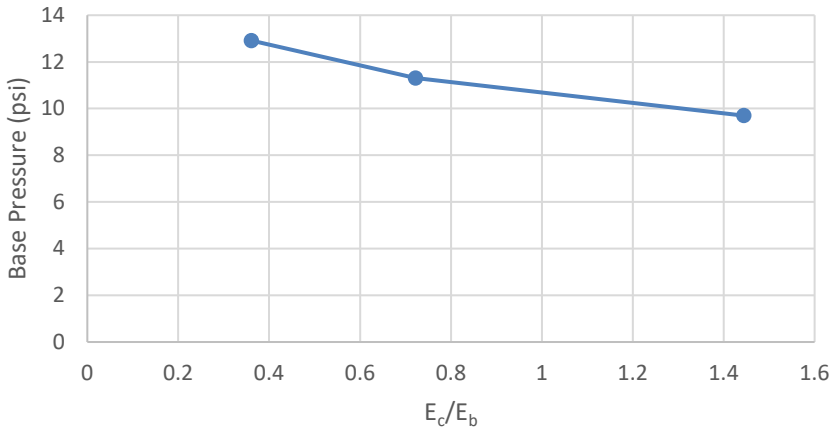

Figure 60. Base pressures for different foundation soils

Figure 60 shows the results of a parametric study on the effect of stiffness of base soil, where E_c and E_b are Young's modulus of the base soil and backfill, respectively. The analysis result shows the weaker base soil gives higher base pressure, and vice versa.

Effect of geosynthetic spacing on the base pressure

The comparison of the base pressures between walls with 4-in and 8-in geosynthetic spacings are shown in Fig. 61. The base pressure of the wall with 8-in. geosynthetic spacing is higher than that

of the wall with 4 in. geosynthetic spacing. The wall no. 3 has less effect of the geosynthetic spacing on the base pressure.

Effect of geosynthetic stiffness on the base pressure

Figure 62 shows the geosynthetic stiffness effect on base pressures is not significant, when compared with the base pressures of two analysis models. The geosynthetic stiffness in the second model (2) is two times of that in the first model (1).

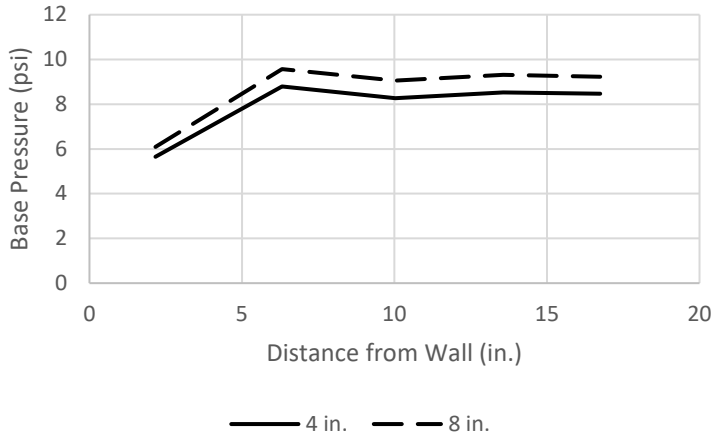

a) 45^0

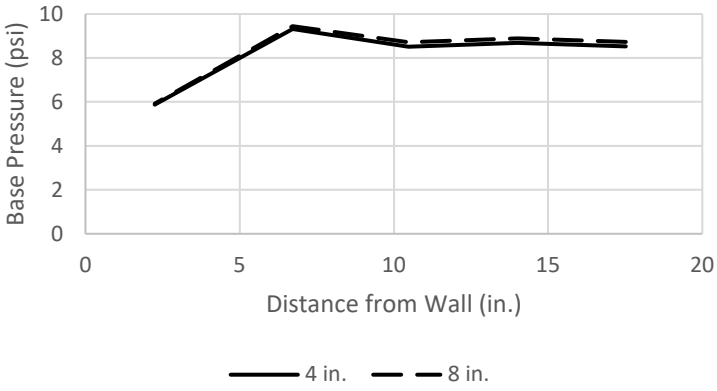

b) 60^0

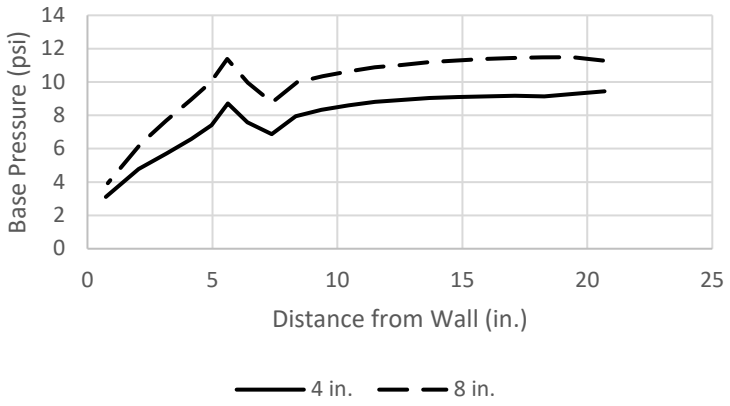

c) 53^0

Figure 61. Effect of geosynthetic spacing on the base pressure

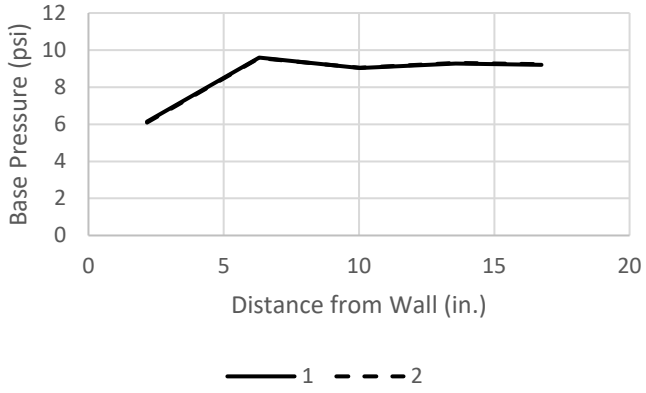

a) 45^0

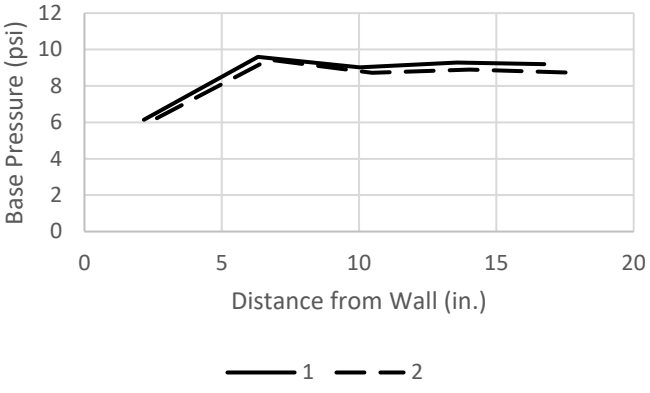

b) 60^0

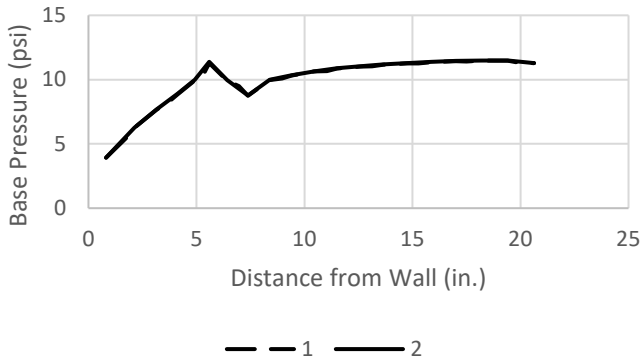

c) 53^0

Figure 62. Effect of geosynthetic stiffness on the base pressure

6. PROPOSED METHOD FOR THE BASE PRESSURE COMPUTATION

6.1.CDOT Work Sheet

CDOT parameters used in MSE Wall LRFD (CDOT 2018) are shown in Table 12 (from B-504-H2).

Table 12: Parameter used in CDOT Work Sheet

Property	Value	Description
φ	34^0	Class I Backfill friction angle
ϒsoil	125 pcf	Unit weight with 95% AASHTO T180
ϒh	1.5	Horizontal earth pressure factor
ϒv	1.35	Vertical earth pressure factor
LS	1.75	Live load surcharge factor
LLSurg	2’	Live load surcharge
dmax	2”	CDOT Class I Backfill Max size
HMAthk	10”	HMA thickness
ϒs	140 pcf	HMA unit weight
ϒHMA	Max.=1.5 Min.=0.65	HMA design factor

Active earth pressure coefficient:

$$K_a = \frac{1-\sin\varphi}{1+\sin\varphi} \tag{20}$$

At rest earth pressure coefficient:

$$K_0 = 1-\sin\varphi \tag{21}$$

$K_r(z) = K_0 - \frac{z}{20}(K_0 - K_a)$ if $z < 20'$, otherwise $K_r(z) = K_a$

Resultant of soil weight and surcharge:

$$R_v(z) = (\gamma_v \gamma_{soil} z + LS\gamma_{soil} LLSurg)\, RL(z) \tag{21}$$

Overturning moment:

$$M_0(z) = \frac{1}{6}K_a\gamma_h\gamma_{soil}z^3 + \frac{1}{2}K_a LS\gamma_{soil}(LLSurg)z^2 + \frac{1}{2}K_a\gamma_{HMA,Max}hma\frac{HMAthk}{12} \tag{22}$$

Righting moment:

$$M_v(z) = \frac{1}{2}R_v(z)R_L(z) \tag{23}$$

Eccentricity of resultant:

$$e = \frac{RL(z)}{2} - \frac{M_r(z) - M_0(z)}{R_v(z)} \tag{24}$$

Overburden with LS

$$\sigma_{v1}(z) = \gamma_v\gamma_{soil}\left(z - \frac{HMAthk}{12}\right) + \gamma_{HMA,Max}\gamma_s\frac{HMAthk}{12} + LS\gamma_{soil}LLSurg \tag{25a}$$

Overburden without LS

$$\sigma_{v2}(z) = \gamma_{soil}\left(z - \frac{HMAthk}{12}\right) + \gamma_s\frac{HMAthk}{12} \tag{25b}$$

Bearing pressure:

$$\sigma_b = \frac{R_y(z)}{RL(z) - 2e} \tag{26}$$

6.2.Governing equations

The following method can be applied for bearing pressure calculation of both truncated base and regular base walls. For the **regular** base, the failure line starts from the toe of the back slope and extend to the surface. The angle between the failure line and the horizontal line is $\theta = 45^0 + \varphi_r/2$ if $\alpha < 45 + \varphi_r/2$ (Fig. 64a) or $\theta = \alpha$ if $\alpha \geq 45^0 + \varphi_r/2$ (Fig. 64b), where φ_r is the friction angle

of backfill. The bearing pressures are evaluated using Meyerhof's overturning analysis method. For the **truncated** base wall (Fig. 64c), geosynthetics extend to the back slope. From the finite element analysis, as shown in Fig. 63, the failure lines occur along the slope and facing wall. The friction angle between the backfill soil and the foundation soil is assumed to be equal to the backfill friction angle, $\delta = \varphi_r$.

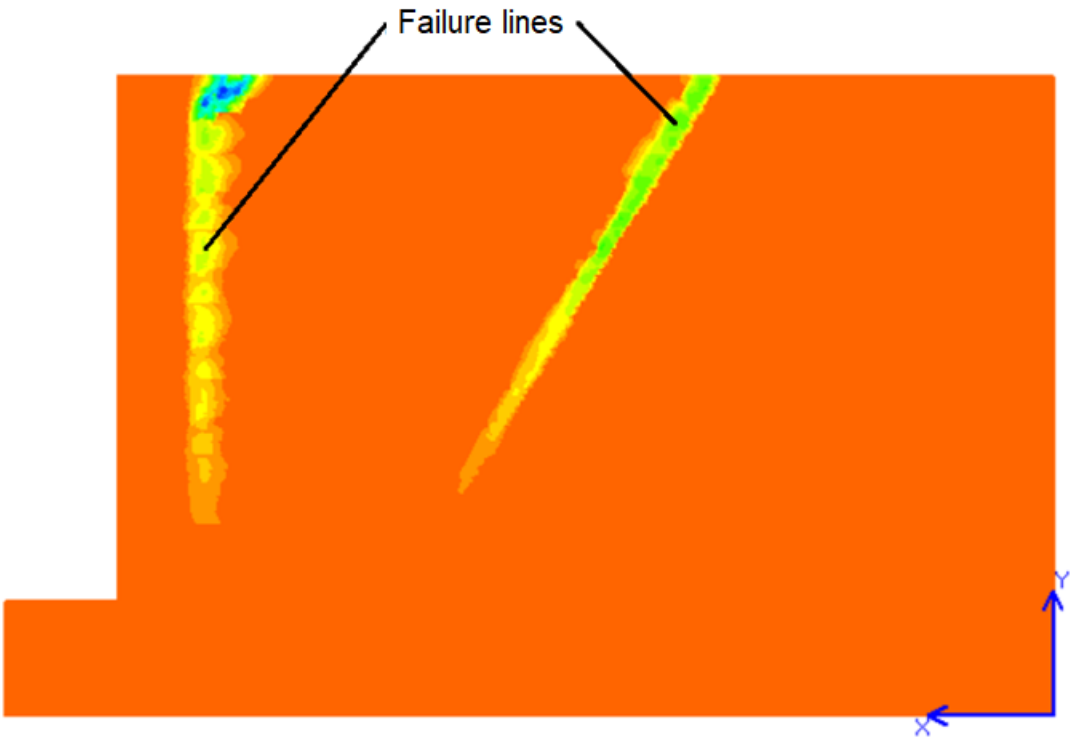

Figure 63. Failure lines for the truncated base wall under high surcharge

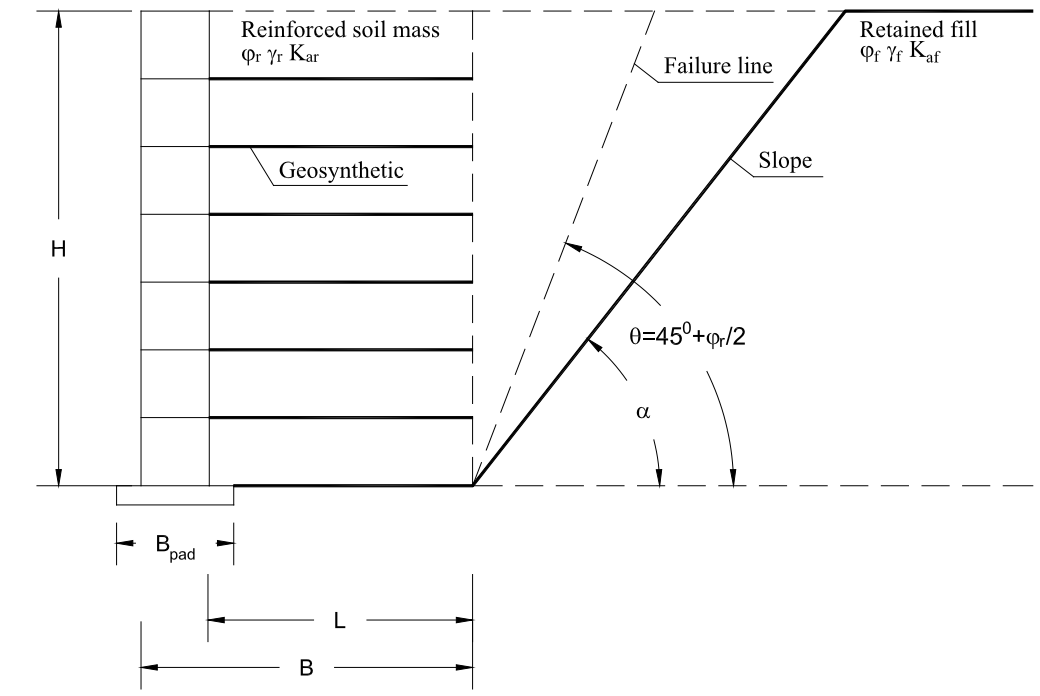

a) Regular base wall $\alpha < 45 + \varphi_r/2$

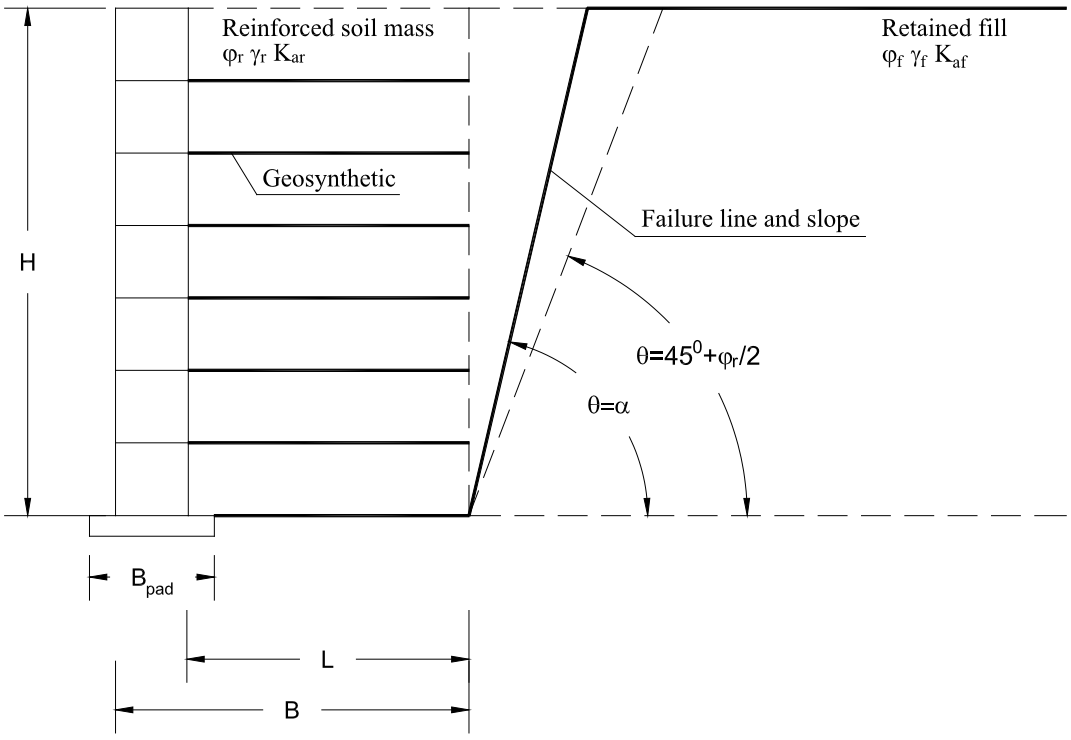

b) Regular base wall $\alpha \geq 45 + \varphi_r/2$

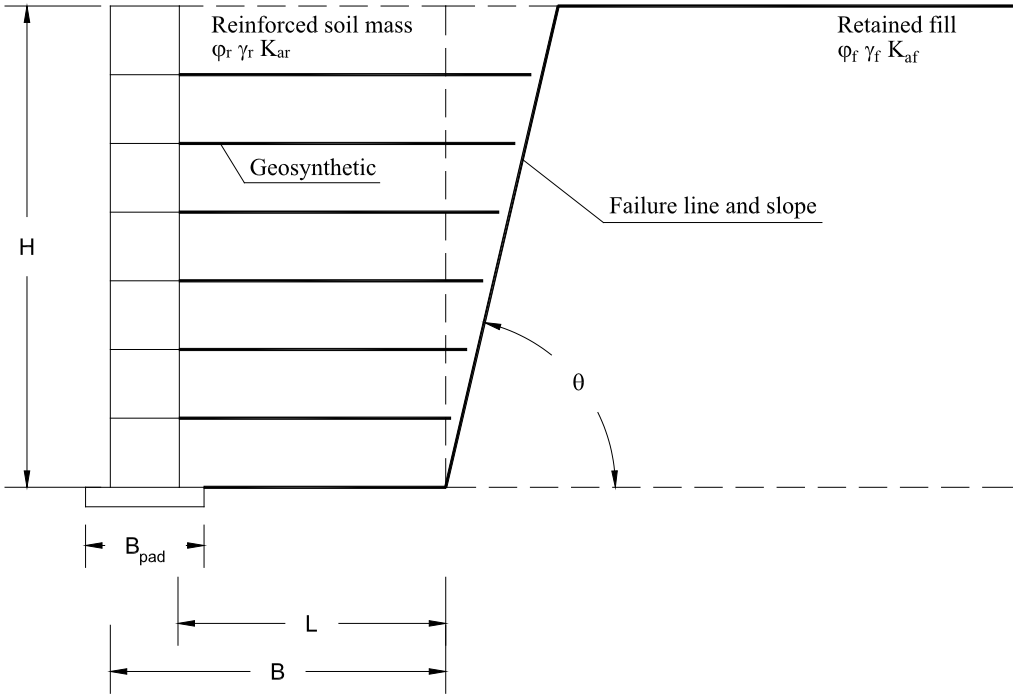

c) Truncated base wall

Figure 64. Failure assumptions

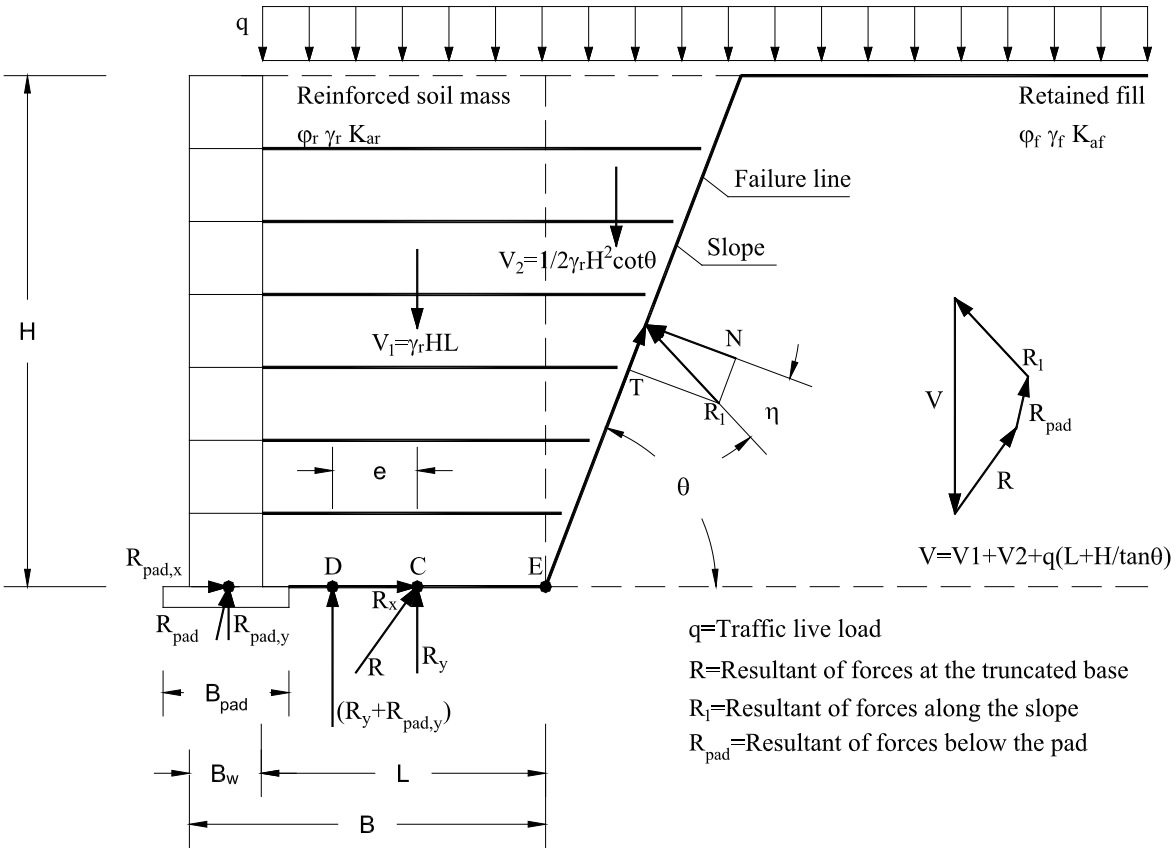

a) Forces apply on the truncated base wall

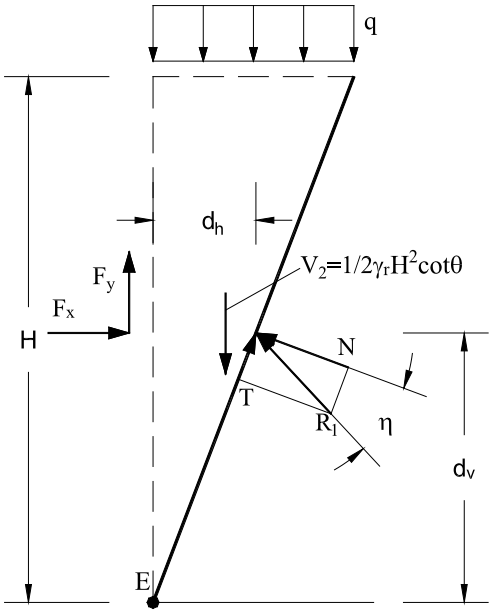

b) Equilibrium condition above the slope

Figure 65. Bearing pressure calculation of the truncated base

The equilibrium equation for the system in the vertical direction based on the free body diagram in Fig. 65a can be written as:

$$V_1 + V_2 + q\left(L + \frac{H}{\tan\theta}\right) + W_f - \left(R_{pad,y} + R_y\right) - T\sin\theta - N\cos\theta = 0 \tag{27}$$

where: V_1 is weight of the soil above the truncated base; V_2 is weight of the soil above the failure line; q is surcharge; T is tangential component of reaction R_1 on the failure line; N is normal component of reaction R_1 on the failure line; H is wall height; W_f is total weight of the facing wall; L is width of the truncated base; R_y is the base reaction in the vertical direction; $R_{pad,y}$ is the reaction below the leveling pad in the vertical direction. The weight of the soil above the truncated base is determined as:

$$V_1 = \gamma_r HL \tag{28}$$

where: γ_r is the unit weight of the backfill soil. The weight of the soil above the failure line:

$$V_2 = \frac{1}{2}\gamma_r \frac{H^2}{\tan\theta} \tag{29}$$

The equilibrium equation for the system in the horizontal direction based on the free body diagram in Fig. 65a can be written as:

$$\left(R_x + R_{pad,x}\right) = N\sin\theta - T\cos\theta \tag{30}$$

where R_x is the base reaction in the horizontal direction; $R_{pad,x}$ is the reaction below the leveling pad in the horizontal direction; The following equations can be obtained along the failure line:

$$T = N\tan\eta \tag{31}$$

where δ is friction angle of the interface between backfill soil and foundation soil, $\delta = \varphi_r$. If $\delta < \theta$ then $\eta = \delta$ and if $\delta > \theta$ then $\eta = \theta$. This condition is used to ensure that the left side of Eq. (30) is not negative.

Consider an equilibrium condition above the slope (Fig. 65b):

$$F_x = N\left(\sin\theta - \tan\eta\cos\theta\right) \tag{32}$$

$$F_y = V_2 + q\frac{H}{\tan\theta} - N\left(\cos\theta + \tan\eta\sin\theta\right) \tag{33}$$

Summing moments about point E (Fig. 65b):

$$F_x d_v = N\sqrt{d_v^2 + d_h^2} - V_2\frac{H}{3\tan\theta} - \frac{q}{2}\left(\frac{H}{\tan\theta}\right)^2 \tag{34}$$

where

$$d_h = \frac{\frac{V_2}{3} + \frac{q}{2}\frac{H}{\tan\theta}}{V_2 + q\frac{H}{\tan\theta}}\frac{H}{\tan\theta} \tag{35}$$

$$d_v = \frac{\frac{V_2}{3} + \frac{q}{2}\frac{H}{\tan\theta}}{V_2 + q\frac{H}{\tan\theta}}H \tag{36}$$

Substituting Eq. (34) into Eq. (32) leads to:

$$N = \frac{V_2\frac{H}{3\tan\theta} + \frac{q}{2}\left(\frac{H}{\tan\theta}\right)^2}{\sqrt{d_v^2 + d_h^2} - \left(\sin\theta - \tan\eta\cos\theta\right)d_v} \tag{37}$$

By introducing Eqs. (31) and (22) into Eq. (27), the total vertical reaction is given by the following equation:

$$\left(R_{pad,y}+R_y\right)=V_1+qL+W_f+F_y \tag{36}$$

Summing moments about point C (Fig. 65a):

$$M=F_x d_v-F_y\frac{B}{2} \tag{37}$$

The following equation can be obtained from Eq. (33):

$$e=\frac{M}{\left(R_{pad,y}+R_y\right)} \tag{38}$$

The average base pressure is calculated as:

$$\sigma_{avg}=\frac{R_{pad,y}+R_y}{B} \tag{39}$$

where $B=L+B_w$ is total base width where B_w is wall thickness.

In design, the maximum pressure, which counts for eccentricity may be used (CDOT, 2018) as the following equations:

$$\sigma_{\max}=\frac{R_{pad,y}+R_y}{B-2e} \tag{40}$$

6.3. Load transfer to facing wall

The pressure at the facing wall is active pressure and a resultant force of this pressure equals to total tension forces in geosynthetic and horizontal padding reaction (Fig. 66):

$$P_a=\sum T_i+R_{pad,x} \tag{41}$$

where T_i is tension force in the ith geosynthetic. As a result, the reaction force from the facing wall to the reinforced soil mass equals $R_{pad,x}$ in the horizontal direction. In the vertical direction, because of friction between the soil and the facing wall, a resultant force can be determined as:

$$R_2=P_a\tan\delta_w \tag{42}$$

where δ_w is friction angle between the soil and the facing wall; P_a is the active force acting on the facing wall. From the direct shear tests for Class Rock Class 1 backfill, $\delta_w=38^0$ or $\delta_w\approx 0.9\varphi$.

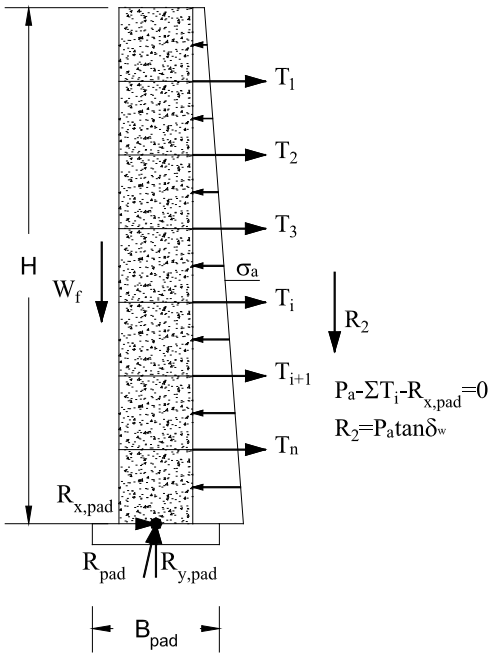

Figure 66. Equilibrium condition at the facing wall

By CDOT worksheets the summation of T_i is always greater than P_a because of the factor safety for assurance of enough resistance from soil reinforcements. Also, there is a 100% long-term connection pullout strength between face blocks and soil reinforcement requirement that ensures 75-years' service life. CDOT worksheet has two fiberglass pins as stoppers installed in panel and block facing for the purpose of resisting lateral earth pressure during construction. Evidently, $R_{pad,x}$ (a horizontal component of R_{pad}) is ideally zero after the concrete block wall is built. With this assumption, the leveling pad is only subject to vertical component R_2 of earth pressure P_a and $R_{pad,x}$ is zero after wall built. The active pressure applies to the facing wall can be calculated by the following equation:

$$P_a = K_a\left(\frac{1}{2}\gamma_r H^2 + qH\right) \tag{43}$$

Vertical reaction along the facing wall is given by:

$$R_2 = P_a \tan\delta_w = K_a\left(\frac{1}{2}\gamma H^2 + qH\right)\tan\delta_w \tag{44}$$

The vertical reaction at the facial pad:

$$R_{pad,y} = R_2 + W_f \tag{45}$$

The leveling pad pressure is calculated as:

$$\sigma_{pad} = \frac{R_{y,pad}}{B_{pad}} = \frac{K_a\left(\frac{1}{2}\gamma H^2 + qH\right)\tan\delta_w + W_f}{B_{pad}} \quad (46)$$

where B_{pad} is the width of the leveling pad; $B_{pad} = 18$ in.

The base pressure is given by:

$$\sigma_b = \frac{R_y}{L} = \frac{R_y + R_{y,pad}}{L} - \frac{K_a\left(\frac{1}{2}\gamma H^2 + qH\right)\tan\delta_w + W_f}{L} \quad (47)$$

Equation (47) is used to compare the base pressures with those from the finite element analyses and the full-scale tests.

6.4. Verification

The proposed method is applied to determine the base pressures of truncated base walls with Class I Backfill soil. Figures 67 and 68 shows the effect of the slope angle on the base pressures of the truncated walls with the same geometry as T-Cage test walls under gravity and 14 psi surcharge, respectively. No load factors are applied and only base pressures (Eq. 47) (without leveling pad pressures) are in the comparison.

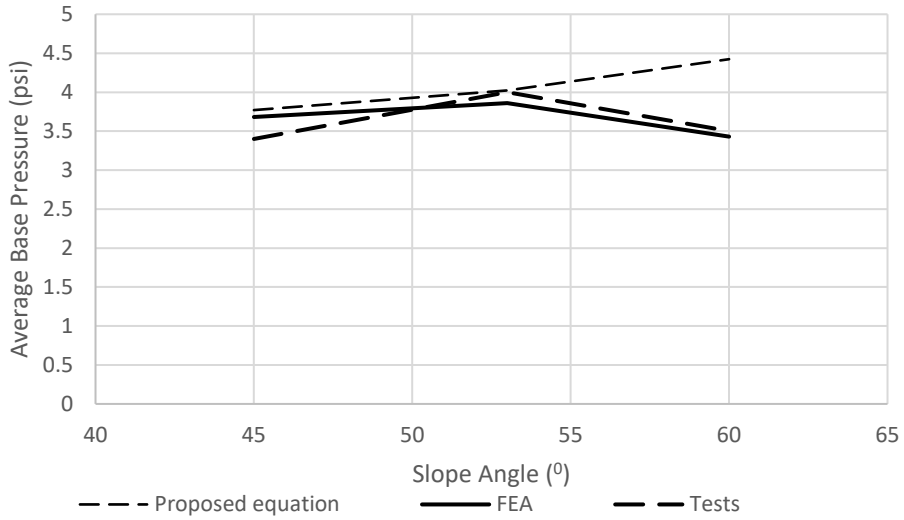

Figure 67. Bearing pressure under gravity load (unfactored)

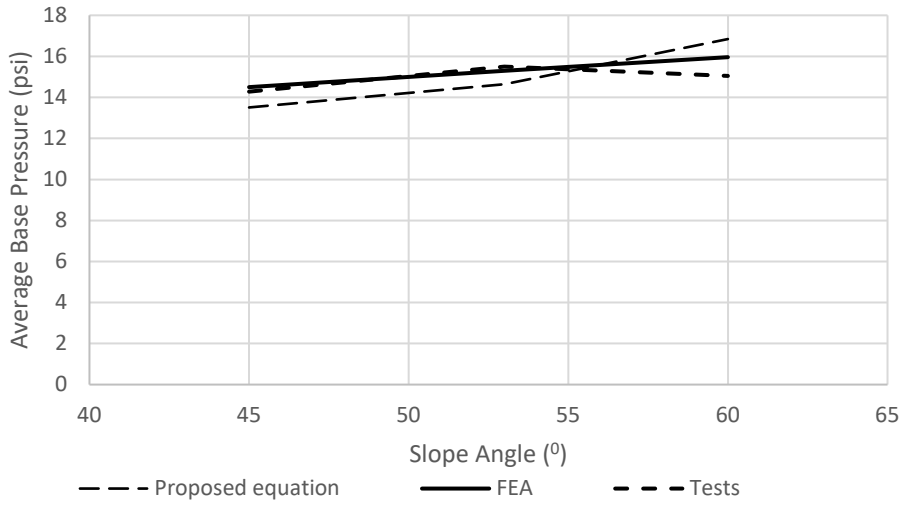

Figure 68. Bearing pressure under 14 psi surcharge and gravity loads (unfactored)

Under the gravity load, the results of the base pressure predicted from the proposed equation are in good agreement with those from FEA and measurement. Under the gravity load and surcharge of 14 psi, the base pressures calculated from the proposed equation are higher than the base pressures from FEA and measurement. A reason for the difference is that the proposed method is derived for the failure state in which stress states on the facing wall and slope reach the failure condition. The load transferred to the facing wall in FEA and measurement is more than that in the proposed method.

6.5.Design procedure

Substituting Eq. (34) into Eq. (32) leads to:

$$N = \frac{V_2 \dfrac{H}{3\tan\theta} + \dfrac{q}{2}\left(\dfrac{H}{\tan\theta}\right)^2}{\sqrt{d_v^2 + d_h^2} - \left(\sin\theta - \tan\eta\cos\theta\right) d_v} \tag{37}$$

where

$$d_h = \frac{\dfrac{V_2}{3} + \dfrac{q}{2}\dfrac{H}{\tan\theta}}{V_2 + q\dfrac{H}{\tan\theta}} \frac{H}{\tan\theta} \tag{35}$$

$$d_v = \frac{\frac{V_2}{3} + \frac{q}{2}\frac{H}{\tan\theta}}{V_2 + q\frac{H}{\tan\theta}} H \tag{36}$$

Consider an equilibrium condition above the slope (Fig. 65b):

$$F_y = V_2 + q\frac{H}{\tan\theta} - N\left(\cos\theta + \tan\eta \sin\theta\right) \tag{33}$$

By introducing Eqs. (31) and (22) into Eq. (27), the total vertical reaction is given by the following equation:

$$\left(R_{pad,y} + R_y\right) = V_1 + qL + W_f + F_y \tag{36}$$

$$F_x = N\left(\sin\theta - \tan\eta\cos\theta\right) \tag{32}$$

Summing moments about point C (Fig. 65a):

$$M = F_x d_v - F_y \frac{B}{2} \tag{37}$$

The following equation can be obtained from Eq. (33):

$$e = \frac{M}{\left(R_{pad,y} + R_y\right)} \tag{38}$$

The average base pressure is calculated as:

$$\sigma_{avg} = \frac{R_{pad,y} + R_y}{B} \tag{39}$$

6.6.Design example

Figure 69 shows the comparison between the proposed method (with load factor shown in Table 13) and the current method used by CDOT (CDOT, 2018) for the most popular MSE wall with 1 (H) to 1 (V) back-fill-slope under 5' surcharge (3' of soil and 2' of traffic loads). Load factors are applied to gravity (1.35) and surcharge (1.75).

The base pressures of the truncated base walls are computed by using the following parameters:

$Q = q\left(L + \frac{H}{\tan\theta}\right)$; $\varphi = 34^0$; $\delta = 34^0$; $\beta = \delta_w = 0.9\varphi = 29^0$;

$q = 1.75(2)125/144 + 1.35(3)125/144 = 6.55$ psi; $\gamma = 1.35(125) = 168.75$ pcf; $B = L + 8$ in.

In this comparison, backfill soil properties and load factors are shown in Table 13. The base pressures are presented in Table 14 to Table 16. The pressures calculated from the proposed method (Eq. 39) are much lower than the current CDOT method.

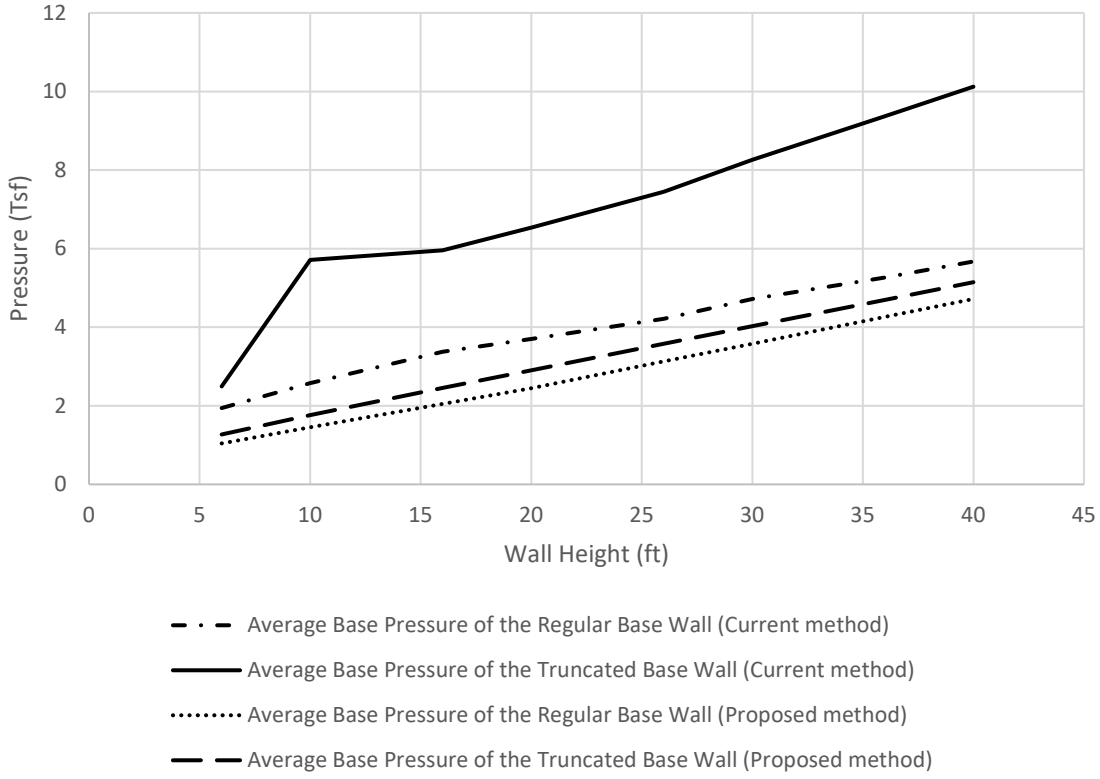

Figure 69. Bearing Pressure Comparison under 5' Surcharge and Gravity

Table 13. Pressures of the truncated base wall for different wall heights (45^0)

H (in.)	L (in.)	V_1 (lb)	V_2 (lb)	Q (lb)	$R_y+R_{pad,y}$ (lb)	σ_{avg} (psi)
72	32.4	227.81	134.59	536.87	522.948	17.637
120	54	632.81	373.86	894.79	1217.992	24.490
192	86.4	1620.00	957.08	1431.66	2780.175	34.085
240	108	2531.25	1495.43	1789.57	4168.042	40.363
312	140.4	4277.81	2527.28	2326.45	6769.460	49.723
360	162	5695.31	3364.72	2684.36	8850.151	55.945
432	194.4	8201.25	4845.20	3221.23	12490.804	65.264
480	216	10125.00	5981.73	3579.15	15264.317	71.472

Table 14. Pressures of the truncated base wall for different wall heights (60^0)

H (in.)	L (in.)	V_1 (lb)	V_2 (lb)	Q (lb)	$R_y+R_{pad,y}$ (lb)	σ_{avg} (psi)
72	32.4	227.81	134.59	536.87	585.021	14.684
120	54	632.81	373.86	894.79	1310.428	21.676
192	86.4	1620.00	957.08	1431.66	2901.629	32.022
240	108	2531.25	1495.43	1789.57	4297.823	38.898
312	140.4	4277.81	2527.28	2326.45	6895.204	49.204
360	162	5695.31	3364.72	2684.36	8962.185	56.074
432	194.4	8201.25	4845.20	3221.23	12565.746	66.379
480	216	10125.00	5981.73	3579.15	15303.513	73.249

Table 15. Pressures of the truncated base wall for different wall heights (53^0)

H (in.)	L (in.)	V_1 (lb)	V_2 (lb)	Q (lb)	$R_y+R_{pad,y}$ (lb)	σ_{avg} (psi)
72	32.4	227.81	134.59	536.87	551.177	16.292
120	54	632.81	373.86	894.79	1256.284	23.164
192	86.4	1620.00	957.08	1431.66	2820.427	32.713
240	108	2531.25	1495.43	1789.57	4200.844	38.918
312	140.4	4277.81	2527.28	2326.45	6777.954	48.132
360	162	5695.31	3364.72	2684.36	8833.682	54.243
432	194.4	8201.25	4845.20	3221.23	12423.758	63.383
480	216	10125.00	5981.73	3579.15	15154.797	69.465

7. SUMMARY, CONCLUSIONS, AND RECOMMENDATIONS

Summary and Conclusions

The three fully instrumented large-scale GRS-Block Facing wall models were tested in a control indoor laboratory environment. The walls were identical except for the differences in excavation slope angles. The backfill soil is Colorado Class I backfill of crushed granite widely used in GRS wall construction in Colorado. Three FE models were developed to numerically simulate the performance of the walls using SSI2D program. The results of the FE analysis were compared with the measured results of the model tests. The backfill behavior was modeled using the modified hyperbolic constitutive model of soil and the clayey soil was modeled using the Mohr-Coulomb

model. In the numerical simulation, geosynthetic was modeled using the nonlinear axial load-displacement curve from the Wide Width tension test. Findings of this study are summarized as follows:

- The three GRS walls were loaded to pressures higher than the service load without observable damage.
- The bearing pressures from measurement and finite element analyses are in good agreement.
- Both the measured and calculated base bearing pressures are much smaller than the sum of overburden and surcharge. This shows that a good part of the vertical load is transferred to the facing wall and excavation slopes. Thus, it is critical to examine the compressive stress variation between each facing blocks, and the bottom block treatment is particularly critical to the performance of the complete block facing wall. A toe kicker and/or backfill might be needed.
- The numerical analyses show that base bearing pressure distribution depends on the base width, the stiffness of backfill, foundation soil and the soil in the excavation slope, and the backfill-facing block interface strength. If the base soil is weaker than the backfill soil, the base stress is increased and vice versa.
- The base pressure increases with increasing geosynthetic spacing. However, the geosynthetic stiffness effect on the base pressures is not significant.
- This study indicates that the performance of the GRS Block Facing Walls depends on the interaction among all elements involved: wall geometry, stiffness, and strength of backfill, facing block, foundation soils and excavation slope, and the interface strength among all elements involved in the wall construction.
- The proposed method for the base bearing pressure evaluation provides the truncated base pressures in good agreement with FEA and measurement.

Recommendations

As is observed in this study, the truncated GRS block facing wall can save much construction cost. However, it is necessary to gain additional knowledge of the details of vertical load balance and transfer, and lateral wall pressures. The TEAM recommends an additional study on the distribution of vertical loads, shear force between neighboring facing blocks and lateral wall pressure of truncated base walls of different excavation slopes, as outlined in the evaluation of the followings:

- Horizontal earth pressures on each facing block, and overall lateral earth wall pressures,
- Block facing and backfill interface transmission of vertical load,
- Inter-block interface vertical and horizontal forces (or stresses) distributions,
- Bearing pressure along the base of the bottom facing block,
- Compressive strength requirement of facing blocks,
- Toe kicker and/or backfill requirement to prevent block sliding, and
- Finally, the bearing capacity requirement of foundation soils.

The current CDOT worksheet adopts an 18-inch width leveling pad. The authors believe that the width of the leveling pad should reflect wall height and strength of geomaterial underlying the pad.

REFERENCES

ASTM D-4595. Standard Test Method for Tensile Properties of Geotextiles by the Wide-Width Strip Method.

AASHTO, LRFD Bridge Design Specifications, 2014, seventh ed. American Association of State Highway and Transportation Officials, Washington, D.C.

Abu-Hejleh, N., Wang, T., Zornberg, J.G., McMullen, M., Outcalt W., 2001. Performance of geosynthetic reinforced walls supporting the Founders/Meadows bridge and approaching roadway structures. Report No. CDOT-DTD-R-2001-12.

Adams, M., Nicks, J., Stabile, T., Wu, J., Schlatter, W., Hartmann, J., 2011a. Geosynthetic Reinforced Soil Integrated Bridge System. Synthesis Report (No. FHWA-HRT-11-027).

Adams, M., Nicks, J., Stabile, T., Wu, J., Schlatter, W., Hartmann, J., 2011b. Geosynthetic Reinforced Soil Integrated Bridge System. Interim Implementation Guide (No. FHWA-HRT-11-026).

Allen, T.M., Christopher, B.R., Holtz, R.D., 1992. Performance of a 41 Foot High Geotextile Wall. Final Report, Experimental Feature WA87-03. Washington State Department of Transportation, Planning, Research and Public Transportation Division.

Ardah, A., Abu-Farsakh, M., Voyiadjis, G., 2017. Numerical evaluation of the performance of a Geosynthetic Reinforced Soil-Integrated Bridge System (GRS-IBS) under different loading conditions. Geotextiles and Geomembranes, 1-12.

Berg, R.R., Christopher, B.R., and Samtani, N.C., *Design of Mechanically Stabilized Earth Walls and Reinforced Soil Slopes, Design & Construction Guidelines*, FHWA-NHI-00-043, Federal Highway Administration, McLean, VA, March 2009.

CDOT (2016). MSE Wall Sheets LRFD.

CDOT (2018). MSE Wall Sheets LRFD.

Duncan, J.M., Chang, C.Y., 1970. Nonlinear analysis of stress and strain in soils. J. Soil Mech. Found. Div. 96 (5), 1629e1653.

Graeme D. Skinner, R.K.R. (2005). "Design and behavior of a geosynthetic reinforced retaining wall and bridge abutment on a yielding foundation." Geotexitiles and Geomembranes. 23: 234-260.

Lee, Y.-B., Ko, H.-Y., and McCartney, J.S. (2010). "Deformation Response of Shored MSE Walls under Surcharge Loading in the Centrifuge." Geosynthetics International. 17(6), 389-402.

Liu, H., 2015. Reinforcement load and compression of reinforced soil mass under surcharge loading. J. Geotech. Geoenvironmental Eng. 141 (6), 04015017.

Morrison, K.F., Harrison, F.E., Collin, J.G., Dodds, A., and Arndt, B., *Shored Mechanical Stabilized Earth (SMSE) Wall Systems Design Guidelines*, Central Federal Lands Highway Division, FHWA-CFL/TD-06-001, Federal Highway Administration, McLean, VA, 2006.

Saghebfar, M., Abu-Farsakh, M., Ardah, A., Chen, Q., Fernandez, B.A., 2017a. Performance monitoring of geosynthetic reinforced soil integrated bridge system (GRS-IBS) in Louisiana. Geotext. Geomembranes 45 (2), 34-47.

Smith, I. M. and Griffiths, D. V. (1997). Programming The Finite Element Method. John Wiley & Sons, Third Edition.

Volmer, B, Chang, N.Y., and Liu, J. G. (2017) "Tiger Cage for Abutment/Retaining Wall and MSB Interaction," ACI SP-316-9.

Woodruff, R., *Centrifuge Modeling for MSE-Shoring Composite Walls*, Master of Science Thesis, Department of Civil Engineering, University of Colorado, Boulder, 2003.

Wu, J. T.H. and Ooi, P.S.K. (2015). Synthesis of Geosynthetic Reinforced Soil Design Topics. FHWA-HRT-14-094.

APPENDICES

A.1 Laboratory tests for the crushed rock backfill

Backfill tests should include: index property tests, like specific gravity, Atterberg's limits tests and gradation analysis, compaction tests (standard and modified) and triaxial compression tests. These tests will provide the index properties for soil classification, maximum dry density and optimum moisture content for guiding field compaction and backfill stress-strain relationship and strength characteristics to evaluate the material parameters for the soil model to be used in finite element analysis. The CGES Geotechnical-structural Laboratory has excellent lab equipment for all the above mentioned tests, refer to the interim report that CGES submitted to CDOT for details of lab test equipment.

A.1.1 Specific gravity test

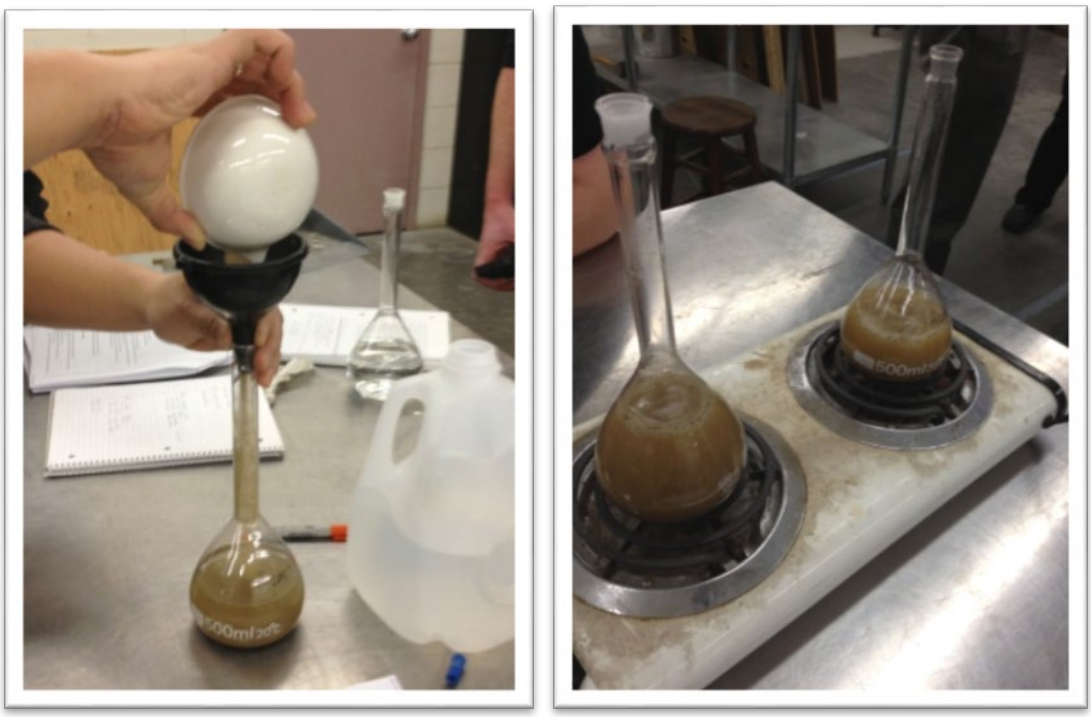

Figure A1. Specific gravity test

The results of this laboratory are reasonable. The table below shows the computations for the specific gravity at room temperature, and also adjusts the value with a temperature correction factor.

Table A1: Specific gravity test

Item	Test No.		
	1	2	3
Temperature of test, T1	24	24	23
Temperature correction factor, A	0.9991	0.9991	0.9993
Mass of flask + water filled to mark, M1 (g)	681.3	645.5	623.5
Mass of flask + soil + water filled to mark, M2 (g)	745.2	708.8	689.3
Mass of dry soil, Ms (g)	99.2	99.3	101.5
Mass of equal volume of water and soil solids, Mw (g) = (M1 + Ms) - M2	35.3	36	35.7
Gs(at T1˚ C) = Ms/Mw	2.81	2.76	2.84
Gs(at 20˚ C) = Gs(at T1˚ C) * A	2.81	2.76	2.84
Average Gs(at 20˚ C)	2.80		

A.1.2Gradation test

Figure A2. Gradation test

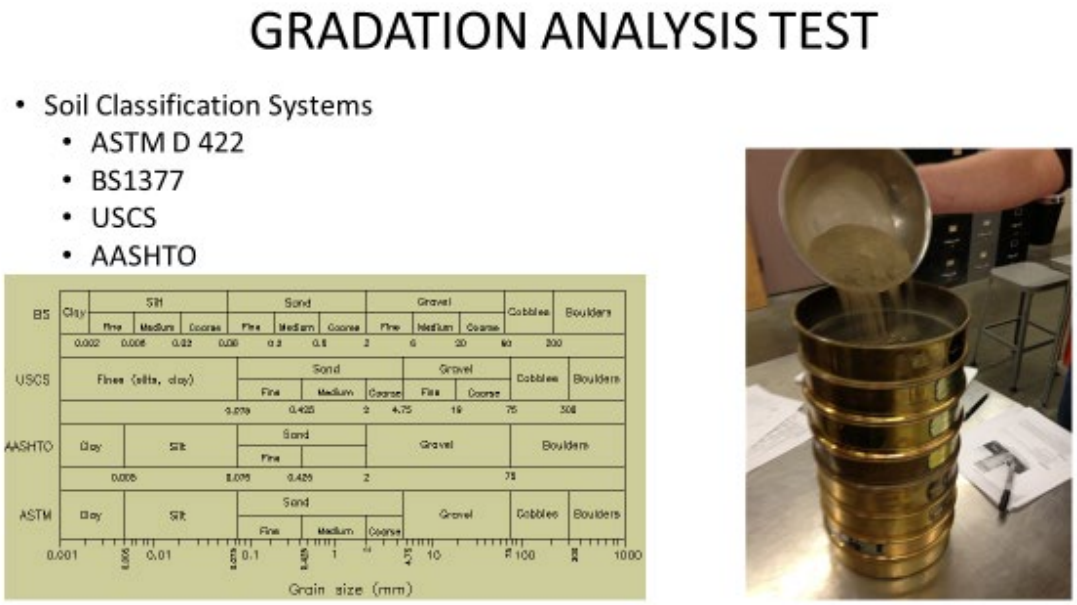

Figure A3. Gradation analysis test

The data gotten after operating the sieve shaker were recorded and calculated by the tabular Excel, the results and the grain size distribution curve (the gradation curve) are shown below:

Mass of dry soil sample, W = 694.6 g

Table A2: Gradation test data

Sieve No.	Sieve Opening (mm)	Mass of soil retained on each sieve, W_n (g)	Percent of mass retained on each sieve, R_n	Cumulative percent retained, $\sum R_n$	Percent finer 100 - $\sum Rn$
4	4.75	208.2	29.97	29.97	70.03
10	2	204.1	29.38	59.36	40.64
20	0.85	92.3	13.29	72.65	27.35
40	0.425	50.1	7.21	79.86	20.14
60	0.25	41.9	6.03	85.89	14.11
100	0.15	35.9	5.17	91.06	8.94
200	0.075	34.1	4.91	95.97	4.03
Pan		28.0	4.03	100.00	0.00
		$\sum$ = 694.6 g		The difference = 0	

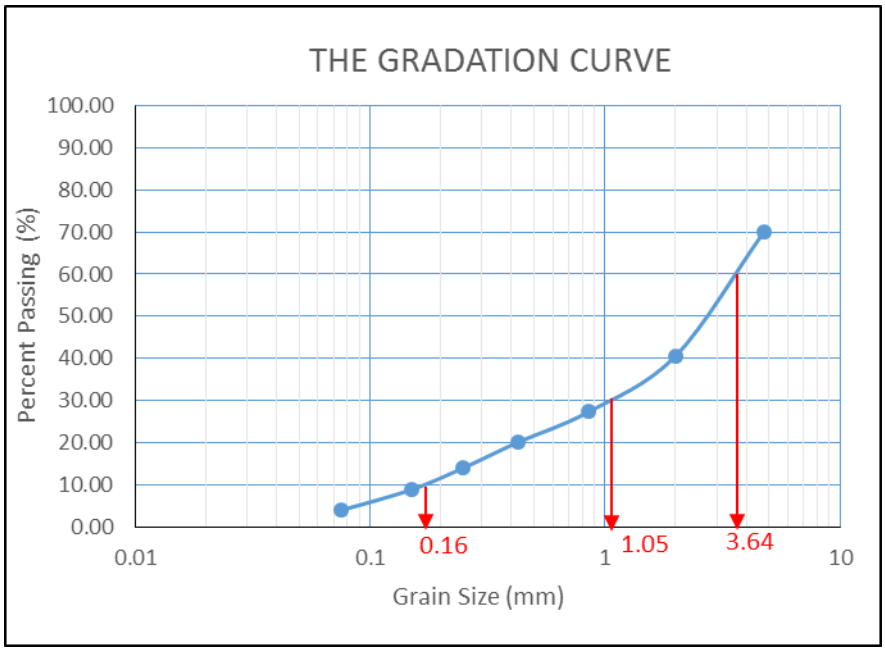

D_{60} = 3.64 mm **D_{30} = 1.05mm** **D_{10} = 0.16 mm**

C_u = 22.75 **C_c = 1.86**

Figure A4. Gradation curve

This soil sample would fall under the category of coarse-grained according to the USCS since more than 50% of the sample (R_{200} = 95.97 %) was retained on No.200 sieve. In addition, more than 50 % of the coarse fraction (F_4 = 70.03 %) passed No. 4 sieve, the uniformity coefficient is 22.5 (> 6) and the coefficient of gradation is 1.89 (in the range of 1 – 3), it is classified as a well graded sand **SW.**

According to the AASHTO, this sample would fall under the category of granular material since less than 35% of the sample passed No. 200 sieve (F_{200} = 4.03 %). In addition, the percentage passing No. 10 sieve is less than 50% (F_{10}= 40.64 %), the percentage passing No. 40 sieve is less than 30% (F_{40} = 20.14 %), and the percent passing No. 200 is less than 15% (F_{200} = 4.03 %), it is classified as an A–1–a. Since the sample is clearly a granular material, it does not need to perform the Atterberg's limits test.

A.1.3Compaction tests

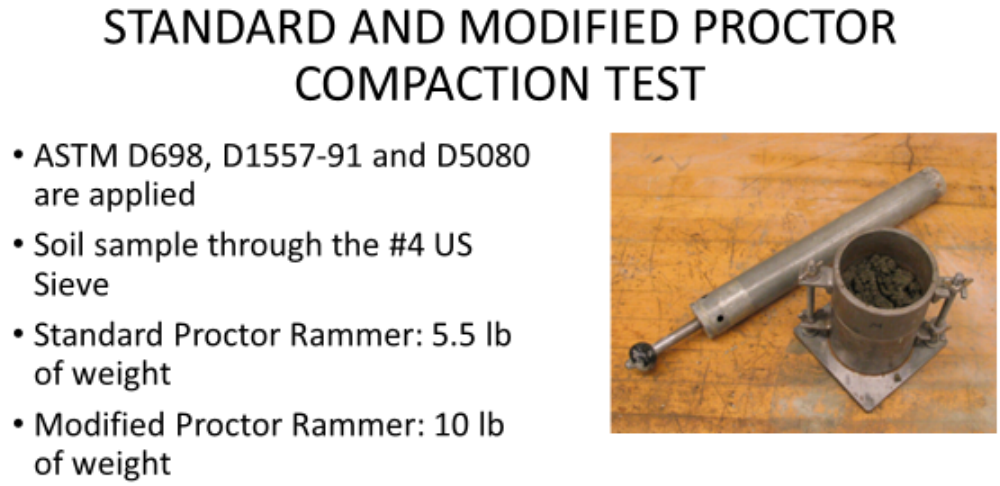

Figure A5. Compaction test

The object of this experiment is to define the laboratory maximum dry unit weight and the optimum water content of the soil sample taken from source of the CDOT Class1 Structural Backfill soil. In order to define the soil density by field compaction, both of two basic tests, the standard and modified compaction tests are performed. The ASTMs: D 698, D 1557-91, and D 5080 would be applied for this test.

Both of two methods of the Proctor Compaction Test (Standard and Modify) are performed to experimentally measure the optimum moisture content and the maximum dry density for the CDOT Class 1 Structural Backfill soil sample. The results obtained from the experiments to be *131.5 lb/ft³* of the maximum dry unit weight with the optimum of *10 %* water content and the maximum dry unit weight of *142 lb/ft³* with the optimum water content of *6.5 %* according to the standard experiment and the modified experiment respectively. The given results are chosen from the fitting A method with the quadratic polynomial aggression curves for the both experiments.

The Proctor compaction test performed to determine the laboratory optimum water content and the dry unit weight of a soil sample. The modified Proctor test gives a higher dry unit weight (140 lb/ft³) with the lower optimum water content (7%) then the standard Proctor test (134.25 lb/ft³ dry unit weight and 9% water content). The result from the modified test should be used for defining the density of soil by field compaction.

Table A3: For the standard proctor compaction test

Test	1	2	3	4	5	6	7
1. Weight of mold, W1 (lb)	9.29	9.29	9.29	9.29	9.29	9.29	9.29
2. Weight of mold + moist soil , W2 (lb)	13.69	13.84	13.97	14.07	14.04	13.97	13.90
3. Weight of moist soil, W2 - W1 (lb)	4.41	4.55	4.68	4.79	4.75	4.68	4.61
4. Moist unit weight, $\gamma = [(W2 - W1) /0.0333]$ (lb)	132.28	136.64	140.48	143.75	142.58	140.62	138.39
5. Moisture can number	3.00	4.00	5.00	6.00	7.00	8.00	9.00
6. Mass of moisture can, W3 (g)	15.60	16.10	16.00	15.20	15.10	15.60	15.10
7. Mass of can + moist soil, W4 (g)	37.80	41.70	42.20	36.20	46.90	46.20	47.20
8. Mass of can + dry soil, W5 (g)	36.70	40.00	40.10	34.30	43.60	42.60	43.20
9. Moisture content, $w(\%) = [(W4-W5)/(W5-W3)]*100$	5.21	7.11	8.71	9.95	11.58	13.33	14.23
10. Dry unit weight of compaction $\gamma d\ (lb/ft^3) = [\gamma/(1+(w(\%)/100))]$	125.73	127.56	129.22	130.75	127.79	124.07	121.15

Table A4: For the modified proctor compaction test

Test	1	2	3	4	5	6	7
1. Weight of mold, W1 (lb)	9.37	9.37	9.37	9.37	9.37	9.37	9.37
2. Weight of mold + moist soil , W2 (lb)	14.01	14.17	14.37	14.42	14.34	14.20	14.15
3. Weight of moist soil, W2 - W1 (lb)	4.64	4.80	5.00	5.05	4.97	4.83	4.78
4. Moist unit weight, $\gamma = [(W2 - W1) /0.0333]$ (lb)	139.34	144.14	150.15	151.65	149.25	145.05	143.54
5. Moisture can number	1	2	3	4	5	6	7
6. Mass of moisture can, W3 (g)	12.00	15.40	15.50	15.10	15.40	15.60	15.20
7. Mass of can + moist soil, W4 (g)	24.60	40.00	42.30	48.90	55.50	52.10	56.00
8. Mass of can + dry soil, W5 (g)	24.4	39.1	40.8	46.3	51.8	48.3	51.5
9. Moisture content, $w(\%) = [(W4-W5)/(W5-W3)]*100$	1.61	3.80	5.93	8.33	10.16	11.62	12.40
10. Dry unit weight of compaction γd (lb/ft^3) $= [\gamma/(1+(w(\%)/100))]$	137.13	138.87	141.75	139.99	135.48	129.94	127.71

The graph of the compaction curves and the zero void curve with G_s = 2. 8 are shown as below:

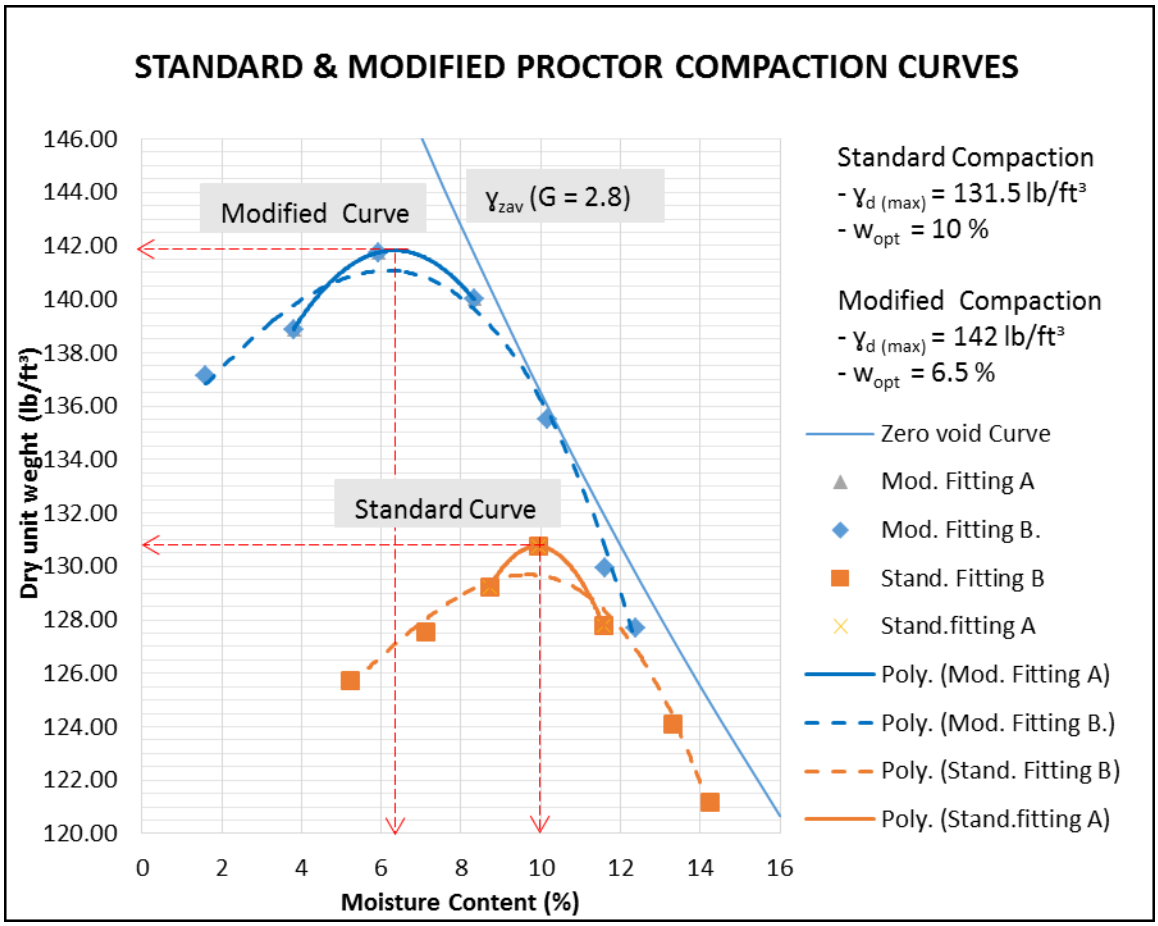

Figure A6. Standard and modified proctor compaction curves

A.2 Laboratory tests of interface between block facing and geosynthetic

The interface between block facing and geosynthetic was tested using the large direct shear box. Block facing was cut to fit the size of the box as shown in Fig.

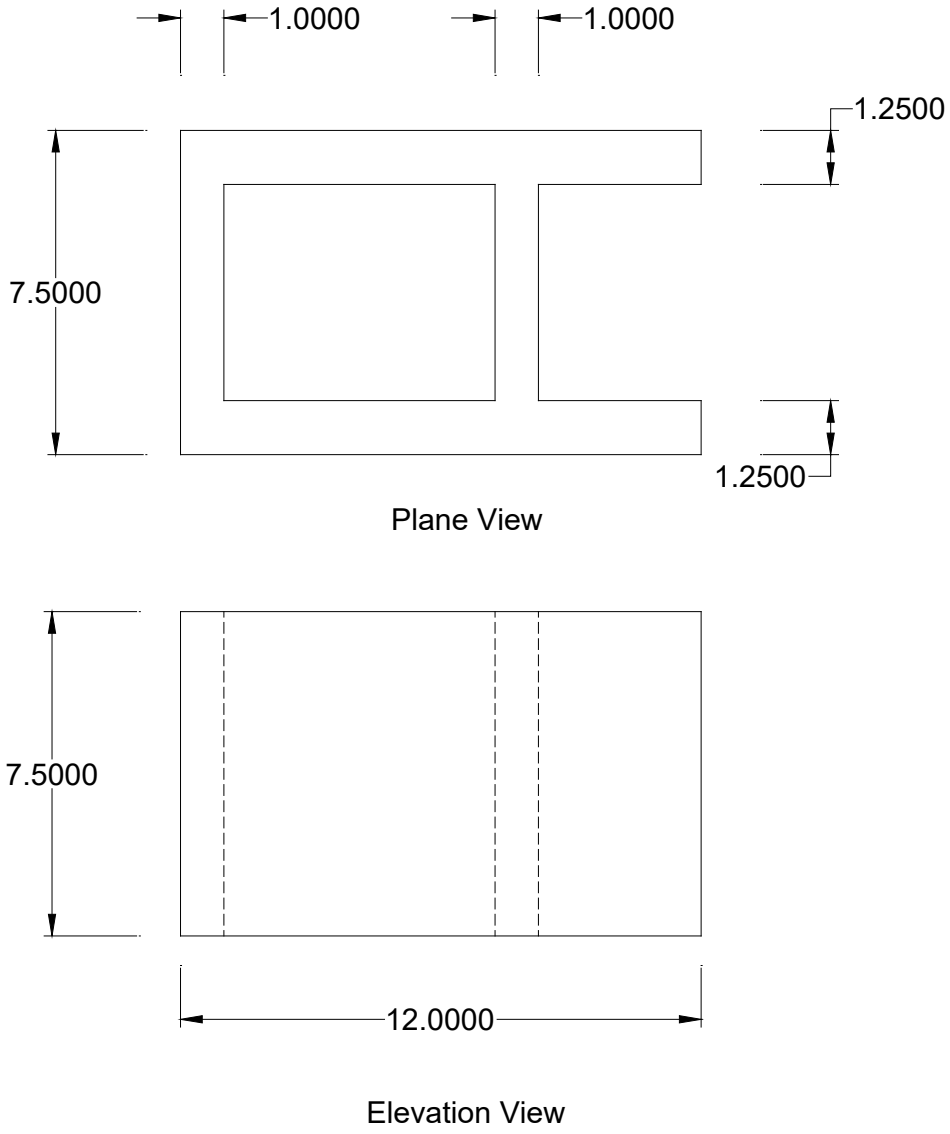

Figure A7. Block facing for the interface test

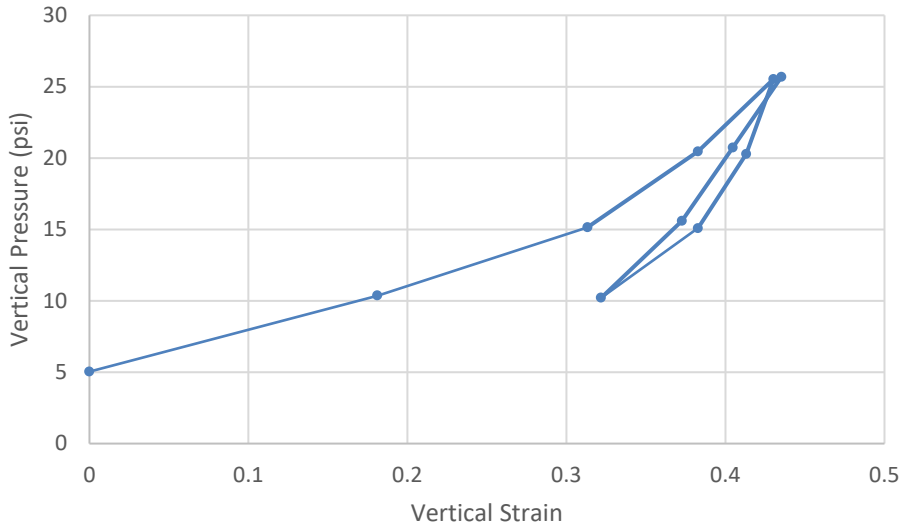

Figure A8. Vertical load test of the interface between block facing and geosynthetic

Table A5: Properties of the block facing and geosynthetic

Object	Stiffness (lb/in)	Modulus (psi)
Block facing	157433	21967
Interface between block facing and geosynthetic	37309	41

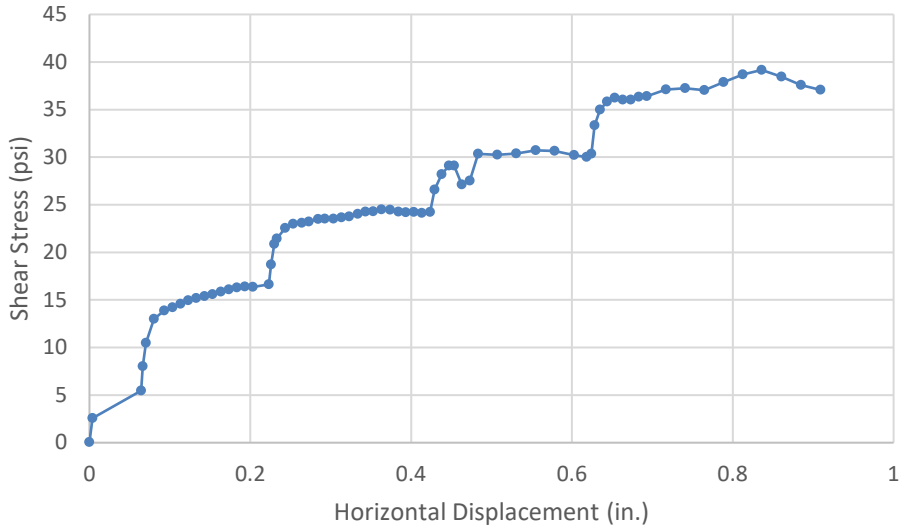

a) Shear stress versus horizontal displacement

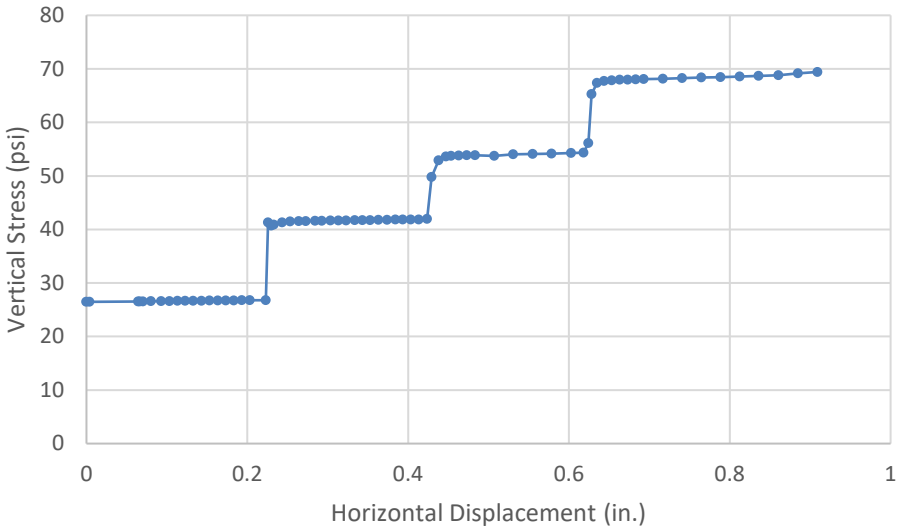

b) Vertical stress versus horizontal displacement

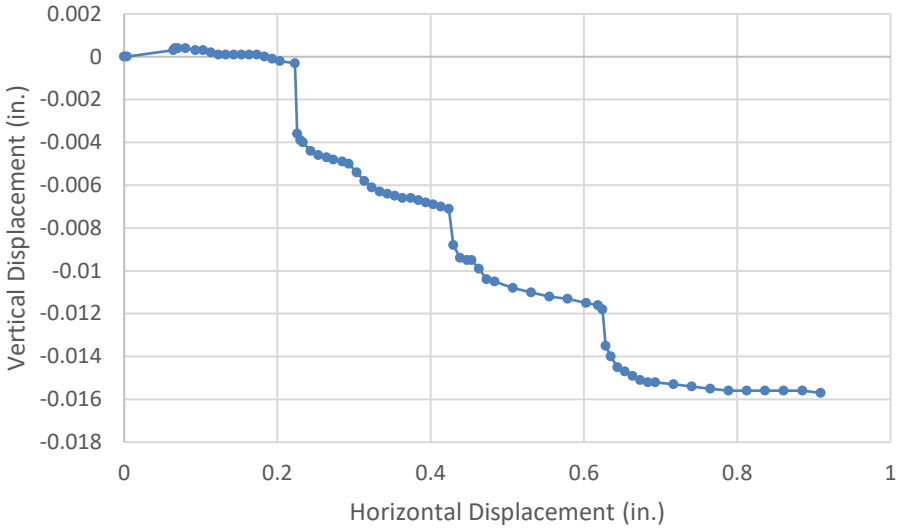

c) Vertical displacement versus horizontal displacement

Figure A9. Test of the interface between block facing and geosynthetic

Table A6: Strength properties of the geosynthetic and block facing interface

Properties	Units	Value
Friction angle, ϕ	(^{0})	28
Cohesion, c	(psi)	1.83

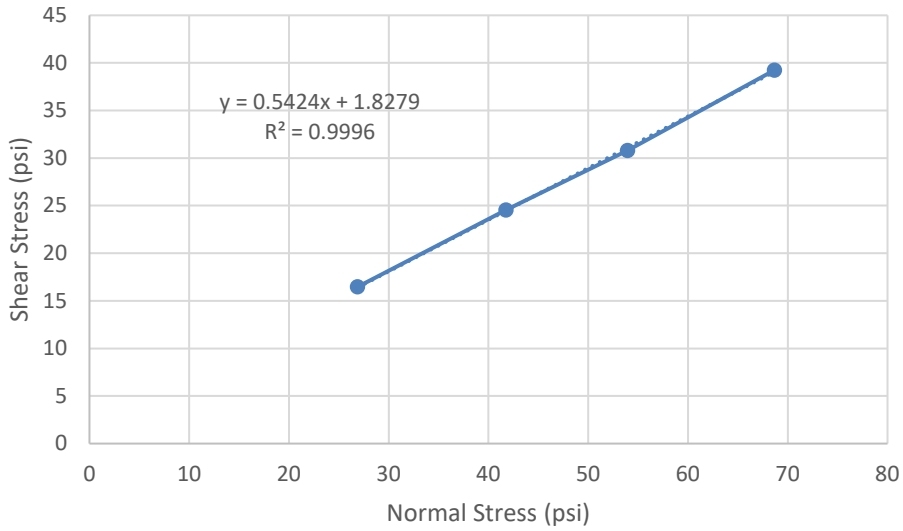

Figure A10. Determination of strength parameter of the interface

A.3 Laboratory tests of interface between backfill soil and concrete

Three tests of interface between backfill soil and concrete were performed under different normal stresses: 10 psi, 20 psi, and 30 psi. The test results are shown in Table A7 and presented in Figs. A12 to A14.

Table A7: Strength properties of the backfill and concrete interface

Properties	Units	Value
Friction angle, ϕ	(^{0})	38
Cohesion, c	(psi)	0.298

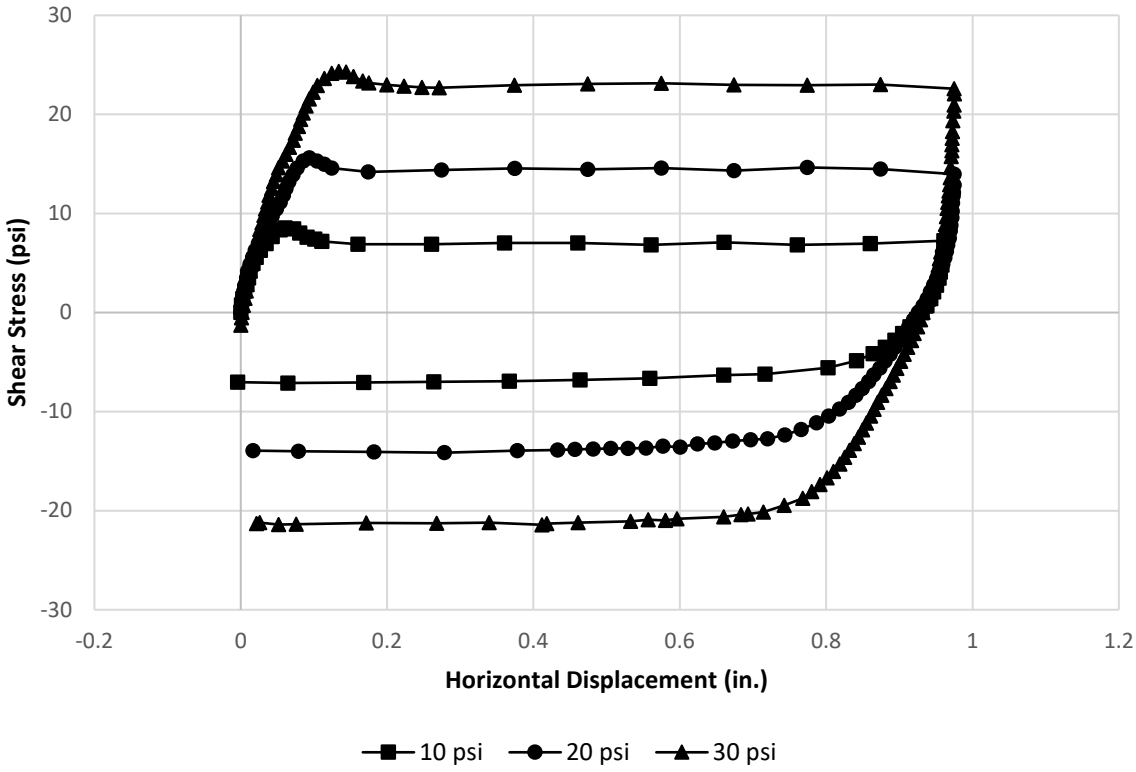

Figure A11. Shear stress and displacement curves

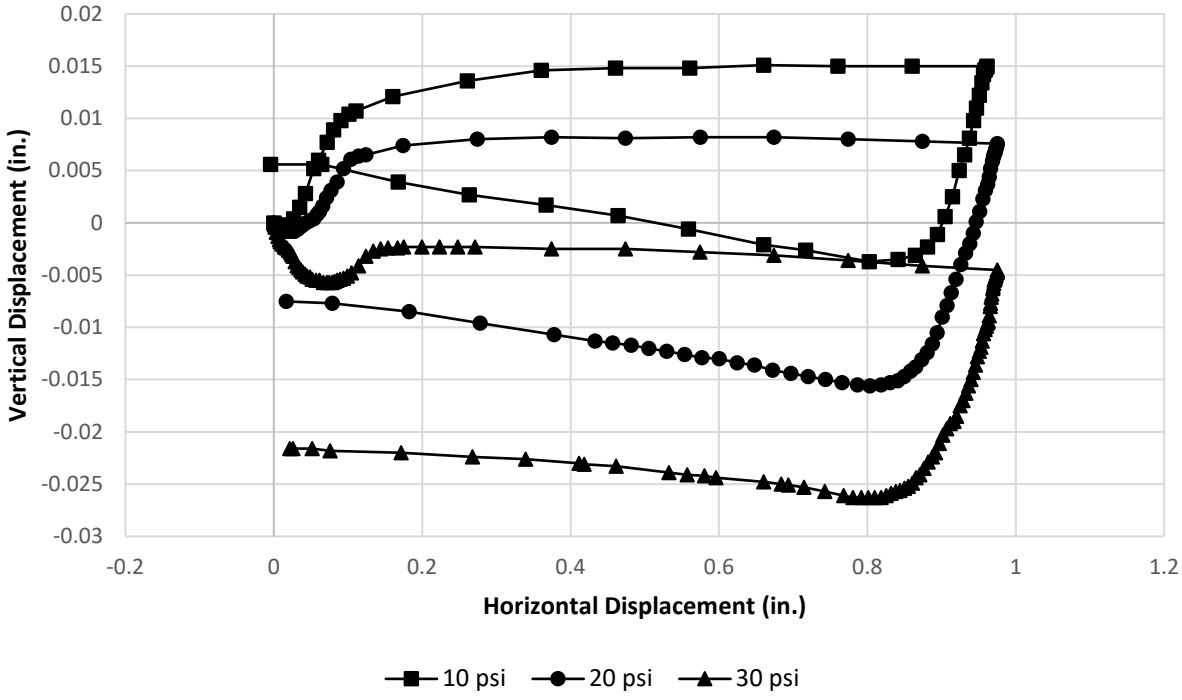

Figure A12. Vertical displacement and horizontal displacement curves

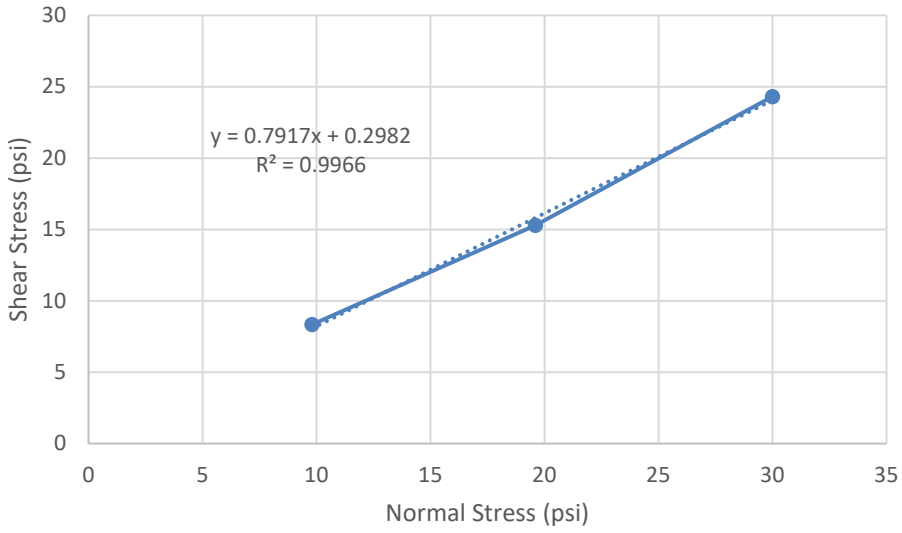

Figure A13: Determination of strength parameter of the interface